INFLATION MODELLING: RISK PREMIA AND DERIVATIVE PRICING

by

Warrick Poklewski-Koziell

Supervisor: Prof. Dr. Markus Leippold

M.Sc. UZH ETH in Quantitative Finance

The Swiss Federal Institute of Technology Zurich and the University of Zurich

Switzerland

September 2013

A thesis submitted in partial fulfilment for the degree of Master of Science

ABSTRACT

This thesis is concerned with the modelling of inflation with the aim of extracting the inflation risk premium (IRP) from asset prices. The pricing of inflation-indexed derivatives is required for this purpose. First, a modelling framework is assumed, whereby all rates in the market are driven by three latent factors, which follow a mean-reverting Vasicek process. Additionally, a price level process is coupled to this. Second, pricing applications of the model are considered and formulae for zero-coupon inflation-indexed swaps, year-on-year inflation-indexed swaps and inflation-indexed caps and floors are presented. Next, the standard and unscented Kalman-filters are presented as means of estimating the sample log-likelihood. Methods for maximising this to estimate model parameters are then considered. Given this setup, the calibration of the model to four data sets in US and European markets is performed. Data sets including swap rates and cap prices are used. The IRP is then extracted from the model and analysed. The thesis concludes with the analysis of a number of applications of the framework, including the use of the IRP in a bond trading strategy.

Keywords: Latent factor model, inflation risk premium, inflation-indexed derivative pricing, Kalman-filter, maximum likelihood estimation, model calibration, bond trading.

ACKNOWLEDGMENTS

I would like to express my sincere gratitude to Raffaele Pellicani[1] for suggesting this thoroughly fascinating research topic. His advice and guidance with the subject matter of this thesis were invaluable.

I would also like to thank Zürcher Kantonalbank and Dr. Thomas Siller for giving me the opportunity to complete this thesis at the bank. The resources and assistance provided to me there proved instrumental in the successful completion of this document.

Moreover, I would like to thank Prof. Dr. Markus Leippold[2] and Nikola Vasiljevic[3] for their supervision of this topic and insightful guidance with many of the themes discussed herein.

Finally, I would like to thank my family and Heather for their wonderful support throughout my studies.

[1]Quantitative analyst at Zürcher Kantonalbank.

[2]Hans Vontobel Professor of Financial Engineering at the University of Zurich.

[3]Ph.D. student in finance at the University of Zurich.

DECLARATION

I declare that this thesis is my own work. It is being submitted in partial fulfilment for the degree of master of science for the program *M.Sc. UZH ETH in Quantitative Finance*. It has not been submitted before for any degree or examination in any other university.

Warrick Poklewski-Koziell

September 2013

Contents

List of Figures

List of Tables

Executive Summary

In this thesis, we consider inflation modelling with the aim of extracting the inflation risk premium (IRP) from asset prices. To do so, we assume a modelling framework in an inflation setting and consider the pricing of inflation-indexed derivatives under this framework. Thereafter, we consider the problems of fitting the model to market data, analysing the adequacy of the model fits to the data and finally, extracting the IRP. We conclude by presenting applications of our research.

Our work is very much a continuation of that of Ho, Huang and Yildirim (2012) [28], who suggest a number of new approaches to analysing the IRP. As a result, a number of sections in this work extend the current scope of the literature. Specifically, we consider the extraction of the IRP from option data, which to our knowledge has not been considered so far. Moreover, we extend a bond trading strategy that makes use of the IRP to detect the over- or underpricing of nominal bonds relative to real bonds.

Modelling Framework. The modelling framework that we make use of in this thesis is the same as that of D'Amico, Kim and Wei (2008) [17] and Ho, Huang and Yildirim (2012) [28]. In this way, we assume that all rates in the market are driven by three latent factors, which follow a mean-reverting Vasicek process. The actual rates (nominal, real and inflation) themselves are simply affine transformations of this process. Additionally, a price level process is coupled to this. This affine framework lends itself nicely to the pricing of nominal and real zero-coupon bonds, as well as the calculation of an expression for the expected inflation rate. The yields on these, as well as the expected inflation rate turn out also to be affine functions of the driving latent factor process. The IRP itself is then simply the difference between the nominal zero-coupon bond yield and the sum of the real zero-coupon bond yield and the expected rate of inflation.

Derivative Pricing. Given this modelling framework, we present pricing formulae for various inflation-indexed derivatives. These are zero-coupon inflation-indexed swaps (ZCI-

ISs), year-on-year inflation-indexed swaps (YOYIIS) and inflation-indexed caps and floors (IICFs). A ZCIIS is a contract where one party agrees to swap a single fixed payment for an inflation-indexed payment at some point in the future. A YOYIIS is similar to a ZCIIS, except that payments are swapped at yearly intervals for the duration of the swap. IICFs are options on inflation. A cap (floor) is a call (put) option on the inflation rate at various points in the future over the life of the option. These instruments can best be understood as the sum of a series of inflation-indexed caplets or floorlets (IICFlets), each of which gives the holder the option to exchange a fixed (inflation-indexed) payment for an inflation-indexed (fixed) one at some point in the future. Typically, IICFs are year-on-year instruments.

Calibration Framework. We calibrate the model to market data by maximising the sample log-likelihood function with respect to the model parameters. To estimate this function, we make use of Kalman-filtering techniques. In the case of instruments whose values are affine functions of the latent factor process (bond yields[4], log-swap rates, CPI levels and expected inflation rates), we employ the standard Kalman-filter. In the case of instruments where the pricing problem is non-linear in the latent factors (caps and floors), we make use of the unscented Kalman-filter. Given the function to compute the sample log-likelihood via a suitable Kalman-filter, we can employ optimisation routines to maximise this with respect to the model parameters. To this end, we use both the *fminsearch* algorithm in Matlab - which is based on the Nelder-Mead simplex algorithm - and a genetic algorithm (details of which are provided in an appendix in the thesis).

Calibration Results and the Inflation-Risk Premium. We consider the calibration of the model to both European and US data sets. Before performing the actual fits, we do a number of principal component analyses of the data sets to determine the number of latent factors needed to explain the variance of the instrument values in the data sets. Here, we find that three factors are sufficient to explain most of the variance in each of the data sets. This is consistent with the notion that yield curves can be explained by a level, slope and curvature factor. We also specify the particular parametrisation of the model that we make use of. This is the same as the one employed by D'Amico, Kim and Wei (2008) [17]. Thereafter, we consider the actual calibration of the model to data.

Here, we make use of four data sets. The first is a synthetic data set which we generate with a Monte-Carlo simulation. The second is taken from the sources specified in Ho, Huang and Yildirim (2012) [28]. Calibrating to these two data sets allows us to benchmark our model and evaluate the performance of our calibration routines. We find, at this point, that

[4]Note, that when we refer to bond yields, we always mean zero-coupon yields, unless otherwise specified.

our model fits are indeed good. Thereafter, we consider two European data sets which have not been used previously in the literature. The first of these is one consisting mainly of ZCIIS rates, as well as nominal bond yields, inflation survey forecasts and HICPxt levels. The second consists mainly of IICF prices, as well as nominal bond yields, inflation survey forecasts and HICPxt levels. In both data sets, the use of nominal bond yields and inflation survey forecasts is to add stability to the calibration process and to produce meaningful results. The calibration to the first of these two is performed via the standard Kalman-filter, whilst that to the second is performed via the unscented Kalman-filter. To our knowledge, the calibration of this inflation model to option data (and therefore the extraction of the IRP from option data) had not been performed before. In the case of the ZCIIS data set, we find that the model fits the data well. In the case of the IICF data set, the fit is not as good, owing mainly to a short timespan of the data set and the illiquidity of IICFs in the European market.

The final section of this chapter analyses the IRP extracted from the European ZCIIS data. Here, we compare the IRP extracted from the model to that found via a model-free approach. We find that the model-implied and model-free approaches produce similar estimates of this quantity. We also consider the historical IRP over the period 2004-2013 and find that it is fairly stable before the recent financial crisis, experiences a large decline at the time of the crisis and remains quite volatile thereafter. Next, we consider the term-structure of the IRP at various points in time and find it to be upward sloping at the end of the data set (May 2013).

Applications. The final chapter of this thesis is concerned with applications of the IRP. The first of these is a bond trading strategy which uses the IRP to determine the over- or underpricing of nominal bonds relative to real bonds. Here, we consider government bond portfolios in both the US and the European (AA grade) markets in periods that include the financial crisis, as well as those before and after the crisis. We implement the bond trading strategy by selecting an in-sample window for the period we are interested in and computing a trigger level for the IRP - above which we buy nominal bonds and below which we buy real bonds - that maximises the risk-adjusted return of the bond trading strategy in that window. Then we implement the strategy in the out-of-sample window, again using this trigger level. We compute the return and the risk-adjusted return in the out-of-sample window and compare the performance of the strategy to three naive buy-and-hold strategies - involving a portfolio of nominal bonds, a portfolio of real bonds and a portfolio equally weighted with real and nominal bonds - as well as to a sample of randomly readjusted portfolios. We find that the bond trading strategy outperforms the other strategies for the

most part in both markets and across all time periods. When we account (naively) for transaction costs in our strategies, however, we find that the performance of the strategy in the European case is reduced. Finally, we propose an extension of the scheme to a multiple bond portfolio setting, where we take the term structure of IRPs into account. In general however, one drawback to the bond trading strategy is that we find it to be somewhat sensitive to the in- and out-of-sample windows chosen to conduct the tests.

Next, we consider the capability of the model to provide a good forecast of future inflation. We find that it performs much better than using past inflation or break-even inflation rates and slightly better than using survey forecasts of inflation. However, the analysis here shows that the model seems to give a forecast of average inflation, but fails to capture the volatility of future inflation.

The final section of this chapter is concerned with the out-of-sample performance of the model. We test this in both a Kalman-filter framework - by calibrating the model to an in-sample window and then running the Kalman-filter in the out-of-sample window - and by performing a linear projection of the model-implied asset prices using expected values. We find the out-of-sample performance of the model to be reasonably good.

Chapter 1

Introduction and Literature Review

The aim of this thesis is to investigate the inflation risk premium (IRP) from instruments in the inflation market, and especially inflation-indexed derivatives. For this purpose, we also need to consider the pricing of such derivatives. The size of the IRP gives an indication of the price of inflation insurance in bond markets and can be used to interpret how certain investors are about expected future inflation. It can also be used as a mechanism to evaluate the over- or underpricing of nominal bonds relative to real bonds, a theme that we will explore in the last chapter of this thesis. Our work in this thesis is very much a continuation of that of Ho, Huang and Yildirim (2012) [28].

The purpose of this current chapter is to introduce the topic of this thesis, the key ideas related to it as well as to examine the current literature available concerning this topic. We start by introducing the IRP, the methods of estimating it and the models that can be used to extract it. Thereafter, we review the types of data used in the literature as well as the results obtained by other authors. Finally, we briefly introduce derivative pricing considerations and applications for the IRP. The remainder of the thesis is arranged as follows.

In Chapter 2, we present the model that we will use for our analysis of the IRP. This is the same model as that used by D'Amico, Kim and Wei (2008) [17] and Ho, Huang and Yildirim (2012) [28]. We explain the dynamics of the model, derive expressions for bond prices, expected inflation and the IRP under the model. Finally, we compare the simulation of rates to the analytical calculation of rates under the model.

Chapter 3 presents pricing equations for a number of inflation-indexed instruments. Specifically, we consider the pricing of zero-coupon inflation-indexed swaps, year-on-year inflation-indexed swaps and inflation-indexed caps and floors.

Chapter 4 is concerned with the theoretical aspects of the calibration of the model to market data. In this chapter, we present both the Kalman and unscented Kalman-filter approaches for estimating the model parameters via maximum likelihood estimation.

Chapter 5 presents the results of the calibration of the model. First, we perform principle component analyses of various rates in nominal and real (or inflation-indexed) markets. Next, we perform the calibration of the model to various data sets and present the results of these calibrations. Here, we consider instrument prices in the US market as well as in the European market. In the European case, we examine instruments that are linked to the Harmonised Index of Consumer Prices, which is a measure of overall inflation among EU countries. We consider the calibration of the model to bond, swap, price level and expected inflation data. Moreover, we extend the current scope of the literature to examine the calibration of the model to cap data. This requires the use of the more sophisticated unscented Kalman-filter. Finally, we interpret the dynamics of the IRP implied by the model.

In Chapter 6, we consider a number of applications of the IRP. The most significant one that we consider here is the use of the IRP in a bond trading strategy. Such a strategy is suggested in the literature, although in a simpler form. We extend that in this thesis by using a modelling approach to obtain an accurate estimate of the IRP and then using this to implement the strategy. We further consider the use of the IRP in the model to decompose break-even inflation rates and thereby obtain a better estimate of expected inflation. This chapter also considers out-of-sample tests for the model.

Chapter 7 concludes the thesis.

1.1 The Inflation Risk Premium

In order to introduce the inflation risk premium, it is helpful to start with Fisher's equation. This is defined as

$$y^N_{t,T} = y^R_{t,T} + i^e_{t,T},$$

where $y^k_{t,T}$, $k = N, R$ are the (continuously compounded) nominal and real yields[1] over $[t, T]$ and $i^e_{t,T}$ is the expected inflation rate over the same time period. This equation suggests that the spread on nominal bond yields over real bond yields is due to expected inflation. There is, however, increasing empirical evidence that indicates that the Fisher hypothesis does not hold (see, for example, Buraschi Jiltsov (2005) [8], Deacon, Derry and Mirfendereski (2004, pg. 61-64 and pg. 83-85) [18], Evans (1998) [21] and Ho, Huang and Yildirim (2012) [28]) and that an additional factor is required to describe the difference between nominal and real rates (also known as the break-even rate). This factor is generally referred to as the inflation risk premium and is defined via the equation

$$y^N_{t,T} = y^R_{t,T} + i^e_{t,T} + \phi_{t,T}, \tag{1.1}$$

where $\phi_{t,T}$ is the IRP over $[t, T]$. We name this expression the extended Fisher equation. It shows that the IRP can be incorporated as a spread over expected inflation to account for the break-even rate.

1.1.1 Intuition and Stylised Facts

The economic intuition for the existence of the IRP stems from the uncertainty associated with expected future inflation. Shen (1998) [41], for example, explains that holders of nominal bonds need to be compensated for the risk of unexpected changes in inflation. Unanticipated increases in inflation cause the real value of nominal bonds to decline unexpectedly and holders of these bonds demand a premium for accepting this risk.

The most commonly stated (see Buraschi and Jiltsov (2005) [8] and Shen (1998) [41]) "stylised fact" for the IRP is that its term structure increases with maturity (see Chen, Liu, Cheng (2005, pg. 45) [12] for an illustration of this). This occurrence might be explained in two ways. Firstly, forecasting difficulties make it hard to accurately estimate expected inflation in the distant future. As a result, there is more uncertainty about inflation at longer maturities and so investors need to be compensated more for holding long-term nominal bonds than for holding short-term nominal bonds. Secondly, an "error" in the estimate of inflation has a bigger impact on the real value of long-term nominal bonds than it does on the real value of short-term nominal bonds due to the greater duration of long-term bonds. Holders of long-term nominal bonds need to be compensated for this.

That being said, however, the shape of the term structure also depends on the level of confidence that investors have in inflation being kept at expected levels (by the central

[1] Note, that when we refer to bond yields, we always mean zero-coupon yields, unless otherwise specified.

bank, say) in the near term. If there is uncertainty about this, then the term structure may indeed decrease with time, reflecting investors beliefs that inflation in the long run should stabilise.

1.1.2 The Importance of Understanding the Inflation Risk Premium

There are a number of reasons for having an interest in understanding the IRP. Firstly, a better understanding of the IRP enables investors with long investment time horizons to better understand the risks to which their portfolios are exposed (see Berkaert and Wang (2010) [4]). It can also be used in detecting the over- or underpricing of inflation insurance and therefore, can be incorporated into bond buying strategies (see Lemaire and Plante (2009) [33]). A better knowledge of the IRP also helps investors to better decompose break-even inflation into its various components, thereby obtaining more accurate estimates of expected future inflation. Secondly, it is important from policy makers' perspectives (see Haubrich, Pennacchi and Ritchken (2012) [27] and Shen (1998) [41]). For them, the size of the IRP indicates how a government can save by issuing real bonds instead of nominal bonds (i.e. they can save the risk premium that they would otherwise have to pay to nominal bond holders). Moreover, the magnitude of the IRP gives an indication of the effectiveness of the inflation targeting policies of governments and how credible markets view their actions to be. Large IRP values would indicate (to an extent at least) that markets do not have much confidence in the abilities of authorities to enforce their policies. Thirdly, it is beneficial for both the supply and demand side of the bond market (see Grishchenko and Huang (2012) [24]). From a supply side, treasuries can better adjust the supply of inflation-indexed securities if they know the term structure of the IRP. From a demand side, investors can better hedge their inflation risks if they know the term structure of the IRP.

These are just a few of the benefits of obtaining a description of the IRP. They provide motivation for us to understand and study it.

1.1.3 Estimating the Inflation Risk Premium

There are two common methods for estimating the IRP in the literature. The first of these uses model-free estimation and the second uses model-implied estimation.

The first method involves estimating the IRP from market instruments without making use of an inflation model. Ho, Huang and Yildirim (2012) [28] provide a simple method for doing this from zero-coupon inflation-indexed swaps (ZCIIS). They show that the fair price

of a ZCIIS is given by

$$P^R_{t,T} = P^N_{t,T}\left(1 + K^{\text{ZCIIS}}_{t,T}\right)^{T-t},$$

where $P^k_{t,T}$, $k = N, R$ are nominal and real zero-coupon bond prices at time t for bonds with maturity T and $K^{\text{ZCIIS}}_{t,T}$ is the ZCIIS rate over $[t, T]$. Taking logarithms and dividing by $-(T-t)$, they get

$$\begin{aligned} y^N_{t,T} &= y^R_{t,T} + \log\left(1 + K^{\text{ZCIIS}}_{t,T}\right) \\ &= y^R_{t,T} + \log\left(1 + K^{\text{ZCIIS}}_{t,T}\right) + \frac{1}{T-t}\mathbb{E}_t\left[\log\left(\frac{Q_T}{Q_t}\right)\right] - \frac{1}{T-t}\mathbb{E}_t\left[\log\left(\frac{Q_T}{Q_t}\right)\right] \\ &= y^R_{t,T} + \frac{1}{T-t}\mathbb{E}_t\left[\log\left(\frac{Q_T}{Q_t}\right)\right] + \left\{\log\left(1 + K^{\text{ZCIIS}}_{t,T}\right) - \frac{1}{T-t}\mathbb{E}_t\left[\log\left(\frac{Q_T}{Q_t}\right)\right]\right\}, \end{aligned} \quad (1.2)$$

where Q_t is the process for the level of prices in the economy. Comparing the last equation to (1.1) and noting that $\frac{1}{T-t}\mathbb{E}_t\left[\log\left(\frac{Q_T}{Q_t}\right)\right]$ is the continuously compounded expected inflation rate over $[t, T]$, it can be seen that the IRP, $\phi_{t,T}$, can be estimated from

$$\log\left(1 + K^{\text{ZCIIS}}_{t,T}\right) - \frac{1}{T-t}\mathbb{E}_t\left[\log\left(\frac{Q_T}{Q_t}\right)\right].$$

The second method involves making use of a modelling framework to imply the IRP. This method is more complicated than the model-free estimation. In general, as Bekaert and Wang (2010) [4] explain, it requires the specification of a no-arbitrage term structure model to price nominal and real bonds as well as the specification of a realistic inflation model, which is linked to the term structure model. These models are then calibrated to market data, which allows for the estimation of the model parameters. Once this is completed, the IRP can be implied from the model. This technique is discussed at length in the literature and will be addressed later in the thesis.

There are also a number of difficulties involved in estimating the IRP. Firstly, the inflation market is a new one and many instruments have not been traded for very long. Treasury inflation protected securities (TIPS), for example, were only introduced in the United States in 1997 (see Ungari (2009) [43]) which means that there are not much data available for these instruments and even the data which are available are possibly biased by illiquidity, at least in the early years of the market (see Bekaert and Wang (2010) [4] and Shen (1998) [41]). On top of this, the relatively short existence of the inflation market could mean that the types of investors in the inflation market are different from those in the nominal market (for example, investors in the inflation market might be more sophisticated than, and have different risk preferences to, those in the nominal market). This is often called the "clientele effect" and it can make comparisons across the markets difficult (see Shen (1998) [41]).

Both of these effects make the accurate estimation of the IRP more challenging. Another difficulty in estimating the IRP is deciding which data to use for expected inflation, which is not observable. Since this is necessary to estimate the IRP, it is important to use data which accurately reflect future inflation expectations. Often inflation surveys are used here, but these rely on the opinions of experts and there are no guarantees that their expectations are the correct ones (see Segreti (2008) [40]).

1.2 Models That Capture the Inflation Risk Premium

The inflation market is a relatively new, but fast growing market and as such, inflation models have attracted considerable interest in recent years. Ungari (2009) [43] gives an overview of many popular inflation models. In particular, he looks at the Heath-Jarrow-Morton (HJM) framework proposed by Jarrow and Yildirim (2009) [30], the inflation market model approach proposed by Belgrade and Benhamou (2004) [5] and a few short-rate modelling approaches. The most famous of these is perhaps the Jarrow-Yildirim (JY) model, which models inflation in an analogous fashion to the HJM approach for foreign exchange, by replacing the domestic, foreign and exchange rate in the foreign exchange framework with the nominal rate, real rate and inflation index respectively. The drawback of these approaches in our situation is that they cannot capture the IRP. For this purpose, we consider alternative models in the literature.

Chen, Liu and Cheng (2005) [12] and Grishchenko and Huang (2012) [24] provide informative reviews of the literature that has shaped the development of modelling techniques for estimating the IRP. Campbell and Shiller (1996) [9] were the first to provide estimates of the IRP by estimating its value from data on nominal bonds. Other significant approaches in the literature are given in the remainder of this section.

Chen, Liu and Cheng (2005) [12] model the IRP using a two-factor Cox-Ingersoll-Ross (CIR) model, which describes the evolution of the real rate and an inflation factor. They use this to derive expressions for real and nominal zero-coupon bonds and then estimate the IRP by subtracting the prices of nominal zero-coupon bonds with risk-neutral parameters from those with real-world parameters.

D'Amico, Kim and Wei (2008) [17] and Ho, Huang and Yildirim (2012) [28] essentially follow the same framework in their approaches to estimating the IRP. Like many others in the literature, they specify a factor model to model nominal and real markets. They do not, however, specify what the factors represent, but rather use latent factors in their approaches.

One departure of the D'Amico, Kim and Wei (2008) [17] paper from the Ho, Huang and Yildirim (2012) [28] paper is that the former explicitly state the number of factors they include in their model. They make use of three factors to drive real and nominal yields, as well as expected inflation, and find the need to incorporate a fourth factor to take account of illiquidity in the TIPS market (they use US data in their approach). Both papers then employ a Vasicek process to describe the evolution of the latent factor vector driving interest rates and inflation. They specify real and nominal rates and market prices of risk as affine functions of this latent factor vector and use these to derive expressions for real and nominal stochastic discount factors as well as for real and nominal zero-coupon bond yields. Their models allow them to derive explicit formulae for the IRP and they obtain estimates of this with the help of inflation expectation surveys.

Ang, Bekaert and Wei (2008) [2] make use of a factor regime switching term structure model. The model is driven by a vector of three factors, two of which are latent and one which acts as an inflation factor. The real rate is specified as an affine transformation of the vector of factors and the authors use this to derive the real, and subsequently the nominal, pricing kernels. Calibrating it to data, they then imply the IRP from the model.

Garcia and Werner (2010) [23] employ a discrete-time affine term structure model. They use this to define a relationship between bond yields and the dynamics of short-term yields and inflation. To do so, they specify a state vector, which follows a VAR(1) (vector autoregressive) process and consists of two latent factors and one inflation factor. They specify the real rate and the market price of risk as affine functions of the state vector and derive an expression for the real pricing kernel. They use this to imply real bond prices, as well as real bond yields (and explain that the same procedure can be followed for nominal rates, bond prices and yields). This allows the authors to obtain a framework to describe break-even inflation rates and find the IRP with the help of survey inflation expectations.

Chernov and Mueller (2012) [13] specify a factor model to capture the state of the economy. Their model consists of a vector of factors, two of which represent the quarterly log-change in GDP and the inflation rate respectively, and the others are latent factors. The vector of factors, or the state vector, follows a VAR(1) process. The authors specify interest rates and the market prices of risk as affine functions of the state vector and derive expressions for the stochastic discount factors. They are able to derive equations defining the yields on real and nominal zero-coupon bonds and they imply the IRP from the dynamics of the model.

A number of other authors follow similar procedures to those outlined above. Grishchenko and Huang [24], for example, use a largely model-free framework in their estimation of the IRP. One of their approaches makes use of a VAR(1) factor model to estimate expected inflation. They make use of TIPS data in their study and find the need to include a liquidity component in the TIPS yield. Christensen, Lopez and Rudebusch (2010) [14] also follow a factor model approach. They analyse real and nominal yields separately, finding the need for three factors (representing the yield curve level, slope and curvature) to model nominal yields and two factors (representing the yield curve level and slope) to model real yields. Aggregating these two approaches, they make use of four factors in a joint model for nominal and real yields. The factors in this model represent a real and a nominal level factor, a slope factor and a curvature factor. They find an analytical expression for the IRP from their model.

1.3 A Review of Results and Data Sources

In this section, we compare various studies on the IRP. Particularly, we consider the values found for the IRP and the data sources used in these studies. For ease of reference, we present this comparison in Table 1.1.

Note that most of the studies make use of the Kalman-Filter to fit their models to market data. The Kalman-filter is a method for linearly projecting (in an optimal way) the state of a system forward in time as current information about the system becomes available. This method allows for the estimation of the sample log-likelihood function, which can then be maximised with respect to the model parameters using numerical optimisation. Informative descriptions of the use of the Kalman-Filter in this setting are given by D'Amico, Kim and Wei (2008) [17] and Ho, Huang and Yildirim (2012) [28].

As can be seen from Table 1.1, most of the studies in the literature make use of bond, swap, CPI and inflation forecast data. They do not, however, make use of data from more sophisticated derivatives. Ho, Huang and Yildirim (2012) [28] suggest that doing so would be a natural extension to the current literature on estimating the IRP. In our study on the IRP, we will therefore make use of other inflation derivative prices and analyse the benefit of considering these sources.

Paper	Data	Calibration Method	Model	IRP Results
Chen, Liu, Cheng (2005) [12]	**US data** including nominal constant maturity Treasury (CMT) rates and TIPS yields. **Data period** from 1998 to 2004. **Maturities** from 3 months to 30 years.	MLE via Unscented Kalman-Filter	Two-factor CIR	Term structure of IRP lies in the range -0.011% to 1.32% (see graph on pg. 45 of their paper for full results).
D'Amico, Kim, Wei (2008) [17]	**US data** including nominal bond yields, CPI-U data, TIPS yields and Michigan and SPF inflation forecast data. **Data period** from 1990 to 2007 for nominal and CPI data and from 1999 to 2007 for TIPS and inflation forecast data. **Maturities** from 3 months to 10 years.	MLE via Kalman-Filter	Latent factor model driven by a Vasicek process	Estimated (historical) IRP lies in the range 0% to 1% for two of their models and in the range -1.5% to 1% for their third model.
Ho, Huang, Yildirim (2012) [28]	**US data** including weekly CPI level data, Treasury yields, TIPS yields, inflation forecast surveys and inflation swap rates. **Data period** from 2004 to 2010. **Maturities** from 3 months to 30 years.	Model-free and MLE via Kalman-Filter	Latent factor model driven by a Vasicek process	Estimated (historical) IRP between -0.5% and 1% (both model-free and model-implied estimation).
Ang, Bekaert, Wei (2008) [2]	**US data** including zero-coupon yield data from CRSP and CPI-U data. **Data period** from 1952 to 2004. **Maturities** from 4 to 20 quarters.	Maximum Likelihood Estimation	Regime switching factor model	IRP estimates range between -0.14% and 1.25%.

Table 1.1 Comparison of studies in the literature.

Paper	Data	Calibration Method	Model	IRP Results
Garcia, Werner (2010) [23]	**European data** including nominal zero-coupon yields on German bonds, real zero-coupon yields, HICP inflation data from Eurostat and SPF inflation forecast data from the ECB. **Data period** from 1995 to 2006. **Maturities** from 3 months to 5 years.	MLE via Kalman-Filter (using a combination of the simplex method and the subgradient method to perform the optimisation)	Factor model driven by a VAR(1) process	Estimated (historical) IRP lies in the range -0.5% and 0.5%.
Chernov, Mueller (2012) [13]	**US data** including nominal Treasury yields, quarterly GDP and CPI data and various inflation survey forecasts. **Data period** from 1970 to 2004. **Maturities** from 3 months to 10 years.	MLE via Kalman-Filter (using a grid search mechanism as well as the simplex and SQP methods to perform the optimisation)	Factor model driven by a VAR(1) process	Estimated (historical) IRP lies in the range -5% to 8% (depending on model and time period).
Christensen, Lopez, Rudebusch (2010) [14]	**US data** including Treasury bond yields, TIPS yields and SPF inflation survey forecasts. **Data period** from 1995 to 2008. **Maturities** from 3 months to 10 years.	MLE via Kalman-Filter	Affine arbitrage-free Nelson-Siegel factor model	Model-implied IRP lies in the range -3.5% and 1.5%.
Grishchenko, Huang (2012) [24]	**US data** including nominal Treasury yields, TIPS yields, CPI-U data, SPF inflation survey forecasts and various real activity measures (see pg. 7-11 and Table 1 in their paper for further details). **Data period** from 2000 to 2008. **Maturities** from 5 to 10 years.	Largely model-free estimation	Largely model-free, but also make use of a VAR(1) model to estimate inflation	Estimated 10-year IRP lies in the range 0.14% and 0.19%.

Table 1.1 Comparison of studies in the literature (continued).

1.4 Inflation-Linked Derivative Pricing and Hedging

Most of the papers reviewed in this section only go as far as to specify pricing formulae for the instruments with which their studies are concerned. As a result, few papers derive pricing formulae for instruments other than bonds. In general, this is due to the fact that the models used to extract to IRP are not appropriate pricing models. Of particular interest to us is the paper by Ho, Huang and Yildirim (2012) [28], which gives a thorough description of various pricing equations within a factor-model framework. In their paper, they derive equations for inflation-indexed swaps (both zero-coupon and year-on-year swaps), swaptions, caplets (floorlets) and caps (floors). The paper by Jarrow and Yildirim (2009) [30] also considers pricing equations for options on the inflation index. Their model is not useful however for computing the IRP.

Hedging is another point of interest when implementing models to price inflation derivatives, but this topic is not generally covered in the literature relating to the IRP for the same reason pricing is not generally covered. Again, Jarrow and Yildirim (2009) [30] consider hedging in the framework of their model. They also present equations for various hedging ratios, or greeks, in their paper.

1.5 Applications of the Inflation Risk Premium

One interesting application of the IRP is as a trading tool for detecting the over- or underpricing of nominal bonds relative to real bonds. This is explored in Lemaire and Plante (2009) [33]. In their paper, they describe a method of using the IRP as a decision tool in a bond buying strategy to decide between buying nominal and real bonds at each point in time. We explore a similar scheme in the last chapter of this thesis.

There are also a number of other applications of the IRP, specifically those described previously, which relate to its use in treasury and central bank activities.

Chapter 2

Modelling Inflation

The model that we make use of in this thesis for modelling inflation and extracting the IRP is the same as that employed by D'Amico, Kim and Wei (2008) [17] and Ho, Huang and Yildirim (2012) [28]. We select it for a number of reasons. Firstly, it is natural to take a factor model approach to modelling yield curves, as different factors can be used to describe different phenomena in the curve. For instance, three factors can be used to describe the level, slope and curvature of a yield curve. Secondly, the model exhibits equations for bond yields and expected inflation rates that are affine in the state vector. In this way, the model lends itself well to calibration via the Kalman-filter. Thirdly, the model is well researched in the literature and it and its variations appear to be the most popularly used for extracting the IRP. It is therefore natural for us to make use of this framework and try to extend it (for instance, by calibrating it to cap prices, which appears not to have been done before in the literature). Finally, it is a robust model, with a reasonably simple and understandable structure, but which can also easily be extended to account for other phenomena, such as the illiqudity of the instruments.

2.1 A Latent Factor Model for Inflation

Here, we follow the formulation of D'Amico, Kim and Wei (2008) [17] and Ho, Huang and Yildirim (2012) [28] closely. We set out a no-arbitrage modelling framework where we specify a vector of latent factors and formulate the nominal rate, real rate, instantaneous inflation rate and the nominal market price of risk as affine functions of this vector. This allows us to find expressions for the nominal and real pricing kernels, nominal and real zero-coupon bond (ZCB) prices, nominal and real yields, as well as expected inflation. Finally, the model admits an expression for the IRP. Here, and in the remainder of the thesis, we refer to this model equivalently as the latent factor model and the Vasicek latent factor

model.

2.1.1 Latent Variables

Heuristically, we define a probability space $(\Omega, \mathcal{F}, \mathbb{P})$, where Ω is the state space, $\mathcal{F}$ is a σ-algebra of subsets of Ω and $\mathbb{P}$ is the objective, or real-world measure. We define an n-dimensional vector process of latent variables on this space by X_s, where s lies in the interval $[t, T]$. This process follows a multivariate Gaussian process, better known as the Vasicek process (see Vasicek (1977) [44]):

$$dX_s = \mathcal{K}(\theta - X_s)\, ds + \Sigma dZ_s, \tag{2.1}$$

where θ is an n-dimensional vector of constants, $\mathcal{K}$ and Σ are $(n \times n)$-dimensional matrices of constants and Z_s is an n-dimensional standard $\mathbb{P}$-Brownian motion. Many papers that make use of this model - the paper by D'Amico, Kim and Wei (2008) [17] included - take n to be 3. The reasoning often given for this is that three factors are enough to explain most of the variation in the yield curves; the three factors are often taken to represent the level, slope and curvature of the yield curve (see Christensen, Lopez and Rudebusch (2010) [14] and Piazzesi (2010) [36]). We follow the specification of the model by Ho, Huang and Yildirim (2012) [28] and leave the number of latent variables unspecified. Later we will perform principal component analysis (PCA) tests to ascertain how many factors are necessary for our situation.

2.1.2 Nominal Rate, Real Rate and Instantaneous Inflation Dynamics

Firstly, we define the dynamics of the nominal and instantaneous expected inflation rates to be

$$r^N(X_s) = \eta_0^N + {\eta_1^N}^\top X_s$$
$$r^e(X_s) = \eta_0^e + {\eta_1^e}^\top X_s,$$

where $r^N(X_s)$ and $r^e(X_s)$ are the nominal short-rate and instantaneous expected inflation rate respectively. Moreover, η_0^N and η_0^e are constants and η_1^N and η_1^e are n-dimensional vectors of constants.

Next, we specify the nominal prices of risk $\lambda^N(X_s)$ as

$$\lambda^N(X_s) = \gamma^N + \Gamma^N X_s,$$

where γ^N is an n-dimensional vector of constants and Γ^N is an $(n \times n)$-dimensional matrix of constants. This now allows us to define the process followed by the nominal pricing kernel

M_s^N as

$$dM_s^N = -r^N(X_s)\, M_s^N ds - \lambda^N(X_s)^\top M_s^N dZ_s.$$

We also define the price level process, Q_s, to be

$$d\log(Q_s) = r^e(X_s)\, ds + \sigma_q^\top dZ_s + \varsigma_q dW_s, \tag{2.2}$$

where σ_q is an n-dimensional vector of positive constants, ς_q is a positive constant and W_s is a standard $\mathbb{P}$-Brownian motion that is independent of Z_s. This shows that the price level process is driven by a stochastic mean growth factor (the instantaneous expected inflation rate), a common shock which also drives the latent factor vector (dZ_s) and an external shock (dW_s). The purpose of these two separate shocks is to capture unexpected movements in the price level that are due to yield curve movements, as well as to external forces.

Specifying the nominal and inflation dynamics in this way allows us now to find an expression for the real dynamics. We achieve this by deriving an expression for the real pricing kernel via

$$M_s^R = M_s^N Q_s,$$

where M_s^R is the real pricing kernel. Applying Itô's (product) formula to this expression yields[1],

$$\begin{aligned} dM_s^R &= d\left(M_s^N Q_s\right) \\ &= -r^R(X_s)\, M_s^R ds - \lambda^R(X_s)^\top M_s^R dZ_s + \varsigma_q M_s^R dW_s, \end{aligned}$$

where

$$r^R(X_s) := \eta_0^R + {\eta_1^R}^\top X_s$$

represents the real rate, with

$$\begin{aligned} \eta_0^R &:= \eta_0^N - \eta_0^e - \frac{1}{2}\left(\sigma_q^\top \sigma_q + \varsigma_q^2\right) + {\gamma^N}^\top \sigma_q \\ \eta_1^R &:= \eta_1^N - \eta_1^e + {\Gamma^N}^\top \sigma_q. \end{aligned}$$

The real prices of risk are defined by

$$\lambda^R(X_s) := \gamma^R + \Gamma^R X_s,$$

where

$$\begin{aligned} \gamma^R &:= \gamma^N - \sigma_q \\ \Gamma^R &:= \Gamma^N. \end{aligned}$$

[1] see Appendix A for the full derivation.

Here, we have seen expressions for the dynamics of the nominal rate, the real rate and instantaneous inflation. The next step is to derive expressions for ZCBs and expected inflation.

2.1.3 Bond Prices, Expected Inflation and the Inflation Risk Premium

The time t prices of real and nominal ZCBs with maturity T can be expressed as

$$P_{t,T}^N = \frac{\mathbb{E}_t\left[M_T^N\right]}{M_t^N}$$
$$P_{t,T}^R = \frac{\mathbb{E}_t\left[M_T^R\right]}{M_t^R}$$

or, equivalently,

$$P_{t,T}^k = \mathbb{E}_t^{\mathbb{Q}^k}\left[\exp\left\{-\int_t^T r^k\left(X_s\right)ds\right\}\right], k = N, R,$$

where $\mathbb{E}_t^{\mathbb{Q}^k}[\cdot]$ represents the expectation under an equivalent (to $\mathbb{P}$) martingale (or risk neutral) measure, $\mathbb{Q}^k$ (that is, the nominal or real risk-neutral measure). Note that here - and in the remainder of the thesis - we take $\mathbb{E}_t^{\cdot}[\cdot]$ to represent $\mathbb{E}^{\cdot}[\cdot|\mathcal{F}_t]$ where $(\mathcal{F}_t)_{t\geq 0}$ is a filtration defined on the probability space.

Defining the time to maturity of these bonds to be $\tau = T - t$, it can be shown (see Duffie and Kan (1996) [19]) that

$$P_{t,T}^k = \exp\left\{\alpha_\tau^k + {\beta_\tau^k}^\top X_t\right\}, k = N, R,$$

where α_τ^k and β_τ^k can be solved with the differential equations

$$\frac{d\alpha_\tau^k}{d\tau} = -\eta_0^k + {\beta_\tau^k}^\top\left(\mathcal{K}\theta - \Sigma\gamma^k\right) + \frac{1}{2}{\beta_\tau^k}^\top\Sigma\Sigma^\top\beta_\tau^k$$
$$\frac{d\beta_\tau^k}{d\tau} = -\eta_1^k - \left(\mathcal{K} + \Sigma\Gamma^k\right)^\top\beta_\tau^k$$

with initial conditions $\alpha_0^k = 0$ and $\beta_0^k = \mathbf{0}$, where $\mathbf{0}$ is an n-dimensional vector of zeros. This allows for the real and nominal yields of these bonds to be expressed as

$$\begin{aligned} y_{t,T}^k &= -\frac{1}{\tau}\alpha_\tau^k - \frac{1}{\tau}{\beta_\tau^k}^\top X_t \\ &=: a_\tau^k + {b_\tau^k}^\top X_t \end{aligned} \tag{2.3}$$

with a_τ^k and b_τ^k taking obvious forms.

Expected inflation over the period $[t, T]$ is given by

$$\frac{1}{\tau}\mathbb{E}_t\left[\log\left(\frac{Q_T}{Q_t}\right)\right] := i^e_{t,T}.$$

D'Amico, Kim and Wei (2008) [17] and Ho, Huang and Yildirim (2012) [28] both demonstrate[2] that this can be expressed as

$$i^e_{t,T} = a^e_\tau + {b^e_\tau}^\top X_t,$$

where

$$a^e_\tau = \eta^e_0 + \frac{1}{\tau}{\eta^e_1}^\top \int_0^\tau \left(\mathbf{I}_n - e^{-\mathcal{K}s}\right)\theta ds \tag{2.4}$$

$$b^e_\tau = \frac{1}{\tau}\int_0^\tau e^{-\mathcal{K}^\top s}\eta^e_1 ds \tag{2.5}$$

and $\mathbf{I}_n$ is the $n \times n$ identity matrix.

Finally, and most significantly, this leads us to an expression for the IRP. Recalling the extended Fisher equation (1.1) and substituting, we have that

$$\begin{aligned}\phi_{t,T} &= y^N_{t,T} - y^R_{t,T} - i^e_{t,T} \\ &= a^N_\tau - a^R_\tau - a^e_\tau + \left(b^N_\tau - b^R_\tau - b^e_\tau\right)^\top X_t.\end{aligned}$$

D'Amico, Kim and Wei (2008) [17] and Ho, Huang and Yildirim (2012) [28] also show that the IRP can be decomposed into a covariance term $\mathcal{C}_{t,T}$ and a "Jensen's effect" term $\mathcal{J}_{t,T}$ such that[3]

$$\phi_{t,T} = \mathcal{C}_{t,T} + \mathcal{J}_{t,T},$$

where

$$\begin{aligned}\mathcal{C}_{t,T} &= -\frac{1}{\tau}\log\left[1 + \frac{\mathbb{C}\text{ov}_t\left[\frac{M^R_T}{M^R_t}, \frac{Q_t}{Q_T}\right]}{\mathbb{E}_t\left[\frac{M^R_T}{M^R_t}\right]\mathbb{E}_t\left[\frac{Q_t}{Q_T}\right]}\right] \\ \mathcal{J}_{t,T} &= -\frac{1}{\tau}\underbrace{\left[\log\left(\mathbb{E}_t\left[\frac{Q_t}{Q_T}\right]\right) - \mathbb{E}_t\left[\log\left(\frac{Q_t}{Q_T}\right)\right]\right]}_{\circledast}.\end{aligned}$$

This expression illustrates that (in the current model) the IRP consists of two terms, one of which is driven by the covariance between the real pricing kernel and the price level process, and the other which reflects the concavity of the logarithmic function. Moreover, due to the concavity of the logarithmic function in the "Jensen's effect" term, $\circledast$ is always positive and so the sign of the IRP depends on the covariance between the real pricing kernel and the price level process.

[2] See Appendix A for further details.

[3] See Appendix A for further details.

2.2 Pricing Comparison

In this section, we briefly consider the implementation of the above pricing formulae for nominal and real bonds, as well as that for expected inflation. We do this in Matlab and compare the results obtained with the above analytical expressions, to those obtained with Monte Carlo simulation. Much of the reason for doing this is to test the implementation of the analytical pricing expressions by comparing them to the simulated values. This is important for the next section as we need to assess the exactness of our implementation of the model, before using these expressions in the calibration routines for the model.

The Monte Carlo scheme that we implement for the model is a simple Euler-Maruyama technique. It essentially follows the same discretisation scheme as seen in the state space representation of the model for the Kalman-filter (see equation (4.1) in the calibration chapter). The parameters that we choose here for the model are somewhat random, however they are chosen so that the IRP is (slightly) positive and that the yield term structures are upward sloping:

$$X_0 = \begin{bmatrix} -0.5 \\ -1 \\ -0.6 \end{bmatrix}, \mathcal{K} = \begin{bmatrix} 0.8 & 0 & 0 \\ 0 & 0.8 & 0 \\ 0 & 0 & 0.8 \end{bmatrix}, \theta = \begin{bmatrix} 0 \\ 0 \\ 0 \end{bmatrix}, \Sigma = \begin{bmatrix} 0.01 & 0 & 0 \\ 0.3 & 0.01 & 0 \\ 0.4 & 0.2 & 0.01 \end{bmatrix},$$

$$\eta_0^N = 0.04, \eta_1^N = \begin{bmatrix} 0.01 \\ 0.015 \\ 0.02 \end{bmatrix}, \gamma^N = \begin{bmatrix} 0.04 \\ 0.06 \\ 0 \end{bmatrix}, \Gamma^N = \begin{bmatrix} 0.05 & 0.02 & 0 \\ 0.04 & 0.05 & 0 \\ 0 & 0 & 0 \end{bmatrix},$$

$$\eta_0^e = 0.015, \eta_1^e = \begin{bmatrix} 0.01 \\ 0.01 \\ 0.005 \end{bmatrix}, \sigma_q = \begin{bmatrix} 0.02 \\ 0.01 \\ 0.08 \end{bmatrix}, \varsigma_q = 0.05.$$

The results of pricing with these parameters are illustrated in the following plot. As can be seen here, both pricing methods produce similar results. This makes us confident that our analytical pricing schemes are indeed working well.

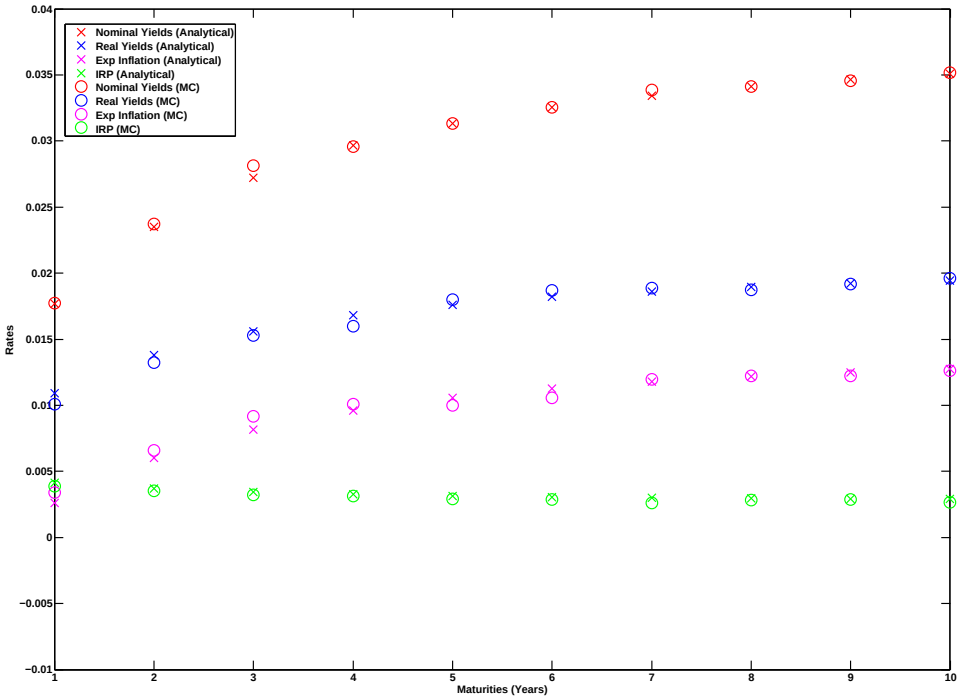

Figure 2.1 Comparison of analytical and Monte Carlo pricing in the Vasicek latent factor inflation model.

Chapter 3

Pricing Inflation-Indexed Derivatives

In this chapter, we will consider the pricing of inflation-indexed derivatives with the latent factor model presented in the previous chapter. We present the pricing of zero-coupon inflation-indexed swaps, year-on-year inflation-indexed swaps and inflation-indexed caps and floors.

3.1 Zero-Coupon Inflation-Indexed Swaps

Zero-coupon inflation-indexed swaps (ZCIISs) are the simplest of the swap contracts in the inflation market, but they are also the most actively traded inflation-indexed swaps (see Ho Huang and Yildirim (2012) [28]). As a result, they are useful instruments to use to obtain more information about inflation risks and expectations. In this section, we derive the fair swap rate for a ZCIIS.

A ZCIIS is a contract which allows the holder to swap a fixed payment for an floating (inflation-indexed) payment at some specified time in the future. Define the time s, $t \leq s \leq T$, value of a ZCIIS that starts at t and matures at T to be $V^{\text{ZCIIS}}(s,t,T)$. Moreover, define the fixed and floating leg values of the swap to be $V^{\text{ZCIIS}}_{\text{Fixed}}(s,t,T)$ and $V^{\text{ZCIIS}}_{\text{Floating}}(s,t,T)$ respectively. Thus,

$$V^{\text{ZCIIS}}(s,t,T) = \alpha\left[V^{\text{ZCIIS}}_{\text{Fixed}}(s,t,T) - V^{\text{ZCIIS}}_{\text{Floating}}(s,t,T)\right]$$

where $\alpha = +1$ for a fixed-for-floating swap and $\alpha = -1$ for a floating-for-fixed swap. At $s = t$, the fair value of this swap is 0, thus

$$V^{\text{ZCIIS}}_{\text{Fixed}}(t,t,T) = V^{\text{ZCIIS}}_{\text{Floating}}(t,t,T). \tag{3.1}$$

Now, the fixed leg of the swap pays $\mathbf{N}\left[\left(1+K_{t,T}^{\text{ZCIIS}}\right)^{\tau}-1\right]$ at time T, where $\tau = T-t$ as usual, $K_{t,T}^{\text{ZCIIS}}$ is the fair swap rate and $\mathbf{N}$ is the swap notional. Without loss of generality, we set $\mathbf{N}=1$ and ignore it for the remainder of this section. Therefore, the value of this leg at time t is

$$V_{\text{Fixed}}^{\text{ZCIIS}}(t,t,T) = P_{t,T}^{N}\left[\left(1+K_{t,T}^{\text{ZCIIS}}\right)^{\tau}-1\right] \tag{3.2}$$

Next, the floating leg of the contract pays $\left[\frac{Q_T}{Q_t}-1\right]$ at time T. Finding an expression for the value of this leg is more complicated than doing so for the fixed leg. Proceeding in a heuristic way,

$$V_{\text{Floating}}^{\text{ZCIIS}}(t,t,T) = \mathbb{E}_t^{\mathbb{Q}^N}\left[\exp\left\{-\int_t^T r_s^N ds\right\}\left(\frac{Q_T}{Q_t}-1\right)\right]$$

where $\mathbb{E}_t^{\mathbb{Q}^N}[\cdot]$ is the expectation under the nominal risk-neutral measure (given the filtration up to time t) and r_t^N is the nominal short rate. To simplify this expression, we follow the foreign exchange framework of Brigo and Mercurio (2006, pg. 45) [7] and perform a change of measure from the nominal risk-neutral measure, to the real risk-neutral measure. To this end, we specify the Radon-Nikodym derivative in the current setting as

$$\frac{d\mathbb{Q}^R}{d\mathbb{Q}^N} = \frac{Q_T A_{t,T}^R}{Q_t A_{t,T}^N},$$

where

$$A_{t,T}^k = \exp\left\{\int_t^T r_s^k ds\right\}, k = N, R$$

and r_s^R represents the real short rate. Brigo and Mercurio (2006) show that this process satisfies the properties of being a positive martingale with unitary expectation (under the nominal risk-neutral measure). Thus,

$$\begin{aligned}
V_{\text{Floating}}^{\text{ZCIIS}}(t,t,T) &= \mathbb{E}_t^{\mathbb{Q}^N}\left[\exp\left\{-\int_t^T r_s^N ds\right\}\frac{Q_T}{Q_t}\right] - \mathbb{E}_t^{\mathbb{Q}^N}\left[\exp\left\{-\int_t^T r_s^N ds\right\}\right] \\
&= \mathbb{E}_t^{\mathbb{Q}^N}\left[\frac{Q_T}{Q_t}\frac{A_{t,T}^R}{A_{t,T}^N}\exp\left\{-\int_t^T r_s^R ds\right\}\right] - P_{t,T}^N \\
&= \mathbb{E}_t^{\mathbb{Q}^R}\left[\exp\left\{-\int_t^T r_s^R ds\right\}\right] - P_{t,T}^N \\
&= P_{t,T}^R - P_{t,T}^N,
\end{aligned} \tag{3.3}$$

where $\mathbb{E}_t^{\mathbb{Q}^R}[\cdot]$ is the expectation under the real risk-neutral measure.

Finally, to obtain the fair swap rate for the ZCIIS, we substitute the expressions for (3.2) and (3.3) into (3.1). This yields

$$P_{t,T}^N \left[\left(1 + K_{t,T}^{\text{ZCIIS}}\right)^\tau - 1 \right] = P_{t,T}^R - P_{t,T}^N$$
$$K_{t,T}^{\text{ZCIIS}} = \left[\frac{P_{t,T}^R}{P_{t,T}^N} \right]^{\frac{1}{\tau}} - 1.$$

This is a model-free derivation for the fair swap rate of a ZCIIS and any model which produces nominal and real bond prices can be used to find the fair ZCIIS rate. In the case of the latent factor model presented in the previous chapter, we get that

$$\begin{aligned} K_{t,T}^{\text{ZCIIS}} &= \left[\frac{\exp\left\{ -\left(a_\tau^R + b_\tau^{R^\top} X_t \right) \tau \right\}}{\exp\left\{ -\left(a_\tau^N + b_\tau^{N^\top} X_t \right) \tau \right\}} \right]^{\frac{1}{\tau}} - 1 \\ &= \exp\left\{ \left(a_\tau^N - a_\tau^R \right) + \left(b_\tau^{N^\top} - b_\tau^{R^\top} \right) X_t \right\} - 1 \\ &=: \exp\left\{ a_\tau^{\text{ZCIIS}} + b_\tau^{\text{ZCIIS}^\top} X_t \right\} - 1, \end{aligned} \tag{3.4}$$

with a_τ^{ZCIIS} and b_τ^{ZCIIS} taking obvious forms. In this way, the model considered in the previous chapter can easily be used to calculate this quantity, as well as to value ZCIISs. The derivation above also gives us a useful tool for fitting the model to ZCIIS data, a technique which is used by Ho, Huang and Yildirim (2012) [28].

3.2 Year-on-Year Inflation-Indexed Swaps

Year-on-year inflation-indexed swaps (YYIISs) are generally less actively traded than ZCIISs and so we do not make use of them in the fitting of the model to inflation data[1]. Nonetheless, we give a brief overview of the pricing of these for completeness, as we will consider the pricing of caps and floors in the next section, and these are typically year-on-year products. For a more thorough overview of the pricing of YYIISs, see Brigo and Mercurio (2006) [7] and Ho, Huang and Yildirim (2012) [28]. We rely on these two sources for the demonstration below.

Assume that a YYIIS starts at time T_m and makes payments at $T_{m+1}, T_{m+2}, \ldots, T_M$, with $0 \leq T_m \leq \cdots \leq T_M$. Define $\Upsilon = \{T_m, \ldots, T_M\}$. In any given year interval, $[T_{i-1}, T_i]$, $i = m+1, \ldots, M$, the fixed leg payer of the swap pays $\mathbf{N} h_i K_\Upsilon^{\text{YYIIS}}$ - where $K_\Upsilon^{\text{YYIIS}}$ is the YYIIS rate and h_i represents the year fraction for the interval $[T_{i-1}, T_i]$ - to the fixed leg receiver at the end of the period and the floating (inflation-indexed) leg payer pays

[1] see Segreti (2008) [40] for an informative description of the inflation-indexed swap market.

$\mathbf{N}h_i\left[\frac{Q_{T_i}}{Q_{T_{i-1}}}-1\right]$ to the floating leg receiver at the end of the period. Again, we can set $\mathbf{N}$ to 1 without loss of generality. The time s $(0 \leq s \leq T_{i-1})$ value of the swap payments in this interval, defined as $V^{\text{YYIIS}}(s, T_{i-1}, T_i)$, is then given by (see Ho, Huang and Yildirim (2012) [28]):

$$\begin{aligned} V^{\text{YYIIS}}(s, T_{i-1}, T_i) &= \alpha\left\{h_i\left(1+K_{\Upsilon}^{\text{YYIIS}}\right)P_{s,T_i}^N - h_i\mathbb{E}_s^{\mathbb{Q}^N}\left[\exp\left(-\int_s^{T_{i-1}} r_u^N du\right)P_{T_{i-1},T_i}^R\right]\right\} \\ &= \alpha\left\{h_i\left(1+K_{\Upsilon}^{\text{YYIIS}}\right)P_{s,T_i}^N - h_i P_{s,T_{i-1}}^N C(T_{i-1}, T_i)\, D(T_{i-1}, T_i)\right\}, \end{aligned}$$

where

$$\begin{aligned} C(T_{i-1}, T_i) &= \exp\left\{-a_{T_i-T_{i-1}}^R \tau_i\right\} \\ D(T_{i-1}, T_i) &= \mathbb{E}_t^{\mathbb{Q}^{N,T_{i-1}}}\left[\exp\left\{-b_{\tau_i}^{R^\top} X_{T_{i-1}}\tau_i\right\}\right] \\ \tau_i &= T_i - T_{i-1} \end{aligned}$$

and $\mathbb{E}_s^{\mathbb{Q}^{N,T_{i-1}}}[\cdot]$ is the expectation under the nominal (T_{i-1}-)forward risk-neutral measure. The expression for $D(T_{i-1}, T_i)$ is computed explicitly in Ho, Huang and Yildirim (2012) [28].

The value of the swap at time t $(0 \leq t \leq T_m)$ over all payment periods, defined as $V^{\text{YYIIS}}(t, \Upsilon)$, is then given by:

$$\begin{aligned} V^{\text{YYIIS}}(t, \Upsilon) &= \sum_{i=m+1}^{M} V^{\text{YYIIS}}(t, T_{i-1}, T_i) \\ &= \alpha\left\{\sum_{i=m+1}^{M} h_i\left(1+K_{\Upsilon}^{\text{YYIIS}}\right)P_{t,T_i}^N - \sum_{i=m+1}^{M} h_i P_{t,T_{i-1}}^N C(T_{i-1}, T_i)\, D(T_{i-1}, T_i)\right\}. \end{aligned}$$

Setting this expression to 0 and solving for $K_{\Upsilon}^{\text{YYIIS}}$ gives the fair swap rate

$$K_{\Upsilon}^{\text{YYIIS}} = \frac{\sum_{i=m+1}^{M} h_i P_{t,T_{i-1}}^N C(T_{i-1}, T_i)\, D(T_{i-1}, T_i) - \sum_{i=m+1}^{M} h_i P_{t,T_i}^N}{\sum_{i=m+1}^{M} h_i P_{t,T_i}^N}.$$

3.3 Inflation-Indexed Caps and Floors

Within inflation-indexed option markets, inflation-indexed caps and floors are the most actively traded instruments. Typically, the most liquid of these are year-on-year instruments (see Segreti (2008) [40]). We consider the pricing problem for such instruments in this section.

In order to value inflation-indexed caps and floors (IICFs), it is first necessary to find expressions for the values of the composite caplets and floorlets (IICFlets). Once this has been achieved, the value of the cap or floor is simply the sum of a string of caplets or floorlets. We follow the specification of Ho, Huang and Yildirim (2012) [28] again in this section.

An inflation-indexed caplet (floorlet) is a call (put) option on the inflation rate over a pre-specified interval of time. As such, the payoff from a IICFlet over the period $[T_{i-1}, T_i]$ (where we define our time points in the same way as for the YYIISs) is given by

$$h_i \mathbf{N} \max\left\{\alpha\left(\frac{Q_{T_i}}{Q_{T_{i-1}}} - \left(1 + K^{\text{IICFlet}}_{T_{i-1},T_i}\right)\right), 0\right\}.$$

Here, $\alpha = 1$ for a caplet and -1 for a floorlet and $K^{\text{IICFlet}}_{T_{i-1},T_i}$ is the strike inflation rate for the IICFlet. Again, without loss of generality, we assume that $\mathbf{N} = 1$. Ho, Huang and Yildirim (2012) [28] show that the time s ($0 \leq s \leq T_{i-1}$) value of this payoff, defined as $V^{\text{IICFlet}}(s, T_{i-1}, T_i)$, is given by

$$\begin{aligned}
V^{\text{IICFlet}}(s, T_{i-1}, T_i) &= h_i \mathbb{E}_s^{\mathbb{Q}^N}\left[\exp\left(-\int_s^{T_i} r_u^N du\right) \max\left\{\alpha\left(\frac{Q_{T_i}}{Q_{T_{i-1}}} - \left(1 + K^{\text{IICFlet}}_{T_{i-1},T_i}\right)\right), 0\right\}\right] \\
&= h_i P^N_{s,T_i} \mathbb{E}_s^{\mathbb{Q}^{N,T_i}}\left[\max\left\{\alpha\left(\frac{Q_{T_i}}{Q_{T_{i-1}}} - \left(1 + K^{\text{IICFlet}}_{T_{i-1},T_i}\right)\right), 0\right\}\right] \\
&= \alpha h_i P^N_{s,T_i}\left[\mu_{\varphi_i}\mathcal{N}(\alpha d_i) - \left(1 + K^{\text{IICFlet}}_{T_{i-1},T_i}\right)\mathcal{N}\left(\alpha\left\{d_i - \sigma_{\log(\varphi_i)}\right\}\right)\right],
\end{aligned}$$

where $\mathbb{E}_s^{\mathbb{Q}^{N,T_i}}[\cdot]$ is the expectation under the nominal (T_i-)forward risk-neutral measure, $\mathcal{N}(\cdot)$ represents the cumulative distribution function of the normal distribution,

$$\begin{aligned}
\varphi_i &:= \frac{Q_{T_i}}{Q_{T_{i-1}}} \\
d_i &:= \frac{\log\left(\frac{\mu_{\varphi_i}}{K^{\text{IICFlet}}}\right) + \frac{1}{2}\sigma^2_{\log(\varphi_i)}}{\sigma_{\log(\varphi_i)}} \\
\mu_{\varphi_i} &:= \mathbb{E}_s^{\mathbb{Q}^{N,T_i}}[\varphi_i] \\
\sigma^2_{\log(\varphi_i)} &:= \mathbb{V}_s^{\mathbb{Q}^{N,T_i}}[\log(\varphi_i)]
\end{aligned}$$

and $\mathbb{V}_s^{\mathbb{Q}^{N,T_i}}[\cdot]$ is the variance under the nominal (T_i-)forward risk-neutral measure. We do not give the full derivation of this equation here, as Ho, Huang and Yildirim (2012) [28] do so in their paper. The full expressions for μ_{φ_i} and $\sigma^2_{\log(\varphi_i)}$ can also be found there; we do not give them here as they are rather cumbersome and do not add much to the intuition behind the cap (floor) pricing equation.

Once we have established pricing expressions for caplets and floorlets, it is simple to find expressions for caps and floors. As in the case with YYIISs, we assume that an IICF starts at T_m and makes payments at $T_{m+1}, T_{m+2}, \ldots, T_M$. The value of the IICF is then given by the sum of a series of IICFlets occurring at each of these payment dates. Thus, defining Υ as before and $V^{\text{IICF}}(t, \Upsilon)$ as the value of the IICF,

$$\begin{aligned} V^{\text{IICF}}(t, \Upsilon) &= \sum_{i=m+1}^{M} V^{\text{IICFlet}}(t, T_{i-1}, T_i) \\ &= \alpha \sum_{i=m+1}^{M} h_i P_{t,T_i}^{N} \left[\mu_{\varphi_i} \mathcal{N}(\alpha d_i) - \left(1 + K_{\Upsilon}^{\text{IICF}}\right) \mathcal{N}\left(\alpha \left\{ d_i - \sigma_{\log(\varphi_i)} \right\}\right) \right] \end{aligned} \tag{3.5}$$

for $0 \leq t \leq T_m$ and where $K_{\Upsilon}^{\text{IICF}}$ is the strike price of the IICF.

Chapter 4

Model Calibration with the Kalman-Filter

In this and the next chapter, we will consider the calibration of the latent factor model to market data. In the present chapter, we present theoretical results relating to the calibration techniques that we employ in this thesis. More specifically, we employ the Kalman-filter and the unscented Kalman-filter as methods to calculate the sample log-likelihood function and then maximise this to with respect to the model parameters to find those that best fit our data sets. The Kalman-filter can only be used on linear systems, while the unscented Kalman-filter can be used on non-linear systems too.

Below, we present the basic setup for the standard and unscented Kalman-filters as they apply to our situation, we outline how they can be used to estimate the sample log-likelihood function and we describe the optimisation framework that we follow to estimate the model parameters that best fit our data sets. For a more general description of the standard Kalman-filter, see Hamilton (1994) [25] and Harvey (1989) [26], and for the unscented Kalman-filter, see Wan and van der Merwe (2001) [45]. In the next chapter, we present actual calibration results.

4.1 Calibration with the Kalman-Filter

The Kalman-filter is a technique for optimally estimating the state of a system. It operates in a sequential manner, taking the most recent point in a time series of noisy observations and providing a linear projection of the system based on this. In this way, it produces a better estimate of the future state of the system than that based on a single observation. In particular, for Gaussian state processes, the Kalman-filter provides the exact likelihood

function for the forecast of the observable variables, thereby yielding a method for estimating the parameters of the state system (i.e. via maximum likelihood estimation). Importantly, the standard Kalman-filter can only be applied to linear systems. In the case of non-linear systems more advanced techniques are required.

D'Amico, Kim and Wei (2008) [17] and Ho, Huang and Yildirim (2012) [28] both give good overviews of the application of the Kalman-filter to the Vasicek latent factor model. We follow their specifications, as well as the more general one of Hamilton (1994) in this section.

The State-Space Representation

In presenting the Kalman-filter, we first introduce the state-space form of the Vasicek latent factor model. Discretising the Vasicek process given in Equation (2.1) with the Euler-Maruyama discretisation scheme gives

$$X_t = X_{t-\tau} + \mathcal{K}\left(\theta - X_{t-\tau}\right)\tau + \Sigma\epsilon_t,$$

for small, positive τ, $t \in [\tau, T]$, $T \geq \tau$ and where $\epsilon_t \sim \mathcal{N}\left(0, \tau\mathbf{I}_n\right)$. $\mathbf{I}_n$ is the $n \times n$ identity matrix. Discretising the price level process (2.2) similarly gives

$$\begin{aligned}\log\left(Q_t\right) &= \log\left(Q_{t-\tau}\right) + r^e\left(X_{t-\tau}\right)\tau + \sigma_q^\top\epsilon_t + \varsigma_q\varepsilon_t \\ &= \log\left(Q_{t-\tau}\right) + \left(\eta_0^e + \eta_1^{e\top}X_{t-\tau}\right)\tau + \sigma_q^\top\epsilon_t + \varsigma_q\varepsilon_t,\end{aligned}$$

where $\varepsilon_t \sim \mathcal{N}\left(0, \tau\right)$, independently of ϵ_t. Denoting $q_t = \log\left(Q_t\right)$ and the augmented state vector as $x_t = \left[q_t, X_t^\top\right]^\top$, we can write the discretised state-space form of the model as

$$x_t = C_\tau + D_\tau x_{t-\tau} + \epsilon_t^x,$$

where

$$C_\tau = \begin{bmatrix} \eta_0^e\tau \\ \mathcal{K}\theta\tau \end{bmatrix},\ D_\tau = \begin{bmatrix} 1 & \eta_1^{e\top}\tau \\ 0 & \mathbf{I}_n - \mathcal{K}\tau \end{bmatrix} \text{ and } \epsilon_t^x = \begin{bmatrix} \sigma_q^\top\epsilon_t + \varsigma_q\varepsilon_t \\ \Sigma\epsilon_t \end{bmatrix}. \tag{4.1}$$

In this way, ϵ_t^x follows a n-dimensional multivariate normal distribution, with mean 0 and covariance matrix

$$\Omega_t^\epsilon = \begin{bmatrix} \sigma_q^\top\sigma_q + \varsigma_q^2 & \left(\Sigma\sigma_q\right)^\top \\ \Sigma\sigma_q & \Sigma\Sigma^\top \end{bmatrix}\tau.$$

Next, we specify the observation equation that we will need to perform the calibration of the Vasicek latent factor model to market data. This can be specified generally as

$$y_t = A + Bx_t + \delta_t.$$

The vector y_t is a m-element vector containing all instrument prices, as well as the price level index, used in the estimation. m is therefore equivalent to the number of calibration instruments plus one for the price level process. In our case, these instruments will include (at least some of) the following: nominal and real zero-coupon yields, expected inflation data and ZCIIS rates. In full form, the vector would then appear as

$$y_t = \left[q_t, {y_t^N}^\top, {y_t^R}^\top, \log\left(1 + K_t^{\text{ZCIIS}}\right)^\top, {i_t^e}^\top\right]^\top,$$

where the individual elements of the above vector represent the log price process and vectors of nominal and real zero-coupon yields, ZCIIS swap rates and inflation expectations, all at time t. The matrices A and B are then given as

$$A = \begin{bmatrix} 0 \\ A^N \\ A^R \\ A^{\text{ZCIIS}} \\ A^e \end{bmatrix}, \; B = \begin{bmatrix} 1 & \mathbf{0} \\ \mathbf{0} & {B^N}^\top \\ \mathbf{0} & {B^R}^\top \\ \mathbf{0} & {B^{\text{ZCIIS}}}^\top \\ \mathbf{0} & {B^e}^\top \end{bmatrix},$$

where the A^k, $k = N, R, \text{ZCIIS}, e$, collect all the a_τ^k defined in Equations (2.3), (2.4) and (3.4) for each instrument in y_t and the B^k, $k = N, R, \text{ZCIIS}, e$, collect all the b_τ^k defined in Equations (2.3), (2.5) and (3.4) for each instrument in y_t. The length of the first dimension of matrices A and B will therefore equal the total number of instruments in the data set, plus one (for the price level process).

Finally, δ_t represents the measurement errors in our data. For simplicity, and as given in both D'Amico, Kim and Wei (2008) [17] and Ho, Huang and Yildirim (2012) [28], we choose them to be independently and identically normally distributed, with mean zero and $m \times m$ covariance matrix Ω_t^δ. δ_t is also assumed to be independent of ϵ_t^x.

Given that x_t is linear in $x_{t-\tau}$ and y_t is linear in x_t, the standard Kalman-filter can easily be applied to the model.

Initialising the Kalman-Filter

To initialise the Kalman-filter, we must first make assumptions about the initial state vector, as well as its covariance matrix. We label these initial guesses $\hat{x}_0$ and Q_0. We also introduce the notation $\hat{x}_{t|s}$ to denote the optimal estimator of x_t at time s ($0 \leq s \leq t$) and $Q_{t|s}$ to denote the corresponding covariance matrix at time s. Finally, we specify $\mathfrak{F}_s$ heuristically as the information process up to time s (from observing all instrument prices up to s).

The first step of the Kalman-filter routine is then to forecast x_t and Q_t from time 0 to time τ based on these initial guesses. We can predict x_τ with $\hat{x}_{\tau|0}$ where

$$\begin{aligned}\hat{x}_{\tau|0} &= \mathbb{E}\left[x_\tau|\mathfrak{F}_0\right] \\ &= C_\tau + D_\tau \hat{x}_0.\end{aligned}$$

The covariance matrix of relating to this forecast (or more specifically, the covariance matrix of the forecast error) is then given by

$$\begin{aligned}Q_{\tau|0} &= \mathbb{E}\left[\left(x_\tau - \hat{x}_{\tau|0}\right)\left(x_\tau - \hat{x}_{\tau|0}\right)^\top\right] \\ &= \mathbb{E}\left[\left(D_\tau\left\{x_0 - \hat{x}_0\right\} + \epsilon_\tau^x\right)\left(D_\tau\left\{x_0 - \hat{x}_0\right\} + \epsilon_\tau^x\right)^\top\right] \\ &= D_\tau Q_0 D_\tau^\top + \Omega_\tau^\epsilon.\end{aligned}$$

More generally, at any time t, given $\mathfrak{F}_{t-\tau}$, we can obtain the optimal estimator of the state vector as

$$\begin{aligned}\hat{x}_{t|t-\tau} &= \mathbb{E}\left[x_t|\mathfrak{F}_{t-\tau}\right] \\ &= C_\tau + D_\tau \hat{x}_{t-\tau|t-\tau}\end{aligned}$$

with corresponding covariance matrix

$$\begin{aligned}Q_{t|t-\tau} &= \mathbb{E}\left[\left(x_t - \hat{x}_{t|t-\tau}\right)\left(x_t - \hat{x}_{t|t-\tau}\right)^\top\right] \\ &= \mathbb{E}\left[\left(D_\tau\left\{x_{t-\tau} - \hat{x}_{t-\tau|t-\tau}\right\} + \epsilon_t^x\right)\left(D_\tau\left\{x_{t-\tau} - \hat{x}_{t-\tau|t-\tau}\right\} + \epsilon_t^x\right)^\top\right] \\ &= D_\tau Q_{t-\tau|t-\tau} D_\tau^\top + \Omega_t^\epsilon.\end{aligned}$$

Forecasting the Observation Equation

Given the forecasted values $\hat{x}_{\tau|0}$ and $Q_{\tau|0}$, the next step is forecast y_t and calculate the corresponding covariance matrix (the covariance matrix of the estimation error) at time τ. To this end, we define $\hat{y}_{t|s}$ to be the optimal estimator of y_t at time s and $V_{t|s}$ to denote the corresponding covariance matrix at time s. We can compute these values as

$$\begin{aligned}\hat{y}_{\tau|0} &= \mathbb{E}\left[y_\tau|\mathfrak{F}_0\right] \\ &= A + B\hat{x}_{\tau|0}\end{aligned}$$

and

$$\begin{aligned}V_{\tau|0} &= \mathbb{E}\left[\left(y_\tau - \hat{y}_{\tau|0}\right)\left(y_\tau - \hat{y}_{\tau|0}\right)^\top\right] \\ &= \mathbb{E}\left[\left(B\left\{x_\tau - \hat{x}_{\tau|0}\right\} + \delta_\tau\right)\left(B\left\{x_\tau - \hat{x}_{\tau|0}\right\} + \delta_\tau\right)^\top\right] \\ &= BQ_{\tau|0}B^\top + \Omega_\tau^\delta.\end{aligned}$$

More generally, at any time t, given $\mathfrak{F}_{t-\tau}$, we can express these as

$$\begin{aligned}\hat{y}_{t|t-\tau} &= \mathbb{E}\left[y_t|\mathfrak{F}_{t-\tau}\right] \\ &= A + B\hat{x}_{t|t-\tau}\end{aligned}$$

and

$$\begin{aligned}V_{t|t-\tau} &= \mathbb{E}\left[\left(y_t - \hat{y}_{t|t-\tau}\right)\left(y_t - \hat{y}_{t|t-\tau}\right)^\top\right] \\ &= \mathbb{E}\left[\left(B\left\{x_t - \hat{x}_{t|t-\tau}\right\} + \delta_t\right)\left(B\left\{x_t - \hat{x}_{t|t-\tau}\right\} + \delta_t\right)^\top\right] \\ &= BQ_{t|t-\tau}B^\top + \Omega_t^\delta.\end{aligned}$$

Updating the Forecast for the State Variables

The power of the Kalman-filter lies in this step. This is also where the normality of the state and the observation equations plays an important role. Updating the forecast for the state equation entails estimating $\hat{x}_{t|t}$ from $\hat{x}_{t|t-\tau}$ once we have observed y_t, the values of the instruments in our data set at time t. We proceed here for general time t, instead of considering the specific case at time τ.

To calculate $\hat{x}_{t|t}$, we need the joint distribution of (x_t, y_t). To this end, we calculate the covariance of the two forecast errors, $U_{t|t-\tau}$, as

$$\begin{aligned}U_{t|t-\tau} &= \mathbb{E}\left[\left(y_t - \hat{y}_{t|t-\tau}\right)\left(x_t - \hat{x}_{t|t-\tau}\right)^\top\right] \\ &= \mathbb{E}\left[\left(B\left\{x_t - \hat{x}_{t|t-\tau}\right\} + \delta_t\right)\left(x_t - \hat{x}_{t|t-\tau}\right)^\top\right] \\ &= BQ_{t|t-\tau}\end{aligned}$$

by the independence of δ_t and x_t. Therefore, the distribution of (x_t, y_t) is multivariate normal

$$\left[\begin{array}{c} x_t \\ y_t \end{array}\right] \Bigg| \mathfrak{F}_{t-\tau} \sim \mathcal{N}\left(\left[\begin{array}{c} \hat{x}_{t|t-\tau} \\ \hat{y}_{t|t-\tau} \end{array}\right], \left[\begin{array}{cc} Q_{t|t-\tau} & BQ_{t|t-\tau} \\ Q_{t|t-\tau}B^\top & BQ_{t|t-\tau}B^\top + \Omega_t^\delta \end{array}\right]\right)$$

and the conditional distribution of x_t given to observation y_t is then

$$x_t|\, y_t \sim \mathcal{N}\left(\hat{x}_{t|t}, Q_{t|t}\right),$$

where

$$\begin{aligned}\hat{x}_{t|t} &:= \hat{x}_{t|t-\tau} + K_{t|t-\tau}\left(y_t - \hat{y}_{t|t-\tau}\right) \\ Q_{t|t} &:= Q_{t|t-\tau} - K_{t|t-\tau}BQ_{t|t-\tau}\end{aligned}$$

and

$$K_{t|t-\tau} := Q_{t|t-\tau}B^\top V_{t|t-\tau}^{-1}$$

is defined as the Kalman-gain.

In this way, the Kalman-filter not only provides forecasts of the state and observation equations at each point in time, but also updates its forecast of the state equation once true values for the variables in the observation equation become available. The Kalman-filter is a recursive algorithm and the steps outlined above are repeated for each time step in the period $[0, T]$. The usefulness of this routine to our situation comes from the log-likelihood function that is a natural output from the Kalman-filter. We will discuss this in the last section of this chapter.

4.2 Calibration with the Unscented Kalman-Filter

For non-linear systems, the Kalman-filter calibration scheme is no longer effective. Instead, we must make use of a method which can handle non-linearities. This is particularly pertinent in the case where the observation equation (as defined in the section on the Kalman-filter) is the pricing equation for a cap or floor. Thus, we turn our attention now to the unscented Kalman-filter (UKF) as a means to handle calibration in non-linear systems. Wan and van der Werwe (2001) [45] give a thorough review of the UKF and we draw from their work here.

The UKF operates by choosing sample points that capture the mean and variance of the Gaussian random variable, both in a prior sense, and in a posterior sense (at least to second order accuracy) when the sample points are passed through the nonlinear system (see Wan and van der Werwe (2001)). The key to this is the unscented transform.

The Unscented Transform

Consider a M-dimensional random variable X, with mean μ_x and covariance Q_x. Moreover, assume that $Y = g(X)$, where $g(\cdot)$ is a nonlinear function. To approximate the mean and covariance of Y, we apply the unscented transform.

First, we calculate the sigma vectors $\mathbf{X}$:

$$\begin{aligned}
\mathbf{X}_0 &= \mu_x \\
\mathbf{X}_k &= \mu_x + \left(\sqrt{(M+\lambda)\,Q_x}\right)_k, \quad k = 1, \ldots, M \\
\mathbf{X}_k &= \mu_x - \left(\sqrt{(M+\lambda)\,Q_x}\right)_k, \quad k = M+1, \ldots, 2M,
\end{aligned}$$

where $\lambda = \nu^2 (M + \upsilon) - M$ is a scaling parameter for ν and υ constant and $\left(\sqrt{(M+\lambda)\,Q_x}\right)_k$ indicates the k^{th} column of the square root matrix (e.g. Cholesky decomposition).

To approximate the mean and covariance of Y, μ_y and Q_y respectively, we compute

$$\mathbf{Y}_k = g\left(\mathbf{X}_k\right), \quad k = 0, 1, \ldots, 2M$$

and

$$\begin{aligned}
\mu_y &\approx \sum_{k=0}^{2M} \omega_k^{(\mu)} \mathbf{Y}_k \\
Q_y &\approx \sum_{k=0}^{2M} \omega_k^{(Q)} \left(\mathbf{Y}_k - \mu_y\right)\left(\mathbf{Y}_k - \mu_y\right)^\top .
\end{aligned}$$

The weights ω_k are given by

$$\begin{aligned}
\omega_0^{(\mu)} &= \frac{\lambda}{M+\lambda} \\
\omega_0^{(Q)} &= \frac{\lambda}{M+\lambda} + 1 - \nu^2 + \varpi \\
\omega_k^{(\mu)} &= \omega_k^{(Q)} = \frac{1}{2\left(M+\lambda\right)},
\end{aligned}$$

where ϖ is a distribution dependent constant parameter. Given the setup for the unscented transform, we can now proceed with the actual UKF algorithm.

State and Observation Equations

The unscented Kalman-filter proceeds in a similar way to the standard Kalman-filter. We specify the state equation for out model as

$$\begin{aligned}
x_t &=: F\left(x_{t-\tau}\right) + \epsilon_t^x \\
&= C_\tau + D_\tau x_{t-\tau} + \epsilon_t^x .
\end{aligned}$$

Moreover, we specify the observation equation as

$$y_t =: G\left(x_t\right) + \delta_t,$$

where the function $G : \mathbb{R}^{n+1} \to \mathbb{R}^m$ is the pricing function for all the instruments in our data set, including inflation-indexed caps (pricing for the other instruments we have considered as well as the price level process are included in G through the same pricing equation that we presented them in the section on the standard Kalman-filter).

Initialising the Unscented Kalman-Filter

As before, we need to make assumptions about the initial state vector, as well as its covariance matrix. We again label these initial guesses $\hat{x}_0$ and Q_0, where

$$\begin{aligned}
\hat{x}_0 &= \mathbb{E}\left[x_0\right] \\
Q_0 &= \mathbb{E}\left[\left(x_0 - \hat{x}_0\right)\left(x_0 - \hat{x}_0\right)^\top\right].
\end{aligned}$$

We now specify the algorithm for the filter at some time t where $t \geq \tau$.

Calculating Sigma Points

We can calculate sigma points (vectors) at $t - \tau$ as described in the subsection on the unscented transform. Thus,

$$\mathbf{X}_{t-\tau|t-\tau} = \left[\hat{x}_{t-\tau|t-\tau} \quad \hat{x}_{t-\tau|t-\tau} + \sqrt{(M+\lambda)\, Q_{t-\tau|t-\tau}} \quad \hat{x}_{t-\tau|t-\tau} - \sqrt{(M+\lambda)\, Q_{t-\tau|t-\tau}}\right].$$

Updating the State Space Equation

Once we have calculated the sigma points, we update the state space equation through

$$\begin{aligned}
\widetilde{\mathbf{X}}_{t|t-\tau} &= F\left(\mathbf{X}_{t-\tau|t-\tau}\right) + \epsilon_t^x \\
\hat{x}_{t|t-\tau} &= \sum_{k=0}^{2M} \omega_k^{(\mu)} \widetilde{\mathbf{X}}_{k,t|t-\tau} \\
Q_{t|t-\tau} &= \sum_{k=0}^{2M} \omega_k^{(Q)} \left(\widetilde{\mathbf{X}}_{k,t|t-\tau} - \hat{x}_{t|t-\tau}\right)\left(\widetilde{\mathbf{X}}_{k,t|t-\tau} - \hat{x}_{t|t-\tau}\right)^\top + \Omega_t^\epsilon,
\end{aligned}$$

where $M = n + 1$ and Ω_t^ϵ is defined as before.

Augmenting Sigma Points

Before we give a forecast of the observation equation in the unscented Kalman-filter, we augment the sigma points as follows

$$\mathbf{X}_{t|t-\tau} = \left[\widetilde{\mathbf{X}}_{t|t-\tau} \quad \widetilde{\mathbf{X}}_{t|t-\tau} + \sqrt{(M+\lambda)\, \Omega_t^\epsilon} \quad \widetilde{\mathbf{X}}_{t|t-\tau} - \sqrt{(M+\lambda)\, \Omega_t^\epsilon}\right].$$

This allows for additional sigma points to be generated from the noise of the state equation. At this point, we need to update M to be $M = 2\,(n+1)$. Next, we forecast the observation equation.

Forecasting the Observation Equation

As with updating the state space equation, we can forecast the observation equation through

$$\begin{aligned}
\widetilde{\mathbf{Y}}_{t|t-\tau} &= G\left(\mathbf{X}_{t|t-\tau}\right) + \delta_t \\
\hat{y}_{t|t-\tau} &= \sum_{k=0}^{2M} \omega_k^{(\mu)} \widetilde{\mathbf{Y}}_{k,t|t-\tau} \\
V_{t|t-\tau} &= \sum_{k=0}^{2M} \omega_k^{(Q)} \left(\widetilde{\mathbf{Y}}_{k,t|t-\tau} - \hat{y}_{t|t-\tau}\right)\left(\widetilde{\mathbf{Y}}_{k,t|t-\tau} - \hat{y}_{t|t-\tau}\right)^\top + \Omega_t^\delta,
\end{aligned}$$

where Ω_t^δ is also defined as it was in the section on the standard Kalman-filter.

Updating the Forecast for the State Variables

Finally, we can update the forecast of the state variable. This is done through

$$\begin{aligned} U_{t|t-\tau} &= \sum_{k=0}^{2M} \omega_k^{(Q)} \left(\mathbf{X}_{k,t|t-\tau} - \hat{x}_{t|t-\tau}\right) \left(\widetilde{\mathbf{Y}}_{k,t|t-\tau} - \hat{y}_{t|t-\tau}\right)^\top \\ \hat{x}_{t|t} &= \hat{x}_{t|t-\tau} + K_{t|t-\tau}\left(y_t - \hat{y}_{t|t-\tau}\right) \\ Q_{t|t} &= Q_{t|t-\tau} - K_{t|t-\tau} V_{t|t-\tau} K_{t|t-\tau}^\top \end{aligned}$$

and

$$K_{t|t-\tau} = U_{t|t-\tau} V_{t|t-\tau}^{-1}$$

In this way, the unscented Kalman-filter operates in much the same way that the standard Kalman-filter does. The main point where the two routines differ is the unscented transform, which allows the unscented Kalman-filter to operate on non-linear systems. The Kalman-filter and the unscented Kalman-filter should produce identical results for linear systems. Again, the usefulness of this routine to our situation comes from the log-likelihood function that is a natural output from the unscented Kalman-filter.

4.3 Maximum Likelihood Estimation

The main use of these two filters in our case is as tools to estimate the parameters of the Vasicek latent factor model. This can be achieved by estimating the sample log-likelihood function of y_t through the filters. If we express the conditional density function of y_t as

$$\begin{aligned} f\left(y_t|\mathfrak{F}_{t-\tau}\right) = (2\pi)^{-\frac{m}{2}} \left|V_{t|t-\tau}\right|^{-\frac{1}{2}} \times \\ \exp\left\{-\frac{1}{2}\left(y_t - \hat{y}_{t|t-\tau}\right)^\top V_{t|t-\tau}^{-1}\left(y_t - \hat{y}_{t|t-\tau}\right)\right\}, \end{aligned}$$

where $f\left(y_t|\mathfrak{F}_{t-\tau}\right)$ is the conditional density function of y_t and m is the number of instruments, then the sample log-likelihood function is:

$$\sum_{t=\tau}^{T} \log \mathfrak{L}\left(y_t|\mathfrak{F}_{t-\tau}\right) := \sum_{t=\tau}^{T} \log\left(f\left(y_t|\mathfrak{F}_{t-\tau}\right)\right),$$

where $\log \mathfrak{L}\left(y_t|\mathfrak{F}_{t-\tau}\right)$ is the log-likelihood function.

To estimate the model parameters, we need a function that estimates the sample log-likelihood, and we maximise this function with respect to the parameter set. This entails running the standard or unscented Kalman-filter many times over in order to find the parameter set which satisfies this optimisation problem. We present this algorithm in a general way in the next section.

4.4 Calibration Routine

To estimate the parameters of the model, we proceed as follows:

1. Initialise the algorithm. Here, we select initial model parameters as well as the initial state vector $\hat{x}_0$ and its covariance matrix Q_0 in the Kalman-filter (standard or unscented).

2. Run the filter (standard or unscented Kalman-filter). The primary purpose of this is to calculate the sample log-likelihood $\sum_{t=\tau}^{T} \log \mathfrak{L}\left(y_t|\mathfrak{F}_{t-\tau}\right)$. We repeat this step numerous times (by running the function that computes the log-likelihood function from the filter through an optimiser), changing the parameters at each step, until we achieve convergence of the sample log-likelihood function to a maximum.

3. Run the filter one last time. Once the sample log-likelihood function has been maximised and the parameters that achieve this are known, we run the filter one last time with these parameters to compute statistics for our optimisation result.

In order to perform maximum likelihood estimation to determine the parameters of the model, we must make use of optimisation routines. We use two routines: the *fminsearch* optimiser in Matlab and a genetic algorithm. The *fminsearch* optimiser in Matlab is an unconstrained, non-linear optimisation method that makes use of the Nelder-Mead simplex algorithm. Genetic algorithms are global optimisation methods that use a form of natural evolution to search the parameter space and settle on an optimal point. The two routines can also be combined, where the genetic algorithm can be use to help find initial inputs for *fminsearch* and we do this on a number of occasions in our search for optimal parameters in the calibration chapter below. Appendix B presents these two algorithms in more detail. In particular, the genetic algorithm that we use was coded by the author, and the specifics of the type of genetic algorithm used can be seen in the appendix. We also present selected Matlab code to run the standard and unscented Kalman-filters in Appendix C.

Chapter 5

Model Calibration Results

In the previous chapter, we described the calibration techniques that we use to fit the latent factor model to market data. In the current chapter, we consider actual calibration results from fitting the model to various data sets, as well as what these results tell us about the IRP.

First, we present principal component analyses of our data sets to analyse the number of factors needed to describe the variations in the data. Thereafter, we present the parametrisation that we use in calibrating the model to the data. Next, we present the actual calibration results when fitting the latent factor model to four different data sets. Finally, we present the implications of our results for the IRP in the European ZCIIS case.

The first data set is a synthetic time series of ZCIIS rates and price levels created using Monte Carlo simulation, and the second is the data set specified in the paper by Ho, Huang and Yildirim (2012) [28]. The reason for using these first two data sets is to check the reliability of the routines that we have implemented, as well as to benchmark our results. The third data set that we use consists mainly of European ZCIIS rates, and the fourth, mainly of European inflation-indexed cap (IIC) prices.

5.1 Data Sets and Principal Component Analyses

In this chapter on the calibration of the Vasicek latent factor model to inflation data, we consider three real world data sets. The first of these comprises nominal bond yields[1], TIPS yields, ZCIIS rates and professional inflation forecasts for US markets. The second data set comprises European ZCIIS rates, nominal bond yields and professional inflation forecasts.

[1]Note, that when we refer to bond yields, we always mean zero-coupon yields, unless otherwise specified.

PC	Nominal Bonds, Real Bonds and ZCIISs
1	0.9352
2	0.9720
3	0.9930
4	0.9967

Table 5.1 Table showing the variance explained by principle components in the US data set.

PC	ZCIISs	ZCIISs and Nominal Bonds
1	0.8658	0.8203
2	0.9849	0.9254
3	0.9954	0.9851
4	0.9982	0.9958

Table 5.2 Table showing the variance explained by principle components in the European ZCIIS data set.

PC	IICs	IICs and Nominal Bonds
1	0.9187	0.9187
2	0.9625	0.9625
3	0.9856	0.9856
4	0.9967	0.9967

Table 5.3 Table showing the variance explained by principle components in the European IIC data set.

Finally, the third comprises IIC prices, as well as nominal bond yields and professional inflation forecasts. The details of these are given in the sections relating to the calibration of the model to the respective data sets.

Previously, we mentioned that we would consider the actual data sets used for our calibration purposes to decide on the number of factors in the model. To this end, we perform principal component analyses (PCAs) on each data set to assess how many factors are needed to explain the variance in each. The results of these are presented in Tables 5.1, 5.2 and 5.3.

Table 5.1 shows how much of the variance in the US data set is explained by the first four principal components (PCs). We have considered all the instruments in the data set in attaining the results shown in this table. From this, we can see that more than 99% of the variance in the data set is explained by the first three PCs. Tables 5.2 and 5.3 give the same analysis for the two European data sets, containing ZCIIS rate data and IIC price data

respectively. Here, we have performed two PCAs for each data set. In the first instance, we perform the PCA on only the primary instruments in each data set, namely the ZCIISs and the IICs. In the second, we perform the PCA on each complete data set. In all instances, we can see that at least 98% of the variance in both data sets is explained by the first three PCs. These results correspond to the general assessment that three factors - a level, slope and curvature factor - drive the yield curve, as reported in D'Amico, Kim and Wei (2008) [17], Litterman and Scheinkman (1991) [34] and Piazzesi (2010) [36]. Consequently, the results of the PCAs appear to make economic sense.

From these results, we determine that a three factor model would be the best suited the instrument prices (or yields) in each of the data sets. Whether we consider the individual instruments (ZCIISs or IICs) separately, or all the instruments in each data set, these results suggest that most of the variance these can be explained by three latent factors. As such, we make use of the three factor version of the Vasicek latent factor model in all of our calibration procedures in the following sections. In the next section, we present the parameter setup that we make use of for the three factor model.

5.2 Calibration Parameters

In running our calibration routines, we calibrate the Vasicek latent factor model to market data by maximising the Kalman-filter (or unscented Kalman-filter) implied log-likelihood function with respect to the parameters

$$\mathcal{K} = \begin{bmatrix} \kappa_{1,1} & 0 & 0 \\ 0 & \kappa_{2,2} & 0 \\ 0 & 0 & \kappa_{3,3} \end{bmatrix}, \theta = \begin{bmatrix} 0 \\ 0 \\ 0 \end{bmatrix}, \Sigma = \begin{bmatrix} 0.01 & 0 & 0 \\ \sigma_{2,1} & 0.01 & 0 \\ \sigma_{3,1} & \sigma_{3,2} & 0.01 \end{bmatrix},$$

$$\eta_0^N, \eta_1^N = \begin{bmatrix} \eta_{1,1}^N \\ \eta_{1,2}^N \\ \eta_{1,3}^N \end{bmatrix}, \gamma^N = \begin{bmatrix} \gamma_1^N \\ \gamma_2^N \\ \gamma_3^N \end{bmatrix}, \Gamma^N = \begin{bmatrix} \Gamma_{1,1}^N & \Gamma_{1,2}^N & \Gamma_{1,3}^N \\ \Gamma_{2,1}^N & \Gamma_{2,2}^N & \Gamma_{2,3}^N \\ \Gamma_{3,1}^N & \Gamma_{3,2}^N & \Gamma_{3,3}^N \end{bmatrix},$$

$$\eta_0^e, \eta_1^e = \begin{bmatrix} \eta_{1,1}^e \\ \eta_{1,2}^e \\ \eta_{1,3}^e \end{bmatrix}, \sigma_q = \begin{bmatrix} \sigma_{q,1} \\ \sigma_{q,2} \\ \sigma_{q,3} \end{bmatrix}, \varsigma_q.$$

In doing so, we constrain the last four parameters, $\sigma_{q,1}$, $\sigma_{q,2}$, $\sigma_{q,3}$ and ς_q, to be non-negative.

It is also important to choose a good starting point for the augmented state vector x_0. This is a tricky task since X_t is a latent vector process and cannot be inferred automatically

from market data. One possible way to avoid this problem is to include x_0 in the calibration setup above. However, this can add instability to the calibration routine. Instead, we use the initial value of the price level process to estimate q_0 and we estimate X_0 by running the calibration routine once with X_0 included in the set of calibration parameters and inferring from the calibrated state variable process the appropriate stating point for the process. To obtain our final results, we run the calibration routine again, fixing x_0 to these values.

The above parameter specification is the same as that given in D'Amico, Kim and Wei (2008) [17] and justifications for their choice are given there. In doing so, they draw from the well known papers by Dai and Singleton (2000) [16] and Duffie and Kan (1996) [19], which explore affine term structure models. The canonical representation of the three factor affine term structure model $\mathbb{A}_0(3)$ in Dai and Singleton (2000), for example, has a very similar specification to the one given above. Particularly, $\theta = 0$ is chosen there to enforce economic interpretation for the model parameters η_0^N, η_0^R and η_0^e. The chosen structure of Σ is also similar in their paper and is used to enforce dependencies between the three driving Brownian motions in the Vasicek latent factor model. The chosen structure of $\mathcal{K}$ is intended to simplify the correlation structure between the model factors. In this way, D'Amico, Kim and Wei (2008) [17] explain that they impose parameter restrictions on the model so as to achieve parameter identification, while preserving a flexible correlation structure. Furthermore, this specification reduces the dimensionality of the calibration problem, therefore simplifying our task in this chapter. For these reasons, we also choose to use this structure.

For the sake of completeness, we also performed the calibration procedures below with $\mathcal{K}$ and θ non-sparse and where the elements on the diagonal of Σ are not preset. We do not report these results here, as they are not an improvement on the ones given in the thesis. For the interested reader, they are available upon request, however.

5.3 Calibration to Synthetic Data

Our first set of calibration results comes from calibrating the Vasicek latent factor model to synthetic data. In order to do this, we use Monte Carlo simulation to generate ZCIIS rate data as well as data for the price level process and then calibrate the model to these data using the Kalman-filter and maximum likelihood estimation. The synthetic data are generated by simulating 50 paths for 12 ZCIISs (with maturities at yearly intervals from 1 to 12 years) and one price level process. The instrument values are simulated at weekly intervals over a 3 year period. To perform this calibration, we use the Matlab optimisation

routine *fminsearch*, as well as initial staring points given by the actual parameter values used to generate the synthetic data. Given this setup, the model should fit the data well and this is the case. Table 5.4 gives the results of the calibration.

Comparison of actual and fitted parameters								
	Actual	**Fitted**		**Actual**	**Fitted**		**Actual**	**Fitted**
$X_0^{(1)}$	-0.5000	-0.5000	$\eta_{1,2}^N$	0.0150	0.0149 (0.0004)	$\Gamma_{3,1}^N$	0.0000	-0.0158 (0.0010)
$X_0^{(2)}$	-1.0000	-1.0000	$\eta_{1,3}^N$	0.0200	0.0201 (0.0003)	$\Gamma_{3,2}^N$	0.0000	-0.0004 (0.0006)
$X_0^{(3)}$	-0.6000	-0.6000	γ_1^N	0.0400	0.0400 (0.0001)	$\Gamma_{3,3}^N$	0.0000	-0.0006 (0.0005)
$\kappa_{1,1}$	0.8000	0.7981 (0.0078)	γ_2^N	0.0600	0.0602 (0.0007)	η_0^e	0.0150	0.0150 (0.0000)
$\kappa_{2,2}$	0.8000	0.7911 (0.0010)	γ_3^N	0.0000	0.0000 (0.0004)	$\eta_{1,1}^e$	0.0100	0.0110 (0.0002)
$\kappa_{3,3}$	0.8000	0.8010 (0.0013)	$\Gamma_{1,1}^N$	0.0500	0.0682 (0.0027)	$\eta_{1,2}^e$	0.0100	0.0099 (0.0003)
$\sigma_{2,1}$	0.3000	0.2993 (0.0154)	$\Gamma_{1,2}^N$	0.0200	0.0215 (0.0006)	$\eta_{1,3}^e$	0.0050	0.0049 (0.0003)
$\sigma_{3,1}$	0.4000	0.4003 (0.0168)	$\Gamma_{1,3}^N$	0.0000	0.0017 (0.0005)	$\sigma_{q,1}$	0.0200	0.0200 (0.0003)
$\sigma_{3,2}$	0.2000	0.1992 (0.0004)	$\Gamma_{2,1}^N$	0.0400	0.0635 (0.0021)	$\sigma_{q,2}$	0.0100	0.0100 (0.0001)
η_0^N	0.0400	0.0828 (0.0466)	$\Gamma_{2,2}^N$	0.0500	0.0474 (0.0018)	$\sigma_{q,3}$	0.0800	0.0800 (0.0002)
$\eta_{1,1}^N$	0.0100	0.0116 (0.0002)	$\Gamma_{2,3}^N$	0.0000	0.0050 (0.0002)	ς_q	0.0500	0.0500 (0.0002)

Error Statistics	
MSE:	2.6579×10^{-7}
Log-likelihood:	2.3864×10^4

Table 5.4 Table of results for the calibration of the Vasicek latent factor model to synthetic data using the Kalman-filter. The table compares the actual model parameters to the fitted model parameters and gives statistics on the mean-squared error (MSE) and the final log-likelihood estimator. Standard errors are reported in parentheses.

The table indicates that the fit to the synthetic data is indeed good. This is shown particularly by the value of the mean-square error (MSE) statistic. Moreover, we can see that most of the fitted parameters are close to their true values (as indicated by the standard errors). This is not the case for all of the parameters, but due to the complexity and high-

dimensionality of the calibration problem, this can be expected. The results are promising as they appear to validate our calibration techniques. Figure 5.1 gives further evidence of the quality of the fit. Here, we can see that the swap rates and the price level process implied from the fitted parameters are very close to their original values. This shows that calibration procedure was able to capture most of the points in the data set.

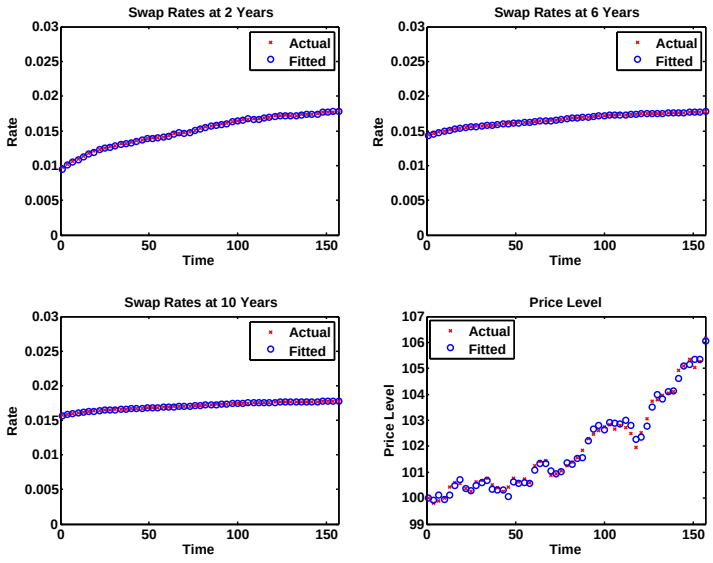

Figure 5.1 Illustration of the quality of the Kalman-filter calibration of the Vasicek latent factor model to synthetic ZCIIS and price level data. In this plot, we have produced the swap rates for 2, 6 and 10 year swaps, as well as the price level process.

We can also evaluate the model-implied 10 year historical IRP in comparison to the "actual" historical 10 year IRP. This is illustrated in Figure 5.2. We obtain the "actual" and the model-implied historical 10 year IRP by deducing them from the Vasicek latent factor model with the actual and the calibrated parameters (as given in Table 5.4) respectively. Again, we can see that the fitted values are close to the actual values.

In general, the Kalman-filter calibration scheme results in a good fit of the Vasicek latent factor model to the synthetically generated data set. It is able to reproduce the (synthetically generated) instrument prices accurately and provide good results for the IRP. This is promising and indicates that the procedure should produce similarly good results for real data sets. We consider the first of these next.

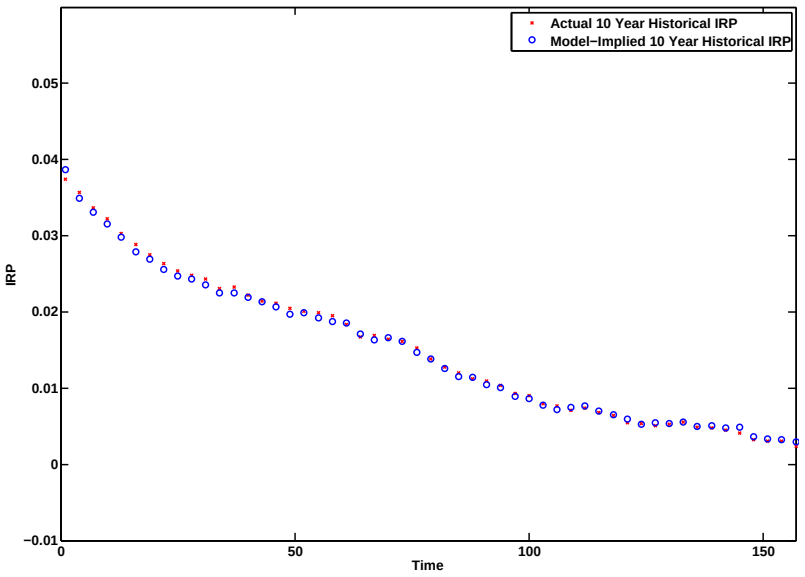

Figure 5.2 Comparison of the actual 10 year historical IRP to that implied by calibrating the Vasicek latent factor model to synthetic data using the Kalman-filter.

5.4 Calibration to US Data

The next set of calibration results that we present are for a US data set. We obtain the data set from the sources given in the paper by Ho, Huang and Yildirim (2012) [28] and the specifics of the data set can be observed in their paper. More generally, however, the data set contains weekly data consisting of US Treasury yields, TIPS yields, the CPI level, SPF inflation forecast data and ZCIIS rates, all taken from the period July 2004 to September 2010. The maturities of the nominal Treasury yields in the data set range from 3 months to 15 years, the maturities of the TIPS range from 10 years to 15 years, the maturities of the ZCIISs range from 10 years to 30 years and the SPF forecasts are for 1 and 10 year horizons.

To start, we produce a plot where we illustrate the 10 year nominal yield, real yield, expected inflation and IRP based on a model-free decomposition. This decomposition is given by Equation (1.2), where the 10 year nominal rate is taken to be the 10 year zero-coupon nominal Treasury yield, the 10 year expected inflation rate is taken from the 10 year SPF forecast and the 10 year IRP is found by subtracting the 10 year SPF forecast from the logarithm of one plus the 10 year ZCIIS rate. The 10 year real rate is then taken as the difference between the 10 year nominal rate and the sum of the 10 year expected

inflation rate and the 10 year IRP. The plot of these is given in Figure 5.3.

Figure 5.3 This plot shows the model-free decomposition of 10 year nominal yields into real yields, expected inflation and the IRP. The various rates in the plot are deduced from Treasury yields, ZCIIS rates and inflation forecasts in the US data set.

Ho, Huang and Yildirim (2012) [28] present a similar plot in their paper, although theirs indicates that the level of the 10 year expected inflation rate oscillates around 1%, while we find that it oscillates around 2.5%. In the plot, two things stand out. Firstly, the line for the expected inflation rate is very flat. This is because the (mean point) forecasts from the SPF for inflation tend to be quite constant. This is perhaps not very realistic, but it is important to include some forecasts in the calibration to add stability to the scheme (see D'Amico, Kim and Wei (2008) [17] and Ho, Huang and Yildirim (2012) [28]). D'Amico, Kim and Wei (2008) [17] make use of Treasury bill forecasts in their estimation instead of inflation forecasts to avoid external impacts on their measure of expected inflation. The second point of interest is the IRP. We can see that the IRP oscillates in a narrow band between 0% and 1%, except during the crisis, when it drops as low as -1%. This indicates that it is feasible for the IRP to become negative (meaning that nominal bond holders are willing to pay an inflation premium to hold bonds). It also seems to suggest that the IRP tends to be quite small. That the IRP can become negative might seem counterintuitive, though the occurrence of this during the crisis could be due to high demand for nominal

bonds at the time. It could also be a result of deflation concerns or liquidity differences between the two types of bonds. Following this, we calibrate the Vasicek latent factor model to the data set and obtain the results given in Table 5.5.

Table of fitted parameters					
$X_0^{(1)}$	0.2000	$\eta_{1,2}^N$	-0.0004	$\Gamma_{3,1}^N$	0.0985
			(0.0016)		(0.0804)
$X_0^{(2)}$	-0.057	$\eta_{1,3}^N$	0.2133	$\Gamma_{3,2}^N$	0.0893
			(0.0134)		(0.0653)
$X_0^{(3)}$	-0.038	γ_1^N	-0.4185	$\Gamma_{3,3}^N$	0.0002
			(0.0929)		(0.0060)
$\kappa_{1,1}$	0.0193	γ_2^N	-0.3874	η_0^e	0.0202
	(0.0035)		(0.0418)		(0.0007)
$\kappa_{2,2}$	-0.0452	γ_3^N	-0.0103	$\eta_{1,1}^e$	0.0429
	(0.0077)		(0.0096)		(0.0095)
$\kappa_{3,3}$	0.3354	$\Gamma_{1,1}^N$	0.0152	$\eta_{1,2}^e$	-0.0430
	(0.0190)		(0.0105)		(0.0078)
$\sigma_{2,1}$	-0.0003	$\Gamma_{1,2}^N$	-0.8243	$\eta_{1,3}^e$	0.0139
	(0.0019)		(0.0965)		(0.0013)
$\sigma_{3,1}$	0.0073	$\Gamma_{1,3}^N$	-0.0296	$\sigma_{q,1}$	0.1489
	(0.0029)		(0.0328)		(0.0039)
$\sigma_{3,2}$	-0.0581	$\Gamma_{2,1}^N$	1.9690	$\sigma_{q,2}$	0.1714
	(0.0031)		(0.2300)		(0.0112)
η_0^N	0.0864	$\Gamma_{2,2}^N$	0.0483	$\sigma_{q,3}$	0.2260
	(0.0084)		(0.0085)		(0.0161)
$\eta_{1,1}^N$	-0.1066	$\Gamma_{2,3}^N$	0.0000	ς_q	0.0761
	(0.0173)		(0.0149)		(0.0184)

Error Statistics	
MSE:	2.5723×10^{-5}
Log-likelihood:	2.5043×10^{4}

Table 5.5 Table of results for the calibration of the Vasicek latent factor model to US data using the Kalman-filter. The table shows the fitted parameters from the calibration of the model to the data. It also gives statistics on the mean-squared error (MSE) and the final log-likelihood estimator. Standard errors are reported in parentheses.

To perform this calibration, we made use of both the genetic algorithm and the *fminsearch* algorithm in Matlab. The genetic algorithm was particularly useful as a first attempt to calibrate the model to the data. It allowed us to search the parameter space broadly and identified regions where a global solution should lie. After this, we could make use of the *fminsearch* algorithm to find an optimum more precisely. We do not have parameters to

compare these fitted ones against, as none are given in the Ho, Huang and Yildirim (2012) [28] paper. However, looking at the error statistics, we can see that the MSE value is quite low, indicating that the calibrated instrument prices are quite close to the actual instrument prices. Figure 5.4 illustrates the decomposition of the 10 year model-implied nominal yields obtained from the calibration of the model to the data set. Again, Ho, Huang and Yildirim (2012) [28] present a similar plot in their paper.

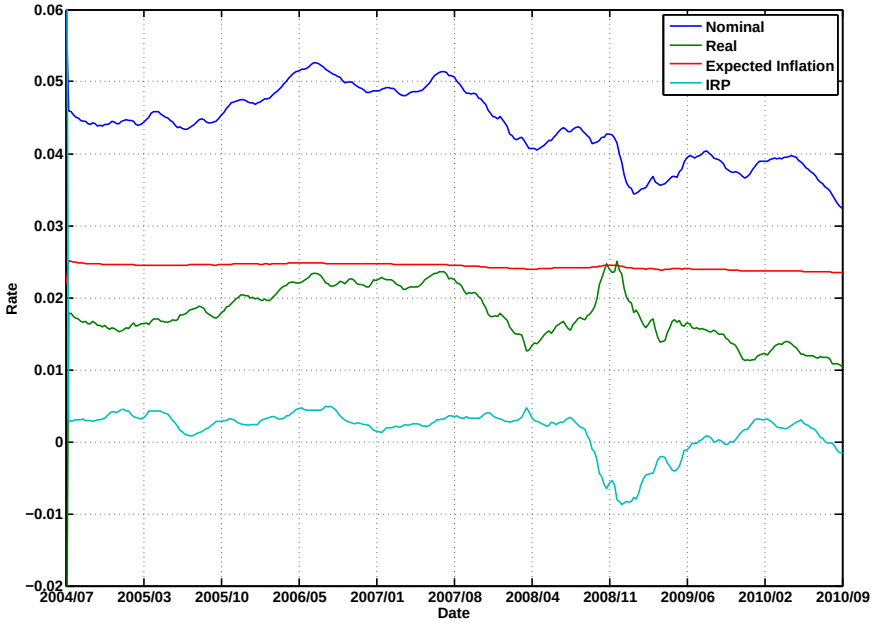

Figure 5.4 This plot shows the model-implied decomposition of 10 year nominal yields into real yields, expected inflation and the IRP (in the US case).

There are two comparisons that can be made here. Firstly, we can compare the model-implied decomposition of 10 year nominal yields to the model-free decomposition thereof. Here, we observe that the model-implied rates are quite similar to the model-free rates. The model-implied rates are slightly smoother than the model-free ones, but the general levels and movements of each of the rates have been well captured by the estimation. It can be expected that the Kalman-filter estimation technique will produced slightly smoothed results, since the Kalman-filter operates by providing a projection of the system from the expectation of its current state. Moreover, the paths followed by the rates in the two plots can be expected to be slightly different, since the model-free estimate takes only some of the instruments in the data set into account, while the model-implied estimate considers the whole data set. Nonetheless, the similarities between the two plots give us confidence that we have achieved a good fit to the market data here.

Secondly, we can compare our plot to that of Ho, Huang and Yildirim (2012, pg. 48) [28]. Here, it can be seen that the real and nominal yield lines in our plot are reasonably similar to those in theirs (at least in terms of the levels of the two lines). However, some more noticeable differences are observable when comparing the IRP and expected inflation lines in the two plots. The level of the IRP line in our plot is, for the most part, quite similar that in their plot. The first half of the line also follows the shape of that in their plot quite closely. The second half of the line in our plot, however, experiences a rapid drop to -1% before recovering to a level slightly above 0% and ending slightly below 0%. In their plot, the same portion of the IRP line experiences only a slight drop below 0% before recovering and ending at a level close to 1%. The level of the expected inflation line in our plot is also quite similar to that in theirs. It is a lot flatter however, whereas the line in their plot moves below the 2% level in the last quarter of the total time period.

Thus, there are some differences between our results and those of Ho, Huang and Yildirim (2012) [28]. These seem to stem mainly from the differences in the 10 year historical expected inflation rate. Given its impact on the IRP, an expected inflation line in our plot more closely resembling that in theirs would produce an IRP line in our plot which was more similar to that in theirs. Considering the level of the expected inflation line in Figure 5.3, however, we are still confident that our calibration of the model to the data has been able to capture the market prices well. These results give us confidence that the calibration procedures that we have implemented are performing as expected.

We now turn our attention to data sets not yet used in the literature. As noted by Ho, Huang and Yildirim (2012) [28], given the fact that many inflation-indexed derivatives are functions of nominal and real bonds, it is possible to calibrate the Vasicek latent factor model to these instruments in order to obtain estimates of the IRP. As such, we will now consider a data set comprised mainly of European ZCIIS rates.

5.5 Calibration to European ZCIIS Data

The previous calibration results to synthetic data and the data set specified in Ho, Huang and Yildirim (2012) [28] give us a sense of the performance of the Kalman-filter calibration scheme that we have implemented. So far, we can see that the scheme captures general market levels and movements quite well. In this section, we calibrate the Vasicek latent factor model to a data set consisting mainly of European ZCIIS rates. In order to add stability to the calibration, we also include nominal bond yields and inflation survey forecasts in our data set. As such, our data set comprises 1, 2, 3, 4, 5, 6, 7, 8, 9, 10, 12, and 15

year swap rates at weekly intervals from 10 September 2004 to 24 May 2013. These rates are obtained from Bloomberg, under the symbol ⟨EUSWIxx Index⟩. The nominal yields that we use are obtained from the website of the European Central Bank (ECB) [42], where we consider spot rates linked to AAA-rated European government bonds at 1, 5, 10 and 15 year maturities. The inflation survey data are used to add stability to our estimation of expected inflation. These we obtain from the ECB's Survey of Professional Forecasters (SPF; also found on the website of the ECB) mean point inflation forecasts for 1 and 5 years. We also make use of price level data for the same period in our calibration. For this, we consider the Harmonised Index of Consumer Prices excluding tobacco (HICPxt) as it is the same index to which the swaps and the SPF forecasts are referenced. Since the price level data are only released on a month-by-month basis, we interpolate linearly between each data point to obtain weekly data. We do this while taking the 3 month lag on the price index into account.

An important consideration when estimating break-even inflation rates (or the IRP) from inflation-indexed securities is the effect of inflation seasonality. We did not mention this issue in the previous subsection because it is not considered in Ho, Huang and Yildirim (2012) [28] and we were attempting to replicate their approach. Ejsing, Garcia and Werner (2007) [20] address the issue of inflation seasonality in the Eurozone thoroughly, and we draw from their paper here. Due to various reasons, such as periodic patterns in sales of consumer goods and seasonal fluctuations in the price and demand for various consumer items, such as food products, inflation exhibits seasonal trends. These trends naturally have an impact on the prices of inflation-indexed securities that make non-yearly payments, or when annually paying instruments are valued in between payments. Since they are not random, they should be factored out of the estimation of break-even inflation rates to avoid misinterpretations of the changes in the level of consumer prices. As such, seasonal adjustment factors should be calculated at each month of the year, and consumer price levels should be adjusted by these factors to account for seasonal changes. Ejsing, Garcia and Werner (2007) show how to do this in the case of inflation-indexed bonds. In our case, the only inflation-indexed products that we consider are ZCIISs. The payment dates for the ZCIISs are at multiples of one year and we do not consider any swaps which are already in existence. As such, seasonality effects do not impact the extraction of the IRP in our case and so we do not need to adjust the security prices with seasonality factors.

The results for the calibration of the model to this data set are given in Table 5.6. In obtaining these results, we have made use of the genetic algorithm as a means to help find the initial points for the *fminsearch* algorithm in much the same way as we did for the

Table of fitted parameters					
$X_0^{(1)}$	0.0600	$\eta_{1,2}^N$	-0.7777	$\Gamma_{3,1}^N$	-0.2198
			(0.1041)		(0.1082)
$X_0^{(2)}$	-0.0430	$\eta_{1,3}^N$	-0.5314	$\Gamma_{3,2}^N$	-0.0060
			(0.0237)		(0.0092)
$X_0^{(3)}$	0.0090	γ_1^N	-0.2224	$\Gamma_{3,3}^N$	-0.0061
			(0.0098)		(0.0259)
$\kappa_{1,1}$	0.0089	γ_2^N	0.0323	η_0^e	0.0218
	(0.0069)		(0.0187)		(0.0012)
$\kappa_{2,2}$	-0.0514	γ_3^N	0.0116	$\eta_{1,1}^e$	-0.0052
	(0.0647)		(0.0079)		(0.0097)
$\kappa_{3,3}$	0.2769	$\Gamma_{1,1}^N$	1.4101	$\eta_{1,2}^e$	0.0700
	(0.0746)		(1.1263)		(0.0247)
$\sigma_{2,1}$	-0.0039	$\Gamma_{1,2}^N$	-2.8220	$\eta_{1,3}^e$	-0.2067
	(0.0009)		(4.5305)		(0.0235)
$\sigma_{3,1}$	-0.0164	$\Gamma_{1,3}^N$	-0.0285	$\sigma_{q,1}$	0.0003
	(0.0023)		(0.0120)		(0.0003)
$\sigma_{3,2}$	-0.0253	$\Gamma_{2,1}^N$	0.3667	$\sigma_{q,2}$	0.0007
	(0.0055)		(0.1863)		(0.0004)
η_0^N	0.0333	$\Gamma_{2,2}^N$	38.2799	$\sigma_{q,3}$	0.0000
	(0.0009)		(7.5610)		(0.0005)
$\eta_{1,1}^N$	0.0408	$\Gamma_{2,3}^N$	-0.0014	ς_q	0.0058
	(0.0729)		(.0133)		(0.0002)

Error Statistics	
MSE:	8.2523×10^{-6}
Log-likelihood:	4.1168×10^4

Table 5.6 Table of results for the calibration of the Vasicek latent factor model to the European ZCIIS data set using the Kalman-filter. The table shows the fitted parameters in the calibration of the model to the data. It also gives statistics on the mean-squared error (MSE) and the final log-likelihood estimator. Standard errors are reported in parentheses.

calibration to the US data set. From the table, it can be seen that the fit of the model to the data set is good. This is indicated by the low value for the MSE (which is only of the order of 10 times larger than the MSE value for the fit to the synthetic data set). It is difficult to make any significant interpretations relating to the actual parameters obtained from the calibration since they don't have any specific economic meaning (except perhaps for η_0^N and η_0^e, which give an indication of the average level of the nominal and inflation short rates). We can see that some of the elements of the matrix Γ are quite large (or have quite large negative values). This is the result of running unconstrained optimisation and also due to the sensitivity of some of the parameters (we noticed that a number of

parameters, especially those in the Γ matrix were quite sensitive). A further illustration of the fit is given in Figure 5.5.

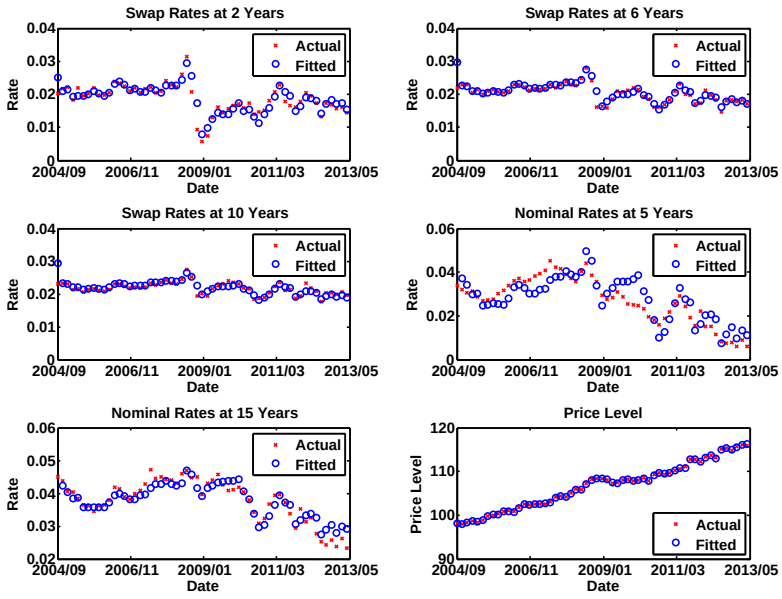

Figure 5.5 This plot shows results of the calibration of the Vasicek latent factor model to a European data set, consisting mainly of ZCIIS rates. In it, we illustrate the fit of the calibrated model to swap rates at 2, 6 and 10 years, nominal spot rates at 5 and 15 years, as well as the price level process (HICPxt).

This plot gives further evidence that the fit of the model to the data set is good. We can see that the calibrated model is able to replicate the swap rates and the price level process closely. It also provides a good fit to the nominal rates at 15 years, although the fit to those at 5 years is not so good. This is probably due to the strong influence of the ZCIIS data on the calibration. We are mostly concerned with the fit to the ZCIIS rates, however, as the purpose for including the nominal rates is only to add stability to the calibration results. As for the case with the calibration of the model to the US data set, we can analyse the model-free and model-implied decomposition of nominal rates into real rates, expected inflation and the IRP. This is illustrated in Figures 5.6 and 5.7.

Figures 5.6 and 5.7 are quite similar, except for the period around the recent financial crisis (and perhaps that around the time of the start of the European crisis), where the nominal and real rates drop significantly in the model-implied decomposition, but not as significantly in the model-free decomposition. The expected inflation rate and the inflation

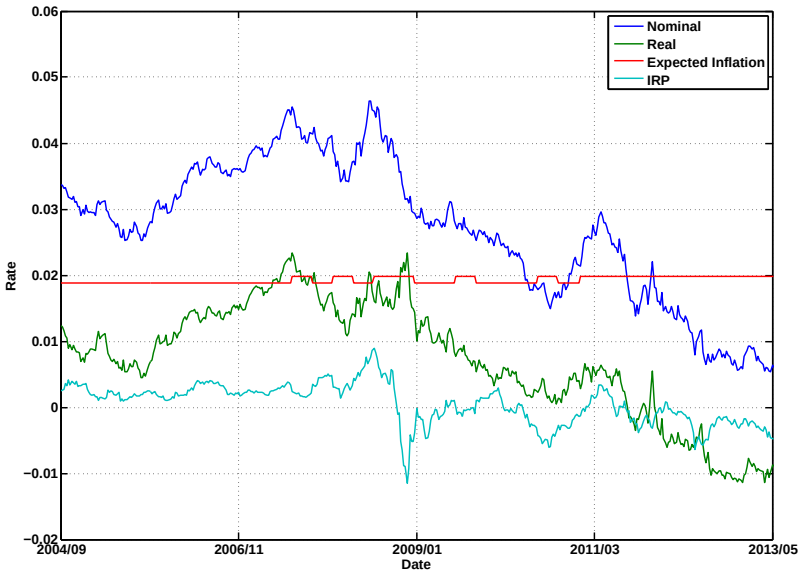

Figure 5.6 This plot shows the model-free decomposition of 5 year nominal yields into real yields, expected inflation and the IRP. The various rates in the plot are deduced from ZCIIS rates and inflation forecasts in the European (ZCIIS) data set.

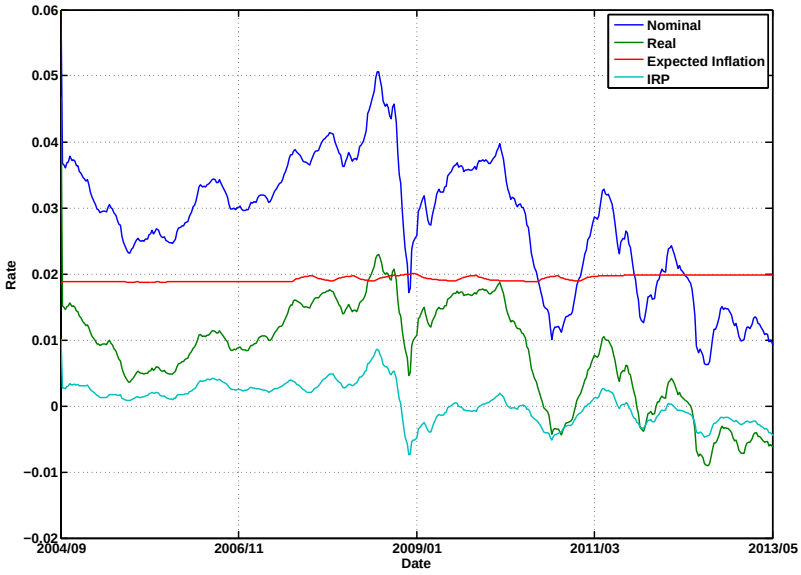

Figure 5.7 This plot shows the model-implied decomposition of 5 year nominal yields into real yields, expected inflation and the IRP (in the European ZCIIS case).

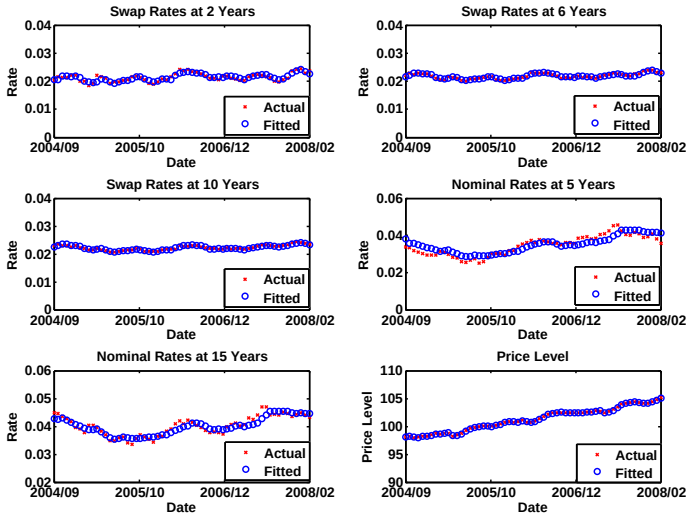

Figure 5.8 This plot shows results of the calibration of the Vasicek latent factor model to a European data set, consisting mainly of ZCIIS rates, in the period before the financial crisis (September 2004 to February 2008). In it, we illustrate the fit of the calibrated model to swap rates at 2, 6 and 10 years, nominal spot rates at 5 and 15 years, as well as the price level process (HICPxt).

risk premium are well captured across the whole time series by the estimation. As mentioned in the section on the calibration of the model to US data, the model-implied decomposition is based on all the instruments in the data set, whereas the model-free decomposition is based only on the nominal rate, expected inflation rate and ZCIIS rate at the specified maturity (5 years). From Figure 5.5, it can be seen that the swap rates experience a bigger drop around the time of the crisis than the nominal rates do. Given the strong influence of the swaps on the calibration, it is not surprising to see such a drop in the real and nominal rates in the model-implied decomposition. Given the impact of the financial crisis on our calibration results, it would also be interesting to consider calibration periods before and after the crisis.

To this end, we first consider the pre-crisis period of September 2004 to February 2008. We calibrate the Vasicek latent factor model to this data in the same way as before and report the results in Table 5.7. The table demonstrates, from the value of the MSE, that the fit to this data period is better than for the full data period. Again, we observe large values for some of the elements of the matrix Γ.

Perhaps of more interest, however, are Figures 5.8 and 5.9. Both plots indicate a better fit to the data than before. They also do not display any big drops in rates, since we have not considered the crisis period in this calibration. Figure 5.8 shows that the model-implied rates match the actual rates very closely, better than in Figure 5.5 (although the rates are significantly flatter in the former plot than in the latter). Moreover, the model-implied and model-free decomposition of 5 year nominal rates are very similar. The model-implied decomposition is smoother than the model-free one, but the levels and paths of the various lines are almost identical in the two plots.

Table of fitted parameters (pre-crisis)					
$X_0^{(1)}$	0.0130	$\eta_{1,2}^N$	0.0604 (0.0104)	$\Gamma_{3,1}^N$	−0.1034 (0.0937)
$X_0^{(2)}$	0.0350	$\eta_{1,3}^N$	−0.0878 (0.0182)	$\Gamma_{3,2}^N$	−0.0081 (0.0081)
$X_0^{(3)}$	0.0650	γ_1^N	−0.0733 (0.0067)	$\Gamma_{3,3}^N$	−0.0129 (0.0156)
$\kappa_{1,1}$	0.1916 (0.0076)	γ_2^N	−0.0769 (0.0202)	η_0^e	0.0197 (0.0002)
$\kappa_{2,2}$	0.0258 (0.0120)	γ_3^N	0.5431 (0.2389)	$\eta_{1,1}^e$	−0.0974 (0.0120)
$\kappa_{3,3}$	0.5845 (0.0916)	$\Gamma_{1,1}^N$	−0.2245 (0.0164)	$\eta_{1,2}^e$	0.1034 (0.0119)
$\sigma_{2,1}$	−0.0055 (0.0023)	$\Gamma_{1,2}^N$	−6.6404 (2.2254)	$\eta_{1,3}^e$	−0.0198 (0.0034)
$\sigma_{3,1}$	0.0223 (0.0065)	$\Gamma_{1,3}^N$	0.2783 (0.3526)	$\sigma_{q,1}$	0.0014 (0.0005)
$\sigma_{3,2}$	−0.0490 (0.0122)	$\Gamma_{2,1}^N$	−19.3139 (1.8078)	$\sigma_{q,2}$	0.0002 (0.0003)
η_0^N	0.0304 (0.0012)	$\Gamma_{2,2}^N$	−3.6872 (0.6480)	$\sigma_{q,3}$	0.0037 (0.0007)
$\eta_{1,1}^N$	0.2827 (0.0652)	$\Gamma_{2,3}^N$	0.0814 (0.0533)	ς_q	0.0021 (0.0012)
Error Statistics					
MSE:		1.4746×10^{-6}			
Log-likelihood:		1.8923×10^4			

Table 5.7 Table of results for the calibration of the Vasicek latent factor model to the European ZCIIS (pre-crisis) data set using the Kalman-filter. The table shows the fitted parameters in the calibration of the model to the data. It also gives statistics on the mean-squared error (MSE) and the final log-likelihood estimator. Standard errors are reported in parentheses.

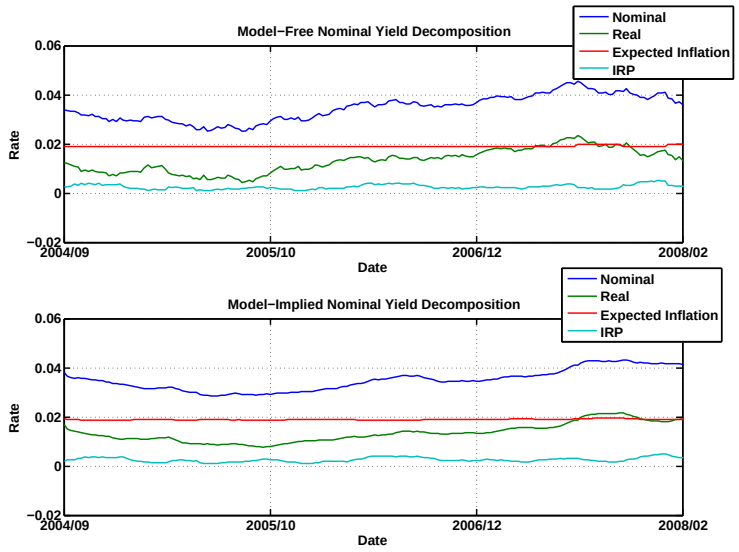

Figure 5.9 This plot shows the model-free and model-implied decomposition of 5 year nominal yields into real yields, expected inflation and the IRP. We consider the pre-crisis data period, September 2004 to February 2008, for the European (ZCIIS) data set in this plot.

We also consider the calibration of the model to the period after the crisis - August 2009 to May 2013. The results of this are given in Table 5.8 and again we can see that the fit in the post-crisis period is better than for the entire period (as indicated by the MSE value). Figures 5.10 and 5.11 also indicate a closer fit to the data than the corresponding figures for the fit to the entire data set do. As with the pre-crisis data set, we do not observe any big drops in rates, since we have not considered the crisis period in this calibration. Moreover, the model-implied and model-free decomposition of 5 year nominal rates are again very similar. Again, the plot for the model-implied decomposition indicates a smoother fit to the data than the model-free decomposition does, but the levels and paths of the various lines in each plot are quite comparable.

These results reveal a good fit of the model to the data. Whether we consider the entire data period, or only that before or after the recent financial crisis, we see that the model is able to match the observed instrument yields and prices well, although the case for the entire data period is not quite as good as when we consider periods on either side of the financial crisis separately. Looking further at the parameter values in Tables 5.7 and 5.8, we can see that there are many differences between the values in each table. This would support the notion that there were structural changes in these markets after the crisis. Some papers

Table of fitted parameters (post-crisis)					
$X_0^{(1)}$	-0.2280	$\eta_{1,2}^N$	0.2956	$\Gamma_{3,1}^N$	1.8895
			(0.0427)		(2.0283)
$X_0^{(2)}$	-0.1300	$\eta_{1,3}^N$	-0.0415	$\Gamma_{3,2}^N$	0.6262
			(0.0073)		(0.4108)
$X_0^{(3)}$	0.6000	γ_1^N	-0.0938	$\Gamma_{3,3}^N$	0.0090
			(0.0369)		(0.0039)
$\kappa_{1,1}$	-0.0132	γ_2^N	-0.3481	η_0^e	0.0205
	(0.0112)		(0.0500)		(0.0003)
$\kappa_{2,2}$	-0.0632	γ_3^N	-0.9487	$\eta_{1,1}^e$	-0.0831
	(0.0157)		(0.5097)		(0.0116)
$\kappa_{3,3}$	0.4647	$\Gamma_{1,1}^N$	-1.1176	$\eta_{1,2}^e$	0.0888
	(0.0880)		(0.1598)		(0.0101)
$\sigma_{2,1}$	-0.0368	$\Gamma_{1,2}^N$	-0.9515	$\eta_{1,3}^e$	-0.0216
	(0.0115)		(0.2246)		(0.0011)
$\sigma_{3,1}$	-0.0960	$\Gamma_{1,3}^N$	0.0366	$\sigma_{q,1}$	0.0012
	(0.0312)		(0.0118)		(0.0007)
$\sigma_{3,2}$	-0.0705	$\Gamma_{2,1}^N$	-3.5301	$\sigma_{q,2}$	0.0000
	(0.0192)		(1.3823)		(0.0007)
η_0^N	0.0146	$\Gamma_{2,2}^N$	4.7852	$\sigma_{q,3}$	0.0000
	(0.0192)		(1.7398)		(0.0008)
$\eta_{1,1}^N$	1.2068	$\Gamma_{2,3}^N$	0.0041	ς_q	0.0069
	(0.3055)		(0.0048)		(0.0004)
Error Statistics					
MSE:		1.4117×10^{-6}			
Log-likelihood:		1.8622×10^4			

Table 5.8 Table of results for the calibration of the Vasicek latent factor model to the European ZCIIS (pre-crisis) data set using the Kalman-filter. The table shows the fitted parameters in the calibration of the model to the data. It also gives statistics on the mean-squared error (MSE) and the final log-likelihood estimator. Standard errors are reported in parentheses.

have suggested the use of regime-switching term-structure models to deal more dynamically with such changes. This is the approach taken in the paper by Ang, Bekaert and Wei (2008) [2]. We do not consider such models in this paper, but these results do suggest that it is wise to identify such changes in the markets when calibrating models to market data and then using the results for forecasting purposes. We will interpret the IRP implied from these results in a later section.

Another point of interest is the similarity that we have seen between the model-free and model-implied decompositions of nominal yields. This might make us wonder why we need

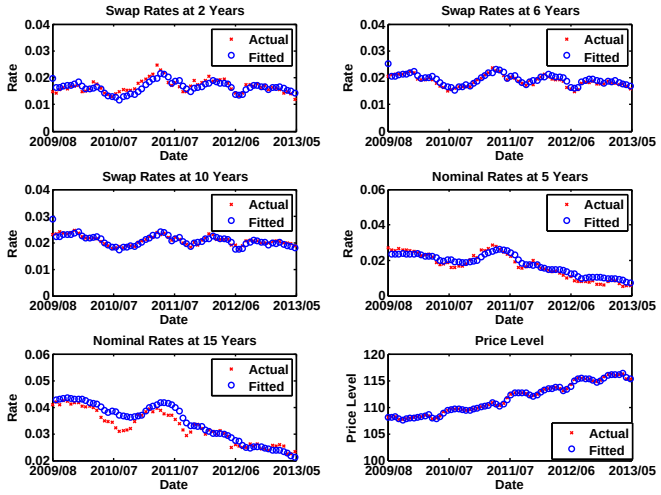

Figure 5.10 This plot shows results of the calibration of the Vasicek latent factor model to a European data set, consisting mainly of ZCIIS rates, in the period after the financial crisis (August 2009 to May 2013). In it, we illustrate the fit of the calibrated model to swap rates at 2, 6 and 10 years, nominal spot rates at 5 and 15 years, as well as the price level process (HICPxt).

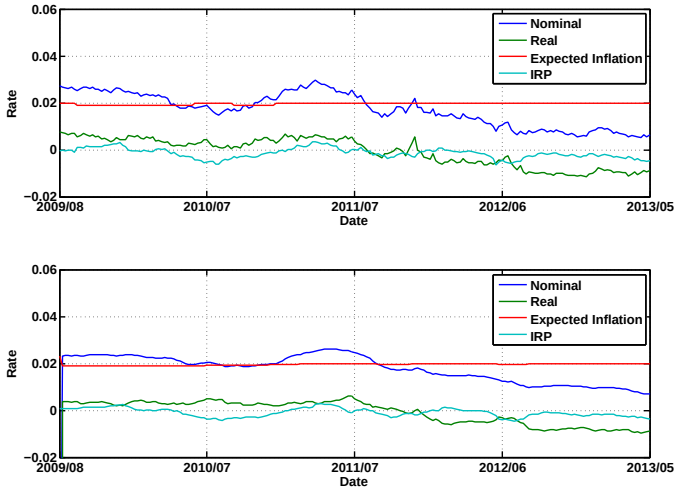

Figure 5.11 This plot shows the model-free and model-implied decomposition of 5 year nominal yields into real yields, expected inflation and the IRP. We consider the post-crisis data period, August 2009 to May 2013, for the European (ZCIIS) data set in this plot.

to use such a complicated model to obtain estimates of the IRP when we could just imply it from observable market data. Implying the IRP from market data is not always possible, however. In the case of the European data set, inflation survey data are only available (on the website of the ECB) for 1, 2 and 5 year ahead forecasts. If we wanted to imply the IRP at a maturity different to one of these, we would somehow need to find a different estimator of expected inflation. This is not a problem in the modelling approach, however, since we only use expected inflation survey data to anchor the model's estimate of expected inflation, but the model can still produce estimates of the IRP outside of these maturities. Moreover, by calibrating the model to an entire data set of various nominal and inflation-indexed instruments, we can capture the overall dynamics of the inflation market. This should enable us to produce better estimates of expected inflation and the IRP than simply using a few of the available instruments for this purpose[2].

5.6 Calibration to European IIC Data

In this section, we consider the calibration of the Vasicek latent factor model to a data set consisting mainly of inflation-indexed cap (IIC) prices. The calibration of inflation models to option price data in the current context (i.e. for the purpose of estimating the IRP) has not been done before (at least according to our research into the literature). This makes it a new and interesting problem to tackle in this area, as it requires the use of different calibration schemes and more complicated pricing scripts. As before, we include nominal zero-coupon yields and inflation survey forecasts to help stabilise the calibration routine. For IIC data, we consider a time series of weekly cap prices for caps with strikes of 2%, 3% and 4% at 1, 3 and 7 year maturities. These prices are obtained from Bloomberg, under the symbol $\langle$EUISCxy Index$\rangle$, where x represents the strike and y represents the maturity of the cap. The nominal rates and the inflation survey forecasts are taken from the same sources as in the data set from the previous section. Finally, we also include price level data as before from HICPxt levels, since the caps that we use are linked to this index. The time period that we consider is from May 2011 to May 2013. We do not consider a longer time period as most of the caps are too illiquid (or non-existent) before May 2011. As with the case for the swap data, we do not consider seasonality impacts on the cap data, since we only consider caps with a whole number of years to expiry.

To perform the calibration here, we make use of the unscented Kalman-filter calibration routine described earlier. We need to do this, since the IIC pricing formula, given by

[2]Of course, with any modelling framework, it is important to consider modelling risk. We try to take care of this by evaluating how well the model reproduces the actual instrument prices to which it is calibrated.

Table of fitted parameters					
$X_0^{(1)}$	-0.4700	$\eta_{1,2}^N$	0.0020	$\Gamma_{3,1}^N$	-0.0011
			(0.0000)		(0.0000)
$X_0^{(2)}$	0.2400	$\eta_{1,3}^N$	-0.1542	$\Gamma_{3,2}^N$	-0.0146
			(0.0002)		(0.0000)
$X_0^{(3)}$	-0.200	γ_1^N	-0.0669	$\Gamma_{3,3}^N$	-0.0085
			(0.0001)		(0.0000)
$\kappa_{1,1}$	0.0536	γ_2^N	-1.6458	η_0^e	0.0061
	(0.0000)		(0.0021)		(0.0000)
$\kappa_{2,2}$	0.0015	γ_3^N	0.0106	$\eta_{1,1}^e$	0.0058
	(0.0000)		(0.0000)		(0.0000)
$\kappa_{3,3}$	0.0799	$\Gamma_{1,1}^N$	4.5491	$\eta_{1,2}^e$	0.0011
	(0.0001)		(0.0045)		(0.0000)
$\sigma_{2,1}$	0.0060	$\Gamma_{1,2}^N$	0.0419	$\eta_{1,3}^e$	-0.0077
	(0.0000)		(0.0000)		(0.0000)
$\sigma_{3,1}$	0.0122	$\Gamma_{1,3}^N$	0.0259	$\sigma_{q,1}$	0.0001
	(0.0000)		(0.0000)		(0.0065)
$\kappa_{3,2}$	-0.0067	$\Gamma_{2,1}^N$	0.0261	$\sigma_{q,2}$	0.0005
	(0.0000)		(0.0000)		(0.0123)
η_0^N	-0.0452	$\Gamma_{2,2}^N$	-0.2337	$\sigma_{q,3}$	0.0009
	(0.0001)		(0.0003)		(0.0049)
$\eta_{1,1}^N$	-0.0686	$\Gamma_{2,3}^N$	-0.0099	ς_q	0.0002
	(0.0000)		(0.0000)		(0.0081)
Error Statistics					
MSE:		3.3761×10^{-5}			
Log-likelihood:		6.1540×10^{3}			

Table 5.9 Table of results for the calibration of the Vasicek latent factor model to the European IIC data set using the unscented Kalman-filter. The table shows the fitted parameters in the calibration of the model to the data. It also gives statistics on the mean-squared error (MSE) and the final log-likelihood estimator. Standard errors are reported in parentheses.

Equation (3.5), is not linear in the state variable X_t. The unscented Kalman-filter handles non-linearities well by efficiently sampling points around the state vector and projecting these through the cap pricing equation to calculate the mean and covariance of the state vector as well as the observation variables. As such, the fundamental concept behind the unscented Kalman-filter is the same as that behind the standard Kalman-filter and we can use it to once again estimate the model parameters via maximum likelihood estimation. As before, we make use of the genetic algorithm to assist us with finding starting parameters for the *fminsearch* algorithm in Matlab. The results of the calibration are given in Table 5.9.

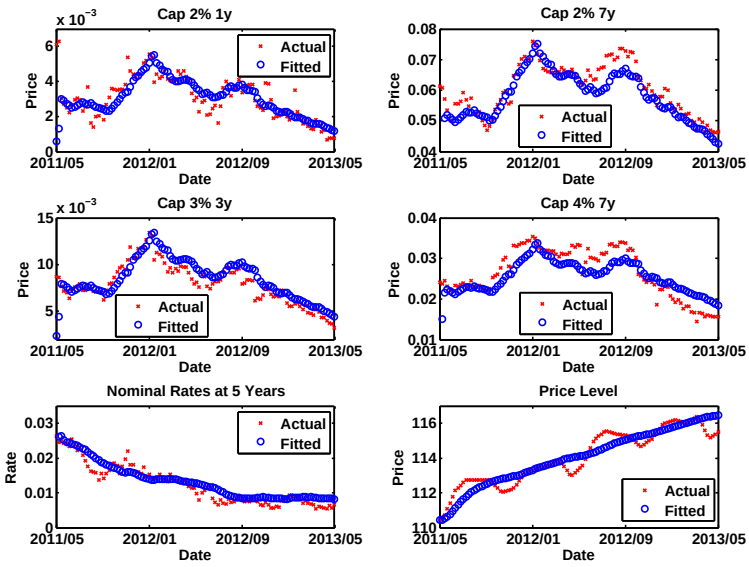

Figure 5.12 This plot shows results of the calibration of the Vasicek latent factor model to a European data set, consisting mainly of IIC prices. In it, we illustrate the fit of the calibrated model to cap prices with strikes of 2% (maturities 1 and 7 years), 3% (maturity 3 years) and 4% (maturity 7 years); nominal spot rates at 5 years; as well as the price level process (HICPxt).

The table indicates a reasonably good fit of the model to the data, although the MSE value that we observe here is the highest amongst all of the model fits so far. The quality of the fit is further illustrated in Figure 5.12. This figure shows that the fit to the IIC and nominal bond data is not as good as was the case for the ZCIISs, although the model still manages to capture the general price movements quite well. The fit to the price level data is rather poor however, as the model manages to capture only the general direction of the process, but not the finer movements. Part of the reason for the poorer fit is the greater dispersion of cap prices. This indicates that the market for caps is thinner than that for swaps in the inflation market. Unfortunately, we were unable to find data for the open interest in the IIC market, so we were not able to explore liquidity issues in the market further.

Figure 5.13 gives an illustration of the model-implied decomposition of 5 year nominal yields into real yields, expected inflation and the IRP. Comparing this to Figure 5.11, which considers a similar data period, there are clearly some differences between the two model-implied decompositions, specifically with regard to the expected inflation and IRP

lines. The nominal and real rate lines are fairly similar across both plots (at the least, with respect to the levels of the respective lines). However, the model seems to fail to capture the levels of expected inflation and the IRP (we have more confidence in the fit of the model to the European ZCIIS data set in the post-crisis period, given the better calibration statistics and model-free plots in that section).

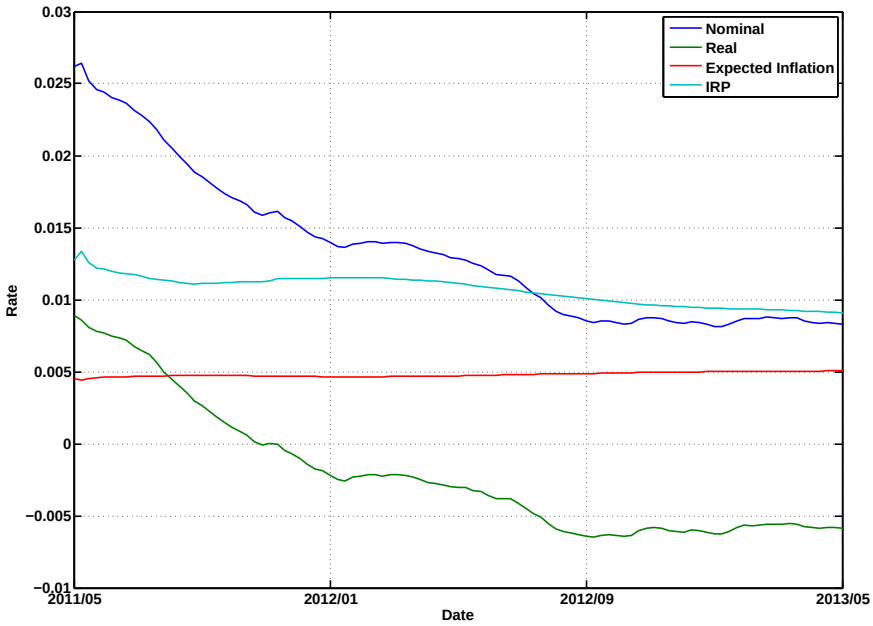

Figure 5.13 This plot shows the model-implied decomposition of 5 year nominal yields into real yields, expected inflation and the IRP (in the European IIC case).

Of interest are also the values of the calibrated parameters. These are quite different to those obtained in the section on the calibration to the ZCIIS data set, specifically those seen in Table 5.8. All these differences, especially in comparison to the model-free decompositions shown in the previous section, lead us to believe that the illiquidity of the IIC market makes it impractical to use for our purposes. In addition to this, the more complicated pricing formula for caps means that the calibration procedure required to fit the model to cap data is more computationally intensive than for the other instrument types that we have considered so far. All of these consideration add to the impracticality of using IIC data to infer the IRP.

Although we do not find a time series of IICs to be very useful in the estimation of the IRP, other uses for these instruments are studied in the literature. Kitsul and Wright (2012) [31], for example, use inflation indexed caps and floors to derive probability densities for

future inflation. These instruments have much better prediction capabilities than swaps and bonds and Kitsul and Wright (2012) [31] find them very useful in not only forecasting future inflation, but also in estimating the volatility of future inflation. Such results make sense, as one would expect option data to give a better description of the higher order moments of the underlying (inflation). The methods that they use to carry out their investigations are different from ours and beyond the scope of this thesis.

5.7 Calibration to Cross-Sectional European IIC Data

The final calibration application that we consider is the calibration of the model to cross-sectional cap data on 31 May 2013. The caps that we consider are from the European market and are linked to the HICPxt. We consider caps at 6 different strikes (from 1% to 6%) and at 11 maturities (from 1 to 10 years and 15 years), obtained from the same source as those in the previous section. As such, the data set that we calibrate the model to consists of 66 data points. The results for the calibration are illustrated in Figure 5.14.

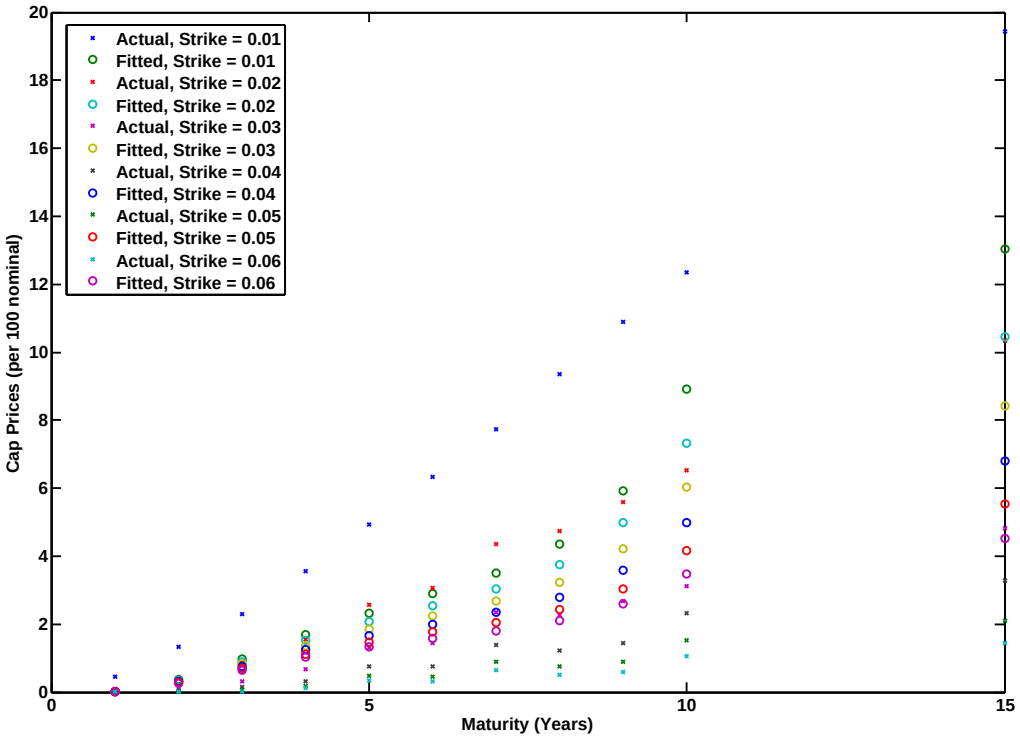

Figure 5.14 This plot shows the results for the calibration of the model to cross-sectional European IIC data on 31 May 2013.

We can see from the figure that the model fails to capture the cross-sectional data well. The first consideration here is the illiquidity of the market. Caps are only available at the strike rates 1%, 2%, 3%, 4%, 5% and 6%. Thus, the number of call options available on inflation is very limited. As a result of this, our data set contains only 66 prices. This is too few points from which to obtain a good fit, especially since the model that we use here has 33 parameters. The second consideration is the model's inability to capture the spread of the cap prices. We can see from the figure that the calibrated prices fall in a relatively narrow band between the actual 6% cap prices and the actual 1% cap prices. This was also observable in the previous section, where the model was not able to fully capture the spread of cap prices in the time series data. The cause of this is most likely the model's inability to capture the volatility in the option market adequately. To model options, it would be better to use a model that can fit the corresponding volatility surface. For these reasons, it can be seen that the latent factor model is not a good model for derivative pricing purposes. Instead, other models such as the Jarrow-Ylilirim model (see Jarrow and Yildirim (2003) [30]) or inflation market-models (see Belgrade and Benhamou (2004) [5], Brigo and Mercurio (2006) [7] and Segreti (2008) [40]) are better suited to this.

5.8 Estimates of the Inflation Risk Premium

In this section, we look closely at the implications of our results for the inflation risk premium. We consider only the results obtained from fitting our model to the European ZCIIS data set.

Figures 5.15 and 5.16 compare the model-implied to the model-free 1 and 5 year IRPs. The time period considered here is from 10 September 2004 to 24 May 2013. From the plots, we can see that the model-implied and the model-free estimates of the IRP follow each other closely. Overall, this indicates that our model has been able to capture the dynamics of the IRP well.

Figures 5.17 and 5.18 illustrate the model-implied historical term structure of IRPs. In Figure 5.17, we have plotted the 1, 5, 10 and 15 year IRPs for the entire time period. Figure 5.18 gives the term structure (out to 15 years) of the IRP at four time points - two before the crisis and two after it. The two figures indicate that the term structure of IRPs is reasonably flat and not very volatile before the financial crisis. For the middle part of this period, the 1 year IRP lies in between the 5 and 10 year IRPs. At the beginning and end of the period, however, the IRPs are arranged in order of increasing maturity, with the 1 year IRP below all the others. This indicates a slight bow shaped IRP term structure curve in

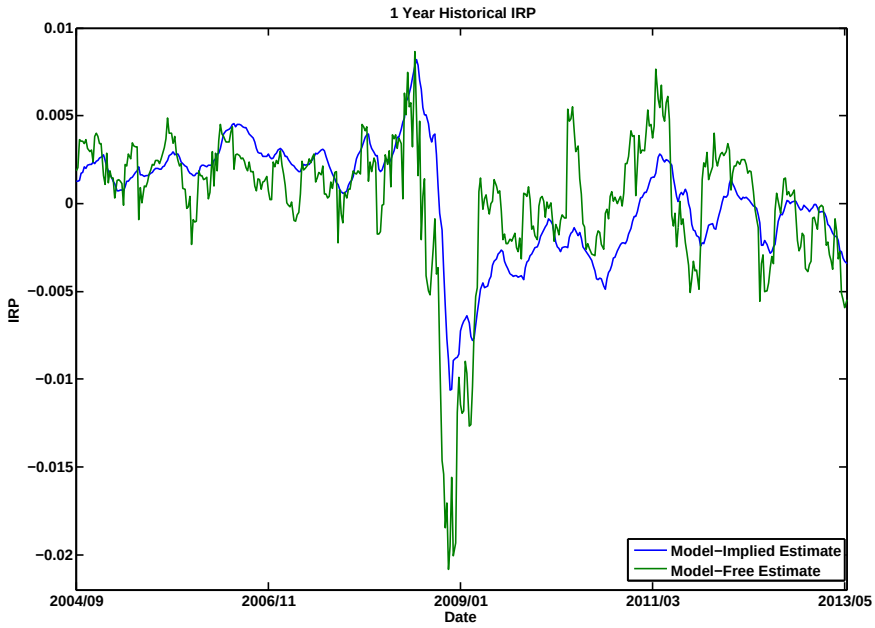

Figure 5.15 This plot shows the model-implied and model-free estimates of the 1 year historical IRP (implied from the European ZCIIS data set).

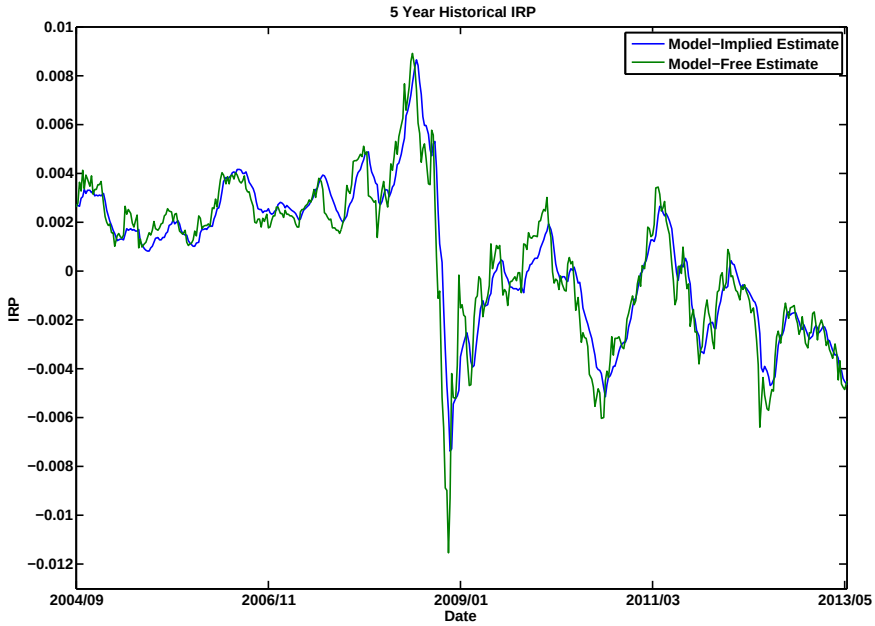

Figure 5.16 This plot shows the model-implied and model-free estimates of the 5 year historical IRP (implied from the European ZCIIS data set).

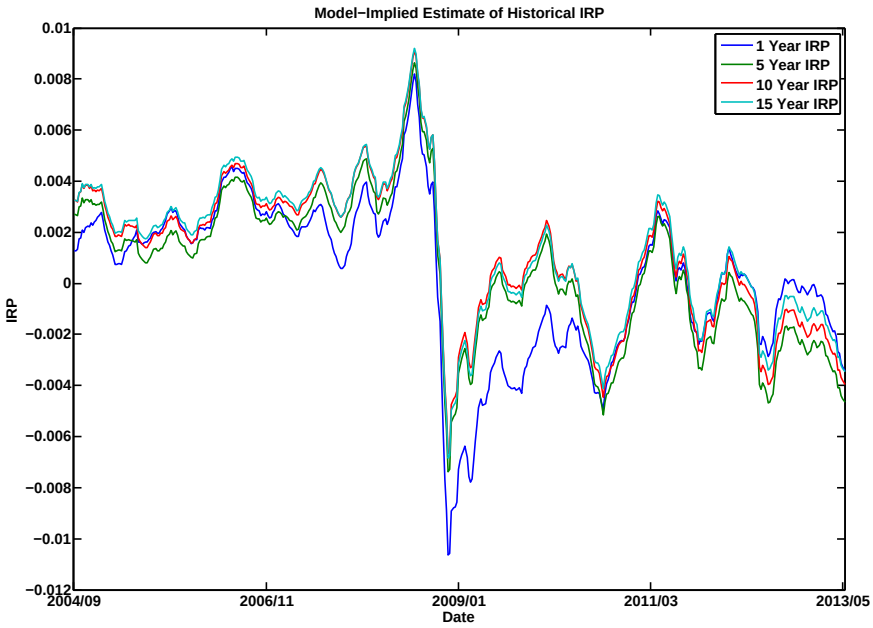

Figure 5.17 This plot shows the model-implied estimates of the 1, 5, 10 and 15 year historical IRPs (implied from the European ZCIIS data set).

the middle of this period, with risk premia at near and far maturities slightly above those at intermediate maturities. At the beginning and end of the period, the term structure is increasing. Moreover, the IRP appears to be (slightly) greater than 0 for the period before the crisis. This makes sense, since there should be a positive risk premium for holders of nominal bonds to compensate them for inflationary risks. The period from the time of the financial crisis until the end of the time series, however, displays markedly different characteristics.

At the time of the financial crisis, the IRP at all maturities dropped significantly to levels well below 0. This is illustrated clearly in Figures 5.15, 5.16 and 5.17 around September 2008, the time when Lehman Brothers collapsed. A number of explanations are given for this occurrence and Campbell, Shiller and Viceria (2009) [10] and Grishchenko and Huang (2012) [24] discuss them at length. Perhaps the most popular is that the observed drop occurred because of a large increase in deflationary risk. At the time of the collapse of Lehman Brothers, there was a large drop in the level of break-even inflation rates, but inflation expectations remained largely the same (at least according to inflation survey data). This, together with the large drop in inflation experienced at the time, would have indicated a rise in deflationary pressures and the occurrence of a negative inflation risk premium. Illiquidity in the inflation market, as well as market segmentation are also cited as reasons for this

drop (see Grishchenko and Huang (2012) [24]). An increase in a "liquidity premium" on real bonds could have lead to break-even inflation rates dropping below expected inflation, hence inducing a negative IRP. The market segmentation proposition refers to the different characteristics of participants in nominal and real bond markets. At the time of the financial crisis, very different preferences between participants in each of these could have caused a narrowing of the spread between nominal and real bond yields, while expected inflation rates remained unchanged, also inducing a negative IRP.

In the period since the financial crisis, the IRP has also been much more volatile than it was before and seems to have oscillated wildly between levels above and below 0. The term structure of IRPs after the crisis also indicates that just after the crisis, one year IRPs were very negative and much lower than risk premia at other maturities, while the term structure curve had a concave down shape. In more recent periods, the spread amongst risk premia at various maturities has been relatively less and the shape of the term structure curve has been concave up. This points towards uncertainty in nominal and real bond markets in recent times in the Eurozone.

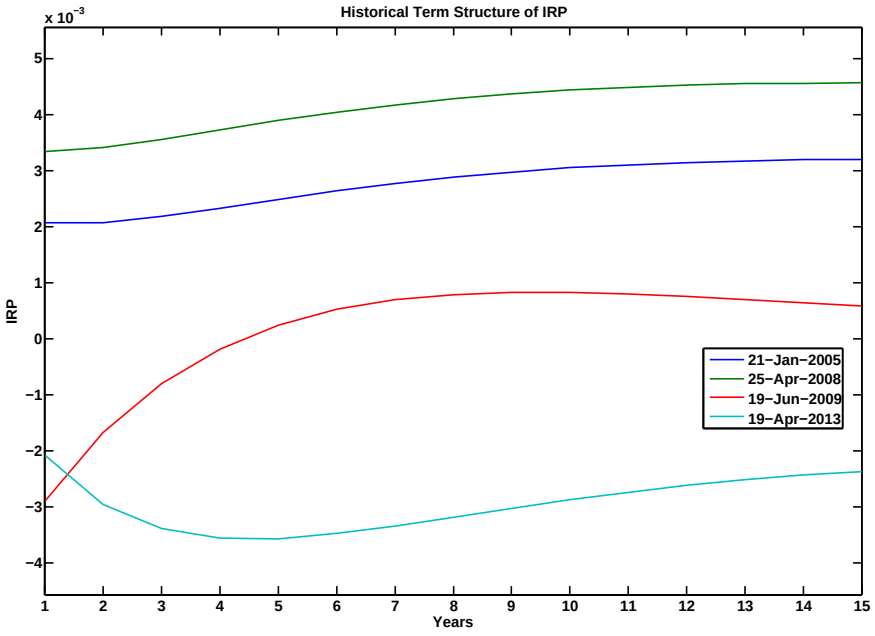

Figure 5.18 This plot shows the historical term structures of the IRP on four different dates, two on each side of the recent financial crisis. The term structures are from 1 year out to 15 years and are implied from the European ZCIIS data set.

It is also interesting to examine what the model says about the term structure of IRPs at the moment. This is illustrated in Figure 5.19, which has been produced by finding the model-implied IRP term structure on 24 May 2013 (the last date of the time series), after calibrating the model to the post-crisis (European ZCIIS) data set. Here we observe, firstly, that the IRP is very small at all maturities in the future, since it ranges between -55 basis points and 0. Moreover, it is negative at all points between now and 15 years in the future, probably pointing to deflationary risks in bond markets. Finally, it is upward sloping (mostly), which suggests that there is less deflationary risk attached to longer term bonds than to shorter term ones.

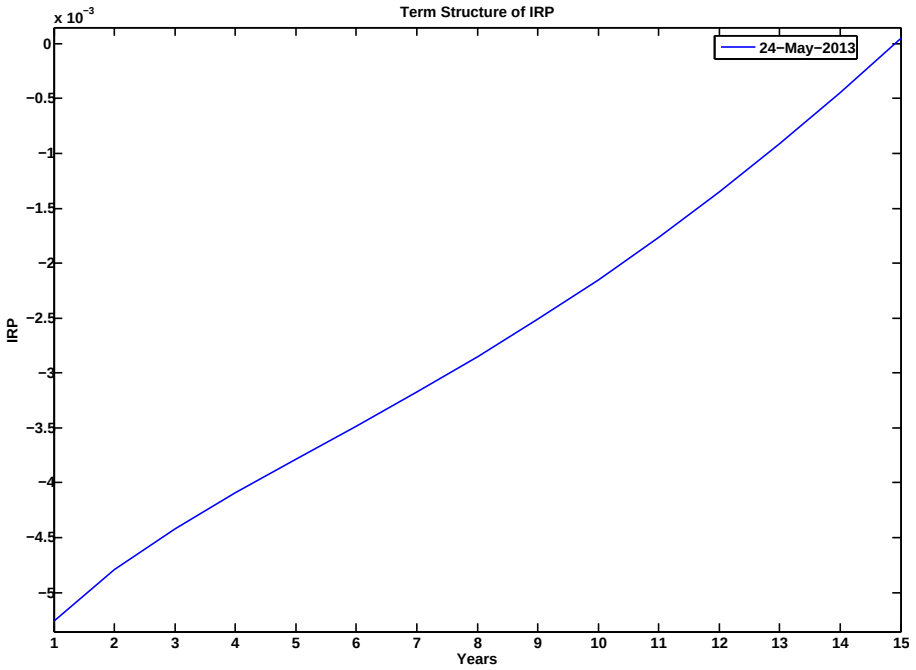

Figure 5.19 This plot shows the term structure of the IRP on the last date of the time series of ZCIIS rates. The term structure is from 1 year out to 15 years and is implied from the European ZCIIS data set (post-crisis).

It is tricky to compare the results for the IRP here to those in the literature. Few studies consider the IRP in a European setting and most studies into the IRP - both in the US case and in the European case - end before the recent financial crisis. Nonetheless, if we compare our results to those of Garcia and Werner (2010) [23] - who consider the IRP in a European setting - in the time period where our two studies overlap (2004-2008), we see that the 1 year model-implied IRP in both studies lies in the 0% to 0.5% range. Looking further at Table 1.1, and comparing the results for the IRP in other studies to those here, we can see that the range of the IRP which we find, is consistent with the literature.

Chapter 6

Applications of the Inflation Risk Premium

In this chapter, we discuss a number of applications for the IRP. The first of these is based on a paper by Lemaire and Plante (2009) [33] who consider how the IRP might be used to detect under or over pricing of real bonds, relative to nominal bonds. We extend their analysis by making use of the Vasicek latent factor model to find the appropriate IRP for this approach. We also consider how the Vasicek model might be used to deduce a better estimate of inflation expectations than that given by inflation forecast surveys or break-even inflation rates. Finally, we consider out-of-sample tests for the model to assess its forecasting capabilities.

6.1 Bond Trading and the Inflation Risk Premium

Here, we extend the approach of Lemaire and Plante (2009) [33], who examine a bond trading strategy based on the IRP. The hypothesis behind this scheme is that the IRP can be used as an indicator of the over or under pricing of real bonds relative to nominal bonds. Under this hypothesis, unusually high (or low) values for the IRP indicate that the price of inflation insurance is too high (or too low) and that it should return to some long-run average level. Considering our results in the previous chapter, this hypothesis seems plausible, since we observe the IRP to oscillate around a certain level (usually close to 0), and not to grow or decline continuously. This also makes sense given the mean-reverting nature of interest rates. Thus we implement a strategy whereby we use the IRP as a trigger level to decide whether to invest in a nominal or a real bond portfolio. At each point in time (at the beginning of each month over the sample period), we compare the actual level of the IRP to the trigger level. If the actual value is larger than or equal to the trigger level,

then we invest our entire portfolio in nominal bonds, otherwise we invest it in real bonds.

To implement this strategy, we consider bond portfolios in the European market and in the US market. For the IRP, we use the results obtained from calibrating the Vasicek latent factor model to the European ZCIIS and US data sets from the previous chapter. For a given time period over which we test this strategy, the appropriate trigger level is found by selecting the one which maximises the risk-adjusted return (annualised return over annualised standard deviation) over a portion of the time period. We then test whether this trigger level still produces superior results over the rest of the time period. In this way, we back-test the strategy. For comparison, we consider four other portfolios: one where we invest exclusively in nominal bonds, one where we invest exclusively in real bonds, one where we invest half our portfolio in nominal bonds and the other half in real bonds, and one where we randomly select to invest in nominal or real bonds at the start of each month.

6.1.1 Trading Strategy with European Bonds

For our first set of results, we use total return indices for European government bonds with 1 to 10 years to maturity as the nominal and real bond portfolios. For nominal bonds, we select the AA-rated bond index from Barclays Indices [3] and for real bonds, we select HICPxt-linked bonds, again from Barclays Indices. These total return indices give a good indication of the return that would accrue to a nominal and a real bond portfolio of short to medium term government bonds in the Eurozone. For the IRP, we choose the model-implied 5 year IRP found by calibrating the Vasicek latent factor model to the entire European ZCIIS data set. We choose this maturity for the IRP because it is approximately equal to the average duration of the bonds in both of the total return indices. Below, we test the effectiveness of this strategy over the entire period of the data set (September 2004 to May 2013), as well as that before and after the crisis.

To start with, we consider results from the entire time period, which includes the recent financial crisis. The in-sample period is 1 October 2004 to 1 November 2006 and during this period, we find that the trigger value of the IRP that maximises the risk-adjusted return is 0.0016. We then test the performance of the strategy with this trigger value in the out-of-sample period, 1 November 2006 to 1 May 2013. The results are presented in Table 6.1, where the column "Strategy" presents the results of the bond trading strategy, the columns "Nominal" and "Real" present the results of investing exclusively in nominal and real bonds respectively, the column "Equal" presents the results of investing an equal amount in the nominal and the real bond portfolios, and the column "Random" presents the results from the random allocation scheme.

Bond strategy results					
	Strategy	Nominal	Real	Equal	Random
Return	0.0575	0.0520	0.0505	0.0512	0.0515
Std. Deviation	0.0362	0.0327	0.0378	0.0317	0.0352
Risk Adj. Return	1.5892	1.5871	1.3365	1.6167	1.4651

Table 6.1 Table of results for the bond trading strategy with European bonds. Here we consider the entire time period of the European data set (2004-2013).

As we can see from the table, the bond strategy outperforms all other strategies considered here from an annualised return perspective. From a risk-adjusted return perspective however, it performs slightly worse than the equally weighted portfolio. Note that the results for the random allocation scheme are taken as an average over a set of 1000 random simulations. We can also plot a histogram of the random allocation results and compare the risk adjusted return from the bond strategy to these. This is given in Figure 6.1.

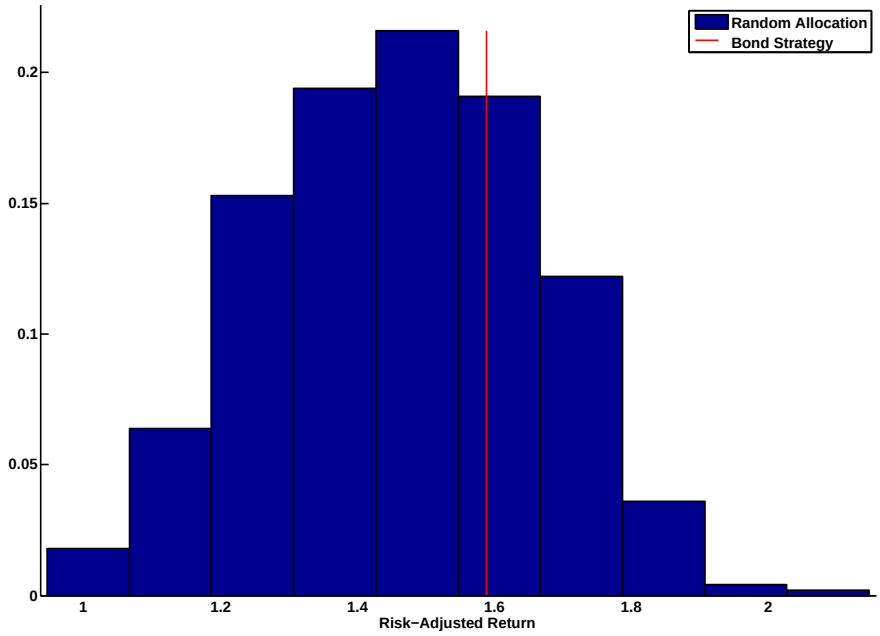

Figure 6.1 Comparison of risk-adjusted return from the bond trading strategy to a histogram of risk-adjusted returns from the random allocation scheme. These results are from the European bond case over the time period 2004 to 2013. 1000 random allocations were used to create the histogram.

This histogram illustrates that the bond trading strategy outperforms the random allocation scheme approximately 75% of the time in the out-of-sample period. We also perform

a hypothesis test to see if the mean of the risk-adjusted returns for the random allocation scheme is significantly different from the risk-adjusted return for the bond trading strategy. To this end, we perform a t-test with the null hypothesis that the mean return of the random allocation scheme is equal to 1.5892 versus the alternative hypothesis that the mean is less than this. We reject the null hypothesis at the 99% level.

We also consider results for the same data set in the pre- and post-crisis periods to see if the strategy was effective before and after the crisis. For the pre-crisis period, we consider an in-sample period of 1 October 2004 to 1 April 2005 and an out-of-sample period of 1 May 2005 to 1 July 2007. The IRP trigger level that maximises the in-sample risk-adjusted return for the bond trading strategy is 0.0006. For the post-crisis period, we consider an in-sample period of 1 August 2009 to 1 December 2009 and an out-of-sample period of 1 January 2010 to 1 May 2013. The optimal IRP trigger level in the in-sample period is 0.0003. The results for these are presented in Tables 6.2 and 6.3. Again, in both instances, the bond trading

Bond strategy results (pre-crisis)					
	Strategy	Nominal	Real	Equal	Random
Return	0.0096	0.0071	0.0048	0.0060	0.0058
Std. Deviation	0.0235	0.0207	0.0308	0.0254	0.0261
Risk Adj. Return	0.4075	0.3451	0.1558	0.2349	0.2253

Table 6.2 Table of results for the bond trading strategy with European bonds. Here we consider the pre-crisis time period of the European data set (2004-2007).

Bond strategy results (post-crisis)					
	Strategy	Nominal	Real	Equal	Random
Return	0.0644	0.0519	0.0552	0.0535	0.0538
Std. Deviation	0.0399	0.0332	0.0390	0.0341	0.0362
Risk Adj. Return	1.6149	1.5633	1.4145	1.5701	1.4891

Table 6.3 Table of results for the bond trading strategy with European bonds. Here we consider the post-crisis time period of the European data set (2009-2013).

strategy outperforms all the other strategies from the perspective of annual returns and from that of risk-adjusted returns. Figure 6.2 plots the histograms of risk-adjusted returns from the random allocation schemes in the periods before and after the financial crisis and compares them to the risk-adjusted returns for the bond trading strategy in each period. In the period before the crisis, the bond trading strategy outperforms the random allocation scheme approximately 85% of the time and in the period after the crisis, it outperforms it approximately 76% of the time. We also conduct hypothesis tests in these two cases to see

if the mean of the random allocation scheme is significantly different from the risk-adjusted return of the bond trading strategy. Again, we reject the null hypotheses at the 99% level. Thus, when we exclude the period of the recent financial crisis, we still find that the bond trading strategy performs better than the other four strategies.

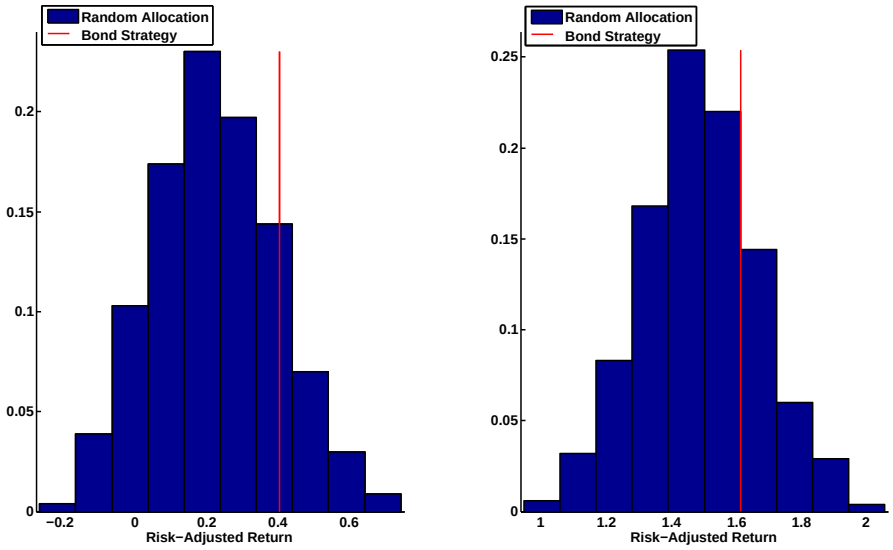

Figure 6.2 Comparison of risk-adjusted returns from the bond trading strategy to histograms of risk-adjusted returns from the random allocation scheme. These results are from the European bond case before and after the recent financial crisis, over the time periods 2004 to 2007 and 2009 to 2013. 1000 random allocations were used to create each histogram.

6.1.2 Trading Strategy with US Bonds

For our second set of results, we consider total return indices for US government bonds. For nominal bonds, we make use of the iShares Treasury bond exchange traded fund (ETF), data for which can be obtained from Bloomberg under the symbol ⟨TLT US Equity⟩. For real bonds, we consider the iShares TIPS exchange traded fund, data for which can be obtained from Bloomberg under the symbol ⟨TIP US Equity⟩. These indices consist primarily of AA-rated US government bonds and, as in the European case, give a good indication of the return on medium to long term nominal and real bond portfolios. We also choose the model-implied 10 year IRP as the reference IRP which we use to to make our bond strategy decisions. This is the same as the IRP that we found in the section on the calibration of the Vasicek latent factor model to the US data set. The period over which we test the bond strategy here is therefore August 2004 to September 2010. Again, we test the effectiveness

of the strategy over the entire time period of the data set, as well as before and after the crisis.

For our results obtained by considering the whole data period, we find that the level of the IRP which maximises the risk-adjusted return of the bond strategy in the in-sample period 1 August 2004 to 1 November 2008 is 0.0036. We then test the effectiveness of this value as a trigger for buying nominal or real bonds in the out-of-sample period 1 December 2008 to 1 September 2010. The results of this are presented in Table 6.4.

Bond strategy results					
	Strategy	Nominal	Real	Equal	Random
Return	0.0755	−0.0179	0.0743	0.0290	0.0298
Std. Deviation	0.0697	0.1757	0.0696	0.1054	0.1310
Risk Adj. Return	1.0831	−0.1017	1.0675	0.2749	0.2738

Table 6.4 Table of results for the bond trading strategy with US bonds. Here we consider the entire time period of the US data set (2004-2010).

The table displays that the bond trading strategy outperforms all the others from a perspective of annualised return and from that of risk-adjusted return. Again, we can plot the histogram of risk-adjusted returns from randomly readjusted portfolios and compare this to the risk-adjusted return of the strategy. This is given in Figure 6.3, which illustrates that the bond trading strategy outperforms a randomly readjusted portfolio about 92% of the time. Performing a hypothesis test where we test the hypothesis that the mean risk-adjusted return of the randomly readjusted portfolio is equal to that of the bond trading strategy, versus the hypothesis that it is smaller than this, we reject the null hypothesis at the 99% level. Thus, the results here lead us to the same conclusions as in the case for the European data set. The use of the IRP as an indicator of the over- or underpricing of inflation risk appears to be reasonably effective.

As before, we analyse the efficacy of the bond trading scheme before and after the crisis. For the pre-crisis period, the in-sample window is from 1 August 2004 to 1 June 2006 and the out-of-sample window is from 1 July 2006 to 1 July 2007. Similarly, for the post-crisis period, these are 1 August 2009 to 1 September 2009 and 1 October 2009 to 1 September 2010 respectively. The optimal IRP values that we find for each period are 0.0034 and 0.0006 respectively and the results for the bond trading strategy in each period are presented in Tables 6.5 and 6.6.

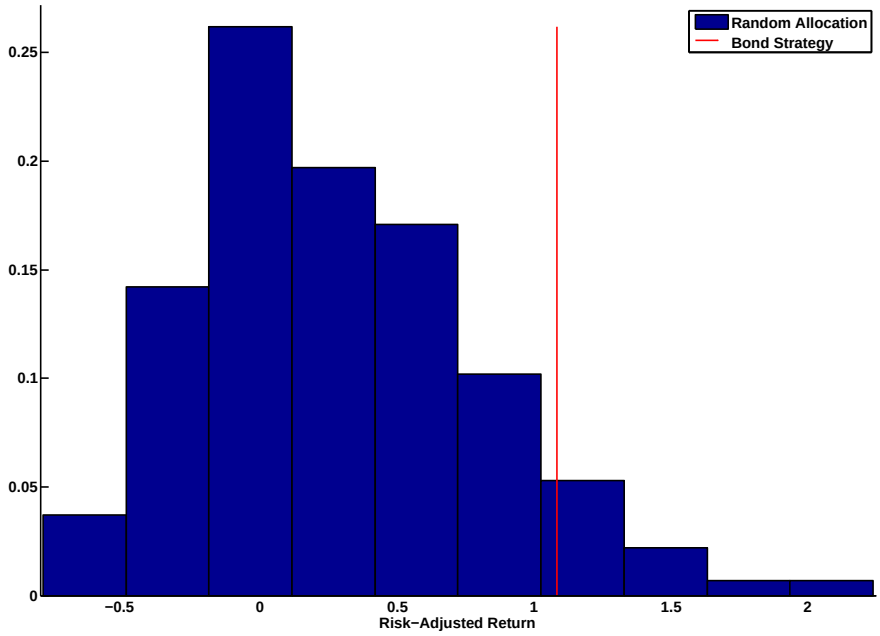

Figure 6.3 Comparison of risk-adjusted return from the bond trading strategy to a histogram of risk-adjusted returns from the random allocation scheme. These results are from the US bond case over the time period 2004 to 2010. 1000 random allocations were used to create the histogram.

Bond strategy results (pre-crisis)					
	Strategy	Nominal	Real	Equal	Random
Return	0.0382	0.0127	−0.0044	0.0041	0.0048
Std. Deviation	0.0649	0.0746	0.0437	0.0575	0.0605
Risk Adj. Return	0.5882	0.1699	−0.1005	0.0720	0.0770

Table 6.5 Table of results for the bond trading strategy with US bonds. Here we consider the pre-crisis time period of the US data set (2004-2007).

Bond strategy results (post-crisis)					
	Strategy	Nominal	Real	Equal	Random
Return	0.1151	0.1035	0.0670	0.0853	0.0860
Std. Deviation	0.1047	0.1397	0.0492	0.0833	0.1024
Risk Adj. Return	1.0994	0.7408	1.3638	1.0230	0.8478

Table 6.6 Table of results for the bond trading strategy with US bonds. Here we consider the post-crisis time period of the US data set (2009-2010).

From Tables 6.5 and 6.6, we see once again that the bond trading strategy outperforms all other strategies on a returns basis in both periods. In the post-crisis period, the strategy

does not outperform the real bond portfolio from a risk-adjusted return perspective. The post-crisis period of the data set is very short, however, as it is taken from the Ho, Huang and Yildirim (2012) [28] paper, and so it is difficult to say how meaningful the results in this period are. Figure 6.4 gives the histograms of risk-adjusted returns form the random allocation scheme in each period and compares them to the risk-adjusted returns for the bond trading strategy. Before the crisis, the bond trading strategy outperforms the random allocation scheme 92% of the time, and after the crisis, it does the same 68% of the time. Performing the same hypothesis tests as before in each period, we twice reject the null hypothesis (at the 99% level) that the mean risk-adjusted return from the random allocation scheme is equal to that of the bond trading strategy.

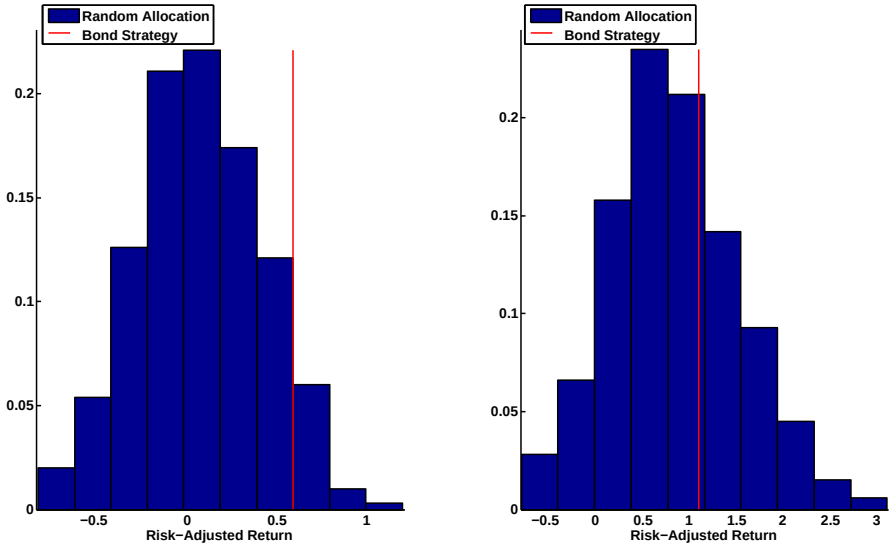

Figure 6.4 Comparison of risk-adjusted returns from the bond trading strategy to histograms of risk-adjusted returns from the random allocation scheme. These results are from the US bond case before and after the recent financial crisis, over the time periods 2004 to 2007 and 2009 to 2010. 1000 random allocations were used to create each histogram.

These results once again hint at the effectiveness of such a bond trading strategy.

6.1.3 Trading Costs

So far, the results we have shown support for the notion that the IRP can be used as a detector of the over- or underpricing of real bonds relative to nominal bonds. The bond strategy that we implemented and tested with European and US bond indices outperformed

the other strategies in most cases. We did not, however, take trading costs into account when making these conclusions. We do that in a simplified way here.

To perform this analysis, we consider the scheme implemented in the post-crisis period for European bonds and over the full period for US bonds. The results of these are given in Tables 6.3 and 6.4. In the European case, we can see that the naive equally weighted nominal and real bond scheme performs best after the bond trading strategy (with regard to risk-adjusted return). We can thus calculate the maximum transaction cost applicable to the bond trading strategy that would still allow it outperform the naive scheme. We find this value to be 9.3 basis points (of portfolio value per trade). Similarly, in the US case, the naive buy and hold scheme for real bonds is the second best performing scheme. Examining the maximum transaction cost that would still permit the bond trading strategy to outperform the naive scheme, we find this figure to be 8.1 basis points. We can now compare these values to bid-ask spreads on funds linked to these bond indices to get an indication of the true market performance of the strategy.

For the European case, we consider two iShares bond indices - the Euro government bond ETF for 5-7 year government bonds and the Euro inflation linked government bond ETF. Descriptions of these can be found on the iShares website [29] and data on them under the Bloomberg codes ⟨IEGY LN Equity⟩ and ⟨IBCI LN Equity⟩. Both funds are designed to track the corresponding Barclays bond indices. Considering the average bid-ask spread as a ratio of mid-price on each of these ETFs over their entire lifetimes, we find values of 10 and 33 basis points respectively. Thus, the trading costs (at least those measured in terms of bid-ask spreads) for trading the bond ETFs are higher than the maximum permissible cost of 9.3 basis points. Taking the average of the trading costs on the two ETFs, 21.5 basis points, as the approximate cost per trade for the bond trading strategy, it would no longer outperform the equally weighted scheme.

For the US case, we can consider trading costs on the same ETFs that we used to test the scheme in the first place. Considering trading costs in the same way as before, we find these (measured in terms of bid-ask spreads) to be 1 and 2.5 basis points for the nominal and real bond ETFs respectively. Comparing these to the maximum permissible cost of 8.1 basis points for the bond trading strategy, we find that they fall below this figure. Even if the trading costs on the scheme were as high as 2.5 basis points, it would still yield a risk-adjusted annual return in excess of those for the other schemes.

As we have seen here, including transaction costs in the assessment of the performance of a strategy is important. In some cases we may find that strategies that performed well when transaction costs are not considered become less attractive after the consideration of these costs. There are also other trading costs (management fees etc.) which should be considered in a thorough investigation on the viability of a trading strategy like this one.

6.1.4 Trading Strategy Extension to a Multiple Bond Portfolio Case

A natural extension of the trading strategies given above is to consider multiple bond portfolios and the whole IRP term structure surface. We do this here in a simple way, by considering two nominal bond portfolios and two real bond portfolios in the European setting. The data for the bond portfolios that we consider come again from Barclays Indices [3] (as in the case of the simple trading strategy above for European bonds). We choose bond portfolios containing bonds with 3-5 years to maturity and 7-10 years to maturity. Correspondingly, we make use of the 4 and 8 year IRP from the calibrated Vasicek latent factor model to implement the same strategy as before. The period that we consider is September 2004 to May 2013, with an in-sample period 1 October 2004 to 1 March 2008 and an out-of-sample period of 1 April 2008 to 1 May 2013. The results of the strategy are given in Table 6.7 and Figure 6.5.

Bond strategy results					
	Strategy	Nominal	Real	Equal	Random
Return	0.0743	0.0691	0.0594	0.0643	0.0643
Std. Deviation	0.0434	0.0443	0.0451	0.0393	0.0423
Risk Adj. Return	1.7111	1.5599	1.3169	1.6359	1.5264

Table 6.7 Table of results for the multiple bond trading strategy with European bonds. Here we consider the entire time period of the European data set (2004-2013).

Again, we can see that the bond trading strategy performs well relative to the other schemes. Conducting a hypothesis test as before, we again reject the null hypothesis that the mean of the risk-adjusted returns for the random allocation scheme is equal to the risk-adjusted return for the bond trading strategy. This method hints at a more dynamic bond allocation scheme than the simple method considered previously. If we could use the full term structure of the IRP, we could formulate a more specific mechanism for buying and selling nominal and real bonds of different maturities. A further extension of this would be to devise a scheme where we do not have to hold only nominal or real bonds, but rather

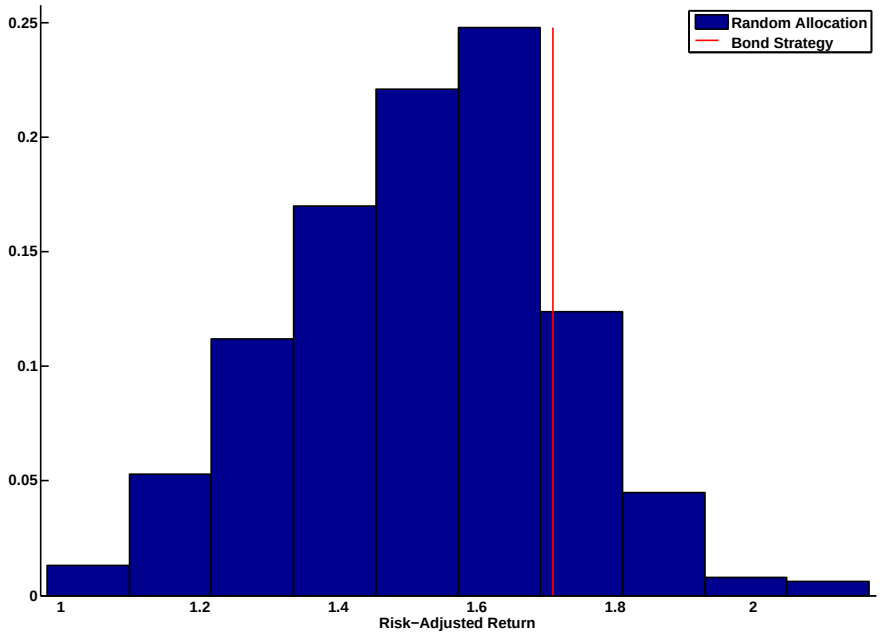

Figure 6.5 Comparison of risk-adjusted return from the multiple bond trading strategy to a histogram of risk-adjusted returns from the random allocation scheme. These results are from the European bond case over the time period 2004 to 2013. 1000 random allocations were used to create the histogram.

where we could hold both types at each point in time (and for each IRP maturity). This would certainly reduce the impact of transaction costs on the strategy.

6.1.5 Drawbacks of the Bond Trading Strategy

There are a number of issues that we found when implementing the bond trading strategy. The first of these is that it is somewhat sensitive to the in-sample and out-of-sample periods chosen to conduct the above tests. In some cases, the results for the strategy with different sample periods were worse than those shown above. Moreover, experimenting with different levels for the IRP as a trigger for the strategy, we did not find any specific region in which "ideal" values lay. Rather, levels of the IRP that produced superior results for the bond trading strategy were scattered in between those that did not. As a result of these considerations, we feel that more research is needed to implement this scheme in practice.

6.2 Estimating Future Inflation

Here, we consider the inflation forecasting abilities of various methods and compare them to that of our calibrated model. We make use of three forecasting methods. The first of these

Inflation Forecasts Performance (RMSE)			
Forecast Type	1 Year	2 Years	5 Years
Model Expected Inflation	10.72	7.67	3.94
Lagged Inflation Rates	16.12	12.09	6.80
Break-Even Inflation Rates	10.98	9.28	9.43
Professional Forecasts	11.11	7.98	4.04

Table 6.8 Table of results showing the forecasting performance of various methods. The values here represent the RMSE of each method in basis points.

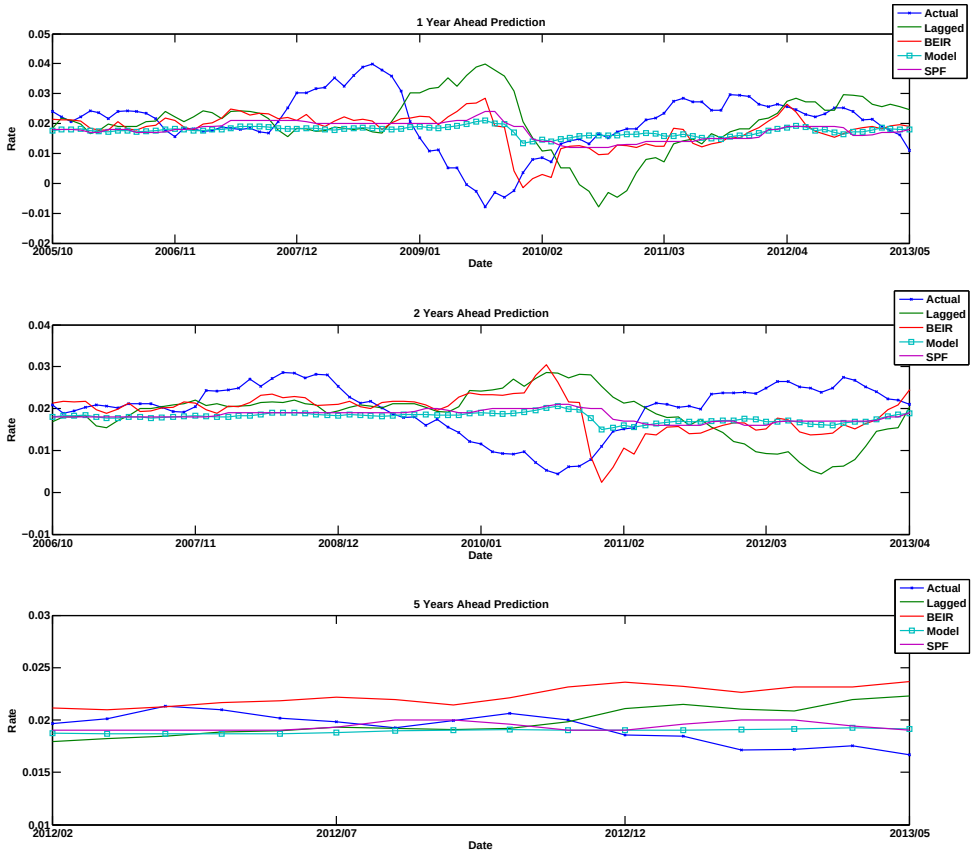

Figure 6.6 Forecasting European HICPxt inflation at 1, 2 and 5 years.

is a naive method whereby we used past inflation as a predictor of future inflation. To do so, we take the inflation rate from as long ago as we would like to forecast inflation in the future (i.e. to forecast inflation 1 year ahead, we take the inflation rate from 1 year ago). The next method is one where we use break-even inflation rates (implied from ZCIISs) as a predictor

of future inflation. Finally, we take inflation forecasts from the ECB's SPF as a method of forecasting inflation. We then compare all of these methods to the actual (realised) inflation rate by computing the RMSE for each method and each forecasting period. This is done only with European data, over the time period October 2004 to May 2013. The results of this are presented in Table 6.8.

The table suggests that the model is able to provide a better forecast of inflation than the other methods are able to. It indicates that the model performs much better than all methods other than that using professional forecasts, where the forecasting accuracy of the two methods is not that different. This reflects the influence of the SPF forecasts on the calibration results, as it is clear that expected inflation in the model follows these quite closely. This is also indicated by the plots in Figure 6.6. Here, we have given an illustrated comparison between the various methods. We can see that the model and SPF forecasts are very flat relative to actual inflation. The methods using lagged inflation and the ZCIIS implied break-even inflation rates, on the other hand, produce more volatile estimates of future inflation. However, their estimations tend to indicate inflation rate movements in the wrong direction, or they fail to capture the timing of the movements. As such, the RMSE values for these methods are relatively high. Thus, it appears that no method produces a convincing estimation of future inflation, although the model-implied method produces the estimate with the smallest error. We could not conclude from these results, however, that the model is a good one to use for expected inflation forecasting and more research would be required to draw such conclusions (see Abrahams, Adrian, Crump and Moench (2012) [1]).

6.3 Out-of-Sample Tests

Another application of the model is to forecast future instrument values. In this section, we perform out-of-sample tests for the model. This gives some indication of the predictive power of the model. To do so, we consider only the European ZCIIS data set - as it was the data set with the longest time period - and calibrate the model to the first part of the data set. We then perform the out-of-sample test on the second part of the data set. The specific time windows that we consider are September 2004 to August 2011 (in-sample) and September 2011 to May 2013 (out-of-sample).

We use two methods for performing the out-of-sample tests. The first is simply to run the Kalman-filter (but not to update the model parameters) on the out-of-sample portion of the data set once the model has been calibrated to the in-sample portion. This illustrates

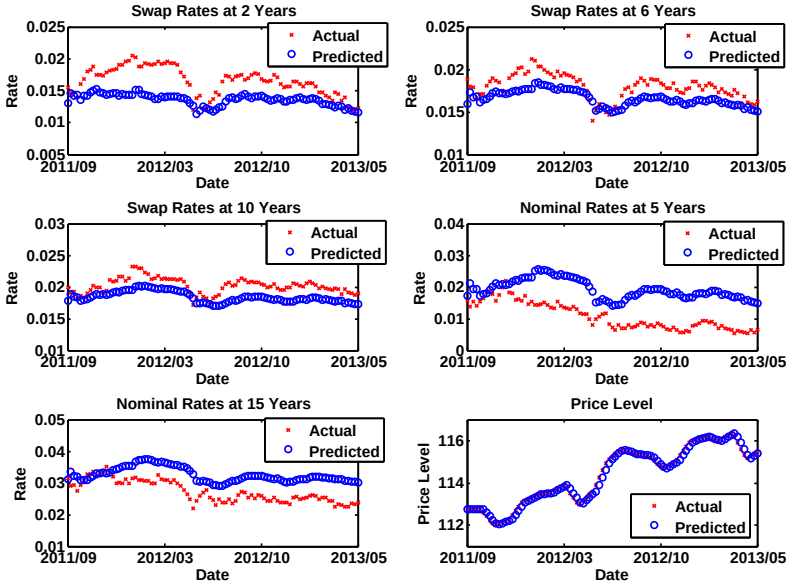

Figure 6.7 Out-of-sample test with Kalman-filter. MSE of fit: 1.4329×10^{-5}.

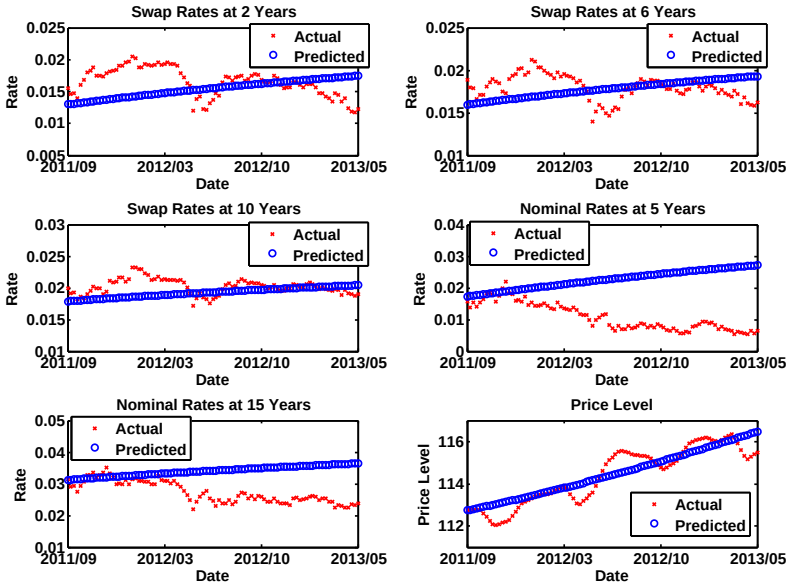

Figure 6.8 Out-of-sample test with model expectations. MSE of fit: 3.2335×10^{-5}.

how well the calibrated model performs in predicting 1 day ahead instrument values in a Kalman-filter framework. The second method is to forecast the state variable by taking its expected value at each point in time, given all information up to the end of the in-sample period. In this way, we get

$$\hat{x}_t = \mathbb{E}\left[x_t | \mathfrak{F}_{t^*}\right],$$

for $t \geq t^*$, where t^* is the end of the in-sample period. Furthermore,

$$\hat{y}_t = A + B\hat{x}_t.$$

This gives us a linear projection of the instrument prices based on the model estimate at the end of the in-sample period. Figures 6.7 and 6.8 illustrate the out-of-sample tests.

From the figures, we can see that performing the out-of-sample test in the Kalman-filter framework allows the model to capture some of the variation of the instrument values, whereas performing the test using model expectations produces a very linear estimate of the asset values. Both out-of-sample tests indicate that the model captures the ZCIIS rates to a reasonable extent. This is more the case for swaps with long maturities than those with short ones. The actual swap rates track the 1 day ahead Kalman-filter implied rates as well as the direction of the linearly projected rates fairly well, although there is a slight spread between the forecasted rates and the actual rates before and after the recent global financial crisis. Considering the nominal rates, we can observe that the predictive power of the model is somewhat worse here than for the other instruments. On the other hand, the model manages to capture the price level process very well out-of-sample. Thus, by considering the plots here, it is hard to say that the model does a perfect job in forecasting the various instrument values out-of-sample, although the performance is not bad. The MSE values of the out-of-sample fits (1.4329×10^{-5} for the Kalman-filter method and 3.2335×10^{-5} for the model expectations method), which are roughly only a multiple of 10 times higher than those for the in-sample fits seen in the previous chapter, also suggest that the model performs reasonably well in this situation. As mentioned already, the data set here is taken over the period of the financial crisis, which is likely to have a negative impact on the forecasting performance of the model. If we consider the same test in the post-crisis period (in-sample: August 2009 to November 2011, out-of-sample: November 2011 to May 2013), we see slightly better results. This is illustrated in Figures 6.9 and 6.10.

Overall, it would appear that the performance of the model out-of-sample is reasonable. It cannot be expected that the model should capture the dynamics of the market as well as it did for the in-sample cases in the previous chapter, but it should be able to predict

the general direction and movement of the market reasonably well. To a reasonable extent, this appears to be the case.

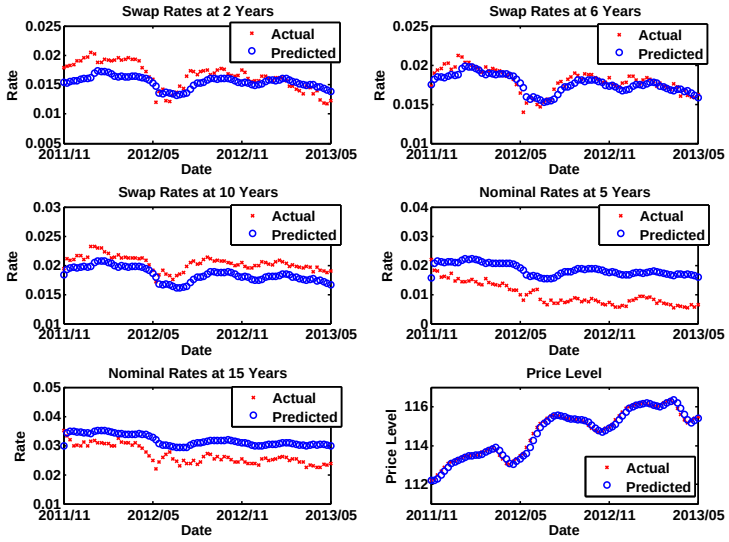

Figure 6.9 Out-of-sample test with Kalman-filter (post-crisis). MSE of fit: 1.2270×10^{-5}.

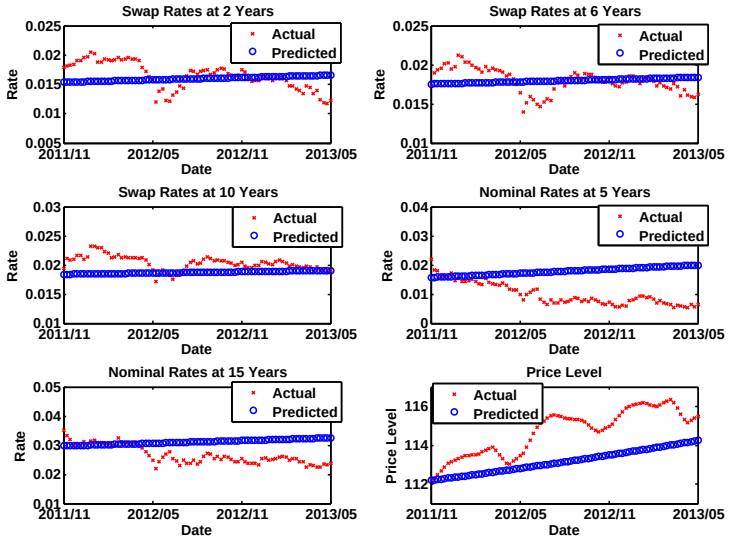

Figure 6.10 Out-of-sample test with model expectations (post-crisis). MSE of fit: 2.5327×10^{-5}.

Chapter 7

Conclusion

In this thesis, we have considered the modelling of inflation with the aim of extracting the inflation risk premium (IRP) from asset prices. For this purpose, it was also necessary to consider the pricing of inflation-indexed derivatives. In a number of sections of this work, we extended the current scope of the literature. Specifically, we considered the extraction of the IRP from option data, which to our knowledge has not yet been considered, and we extended a bond trading strategy that makes use of the IRP to detect the over- or underpricing of nominal bonds relative to real bonds. This work is also continuation of that in Ho, Huang and Yildirim (2012) [28], who suggested a number of new research avenues that could be taken into investigating the IRP.

In the first chapter, we introduced the topic and gave a definition of the IRP. We considered two different methods for extracting the IRP (model-free and model-implied) and we reviewed some of the current literature relating to the modelling of inflation and the extraction of the IRP.

The second chapter was concerned with the modelling framework that we made use of in this thesis. We considered the same framework as that of D'Amico, Kim and Wei (2008) [17] and Ho, Huang and Yildirim (2012) [28] where we assumed that all rates in the market were driven by three latent factors following a mean-reverting Vasicek process. A price level process was coupled to this model and all rates (nominal, real and inflation) in the framework were then shown to be affine transformations of the state vector. This allowed for the specification of nominal and real zero-coupon yields, as well as expected inflation rates as affine transformations of the state vector. From here, we could simply extract the IRP as the difference between the nominal zero-coupon bond yield, and the sum of the real zero-coupon bond yield and the expected inflation rate.

The third chapter of the thesis was concerned with pricing applications. Specifically, we presented formulae for the pricing of zero-coupon inflation-indexed swaps (ZCIISs), year-on-year inflation-indexed swaps (YOYIISs) and inflation-indexed caps and floors (IICFs).

In the fourth chapter, we analysed a Kalman-filter framework for calibrating the model to market data. Here, we presented both the standard and the unscented Kalman-filters as means of approximating the sample log-likelihood function. We also considered methods of maximising this so as to estimate the model parameters.

With the theoretical framework in place, the fifth chapter presented the results of the calibration of the model to market data. First, we performed principal component analyses on our data sets to determine the number of latent factors required to explain the variance of the instruments in the data sets. We also specified the precise parametrisation of the latent factor model that we made use of in the calibration section. For the actual calibration of the model to data, we considered four data sets: a synthetic one, a US one which was taken from the sources specified in Ho, Huang and Yildirim (2012) [28], a European one consisting mainly of ZCIIS rates, as well as a European one consisting mainly of IICF prices. Calibrating the model to the first two data sets allowed us to benchmark our model and evaluate the performance of our calibration routines. We found the performance of these aspects to be good at this point. Calibrating the model to the last two data sets, we obtained good fits of the model to the one consisting mainly of ZCIIS rates, but not as good fits to the one consisting mainly of IICF prices. The latter case required the use of the unscented Kalman-filter (where all previous ones required only the standard Kalman-filter), which to our knowledge had not been performed before. The final section of this chapter was concerned with the extraction of the IRP from the European ZCIIS data. Here, we found that the model-implied IRP was consistent with the model-free IRP. We also considered the model-implied historical IRP over the period 2004-2013 and found that it experienced a large decline at the time of the recent financial crisis. Finally, the term-structure of the IRP at the end of the data set (May 2013) was found to be upward sloping.

The final chapter of the thesis was concerned with applications of the modelling framework. First, we analysed a bond trading strategy in both the US and European markets, which used the IRP to determine the over- or underpricing of nominal bonds relative to real bonds. Our treatment of this strategy was an extension to that in the literature. We found that the strategy performed quite well (on a return and risk-adjusted return basis) relative to three other naive strategies and a random allocation strategy. Considering transaction costs, however we found the performance of the strategy in the European case to be some-

what reduced. Next, we considered the capability of the model in providing a forecast of future inflation. Here, we saw that it provided a better forecast than a number of other methods, but that it seemed to give a forecast of average inflation and failed to capture the volatility of future inflation. Finally, we considered the out-of-sample performance of the model and found this to be reasonably good.

There are also a number of avenues through which our research could be extended. Firstly, it would be interesting to consider other models for the use of extracting the IRP and compare them to this one. The universe of models for such purposes is still quite small and such research would be valuable, particularly if it resulted in the "discovery" of a robust model that was less complex than this one considered here. Secondly, it would be interesting to assess whether the inflation option market could provide better estimates of the IRP as it grows in size. The research into that market in this thesis was limited by the illiquidity of inflation-indexed caps and floors. Moreover, investigations into the use of options to estimate the distribution of future inflation could be a quite useful and an interesting research path to follow into inflation-indexed options. Finally, a number of the applications of the IRP could be explored further; particularly the bond trading strategy and the use of the IRP to help provide a better prediction of future expected inflation, or even as a predictor of future inflation volatility. In the case of the bond trading strategy, it would be interesting to know if a more robust way of choosing a trigger level for the strategy exists. It would also be interesting to assess whether the strategy could be extended to include more bonds and if a more dynamic way of trading such bonds could be found. We hope that further research along these lines is undertaken.

Appendix A

Model Related Derivations

A.1 Deriving the Real Pricing Kernel in the Latent Factor Model

Applying Itô's (product) formula to the expression $M_t^R = M_t^N Q_t$ yields,

$$\begin{aligned}
dM_t^R &= d\left(M_t^N Q_t\right) \\
&= M_t^N dQ_t + Q_t dM_t^N + d\left\langle M^N, Q\right\rangle_t \\
&= M_t^N \left[Q_t \left(r^e\left(X_t\right) + \frac{1}{2}\sigma_q^\top \sigma_q + \frac{1}{2}\varsigma_q^2\right) dt + Q_t\left(\sigma_q^\top dZ_t + \varsigma_q dW_t\right)\right] \\
&\quad \text{(by applying Itô's formula to } f\left(\log\left(Q_t\right)\right), \text{ where } f\left(x\right) = e^x\text{)} \\
&\quad + Q_t\left[-r^N\left(X_t\right) M_t^N dt - \lambda^N\left(X_t\right)^\top M_t^N dZ_t\right] \\
&\quad - \lambda^N\left(X_t\right)^\top \sigma_q M_t^N Q_t dt.
\end{aligned}$$

Substituting for $M_t^N Q_t, r^e\left(X_t\right), r^N\left(X_t\right)$ and $\lambda^N\left(X_t\right)$ and then grouping terms we get

$$\begin{aligned}
dM_t^R &= M_t^R\left(\eta_0^e + \eta_1^{e\top} X_t - \eta_0^N - \eta_1^{N\top} X_t + \frac{1}{2}\sigma_q^\top \sigma_q + \frac{1}{2}\varsigma_q^2 - \gamma^{N\top}\sigma_q - X_t{}^\top \Gamma^{N\top}\sigma_q\right) dt \\
&\quad + M_t^R\left(\sigma_q^\top - \gamma^{N\top} - X_t{}^\top \Gamma^{N\top}\right) dZ_t \\
&\quad + \varsigma_q M_t^R dW_t \\
&= M_t^R\left[\left(\eta_0^e - \eta_0^N + \frac{1}{2}\left(\sigma_q^\top \sigma_q + \varsigma_q^2\right) - \gamma^{N\top}\sigma_q\right) + \left(\eta_1^{e\top} - \eta_1^{N\top} - \sigma_q^\top \Gamma^N\right) X_t\right] dt \\
&\quad + M_t^R\left(\sigma_q^\top - \gamma^{N\top} - X_t{}^\top \Gamma^{N\top}\right) dZ_t \\
&\quad + \varsigma_q M_t^R dW_t \\
&= M_t^R\left[-r^R\left(X_t\right) dt - \lambda^R\left(X_t\right)^\top dZ_t + \varsigma_q dW_t\right],
\end{aligned}$$

where

$$r^R(X_t) := \eta_0^R + {\eta_1^R}^\top X_t,$$

is the formulation we obtain for the dynamics of the real rate, with

$$\begin{aligned}\eta_0^R &:= \eta_0^N - \eta_0^e - \frac{1}{2}\left(\sigma_q^\top \sigma_q + \varsigma_q^2\right) + {\gamma^N}^\top \sigma_q \\ \eta_1^R &:= \eta_1^N - \eta_1^e + {\Gamma^N}^\top \sigma_q.\end{aligned}$$

Furthermore, the real prices of risk are defined by

$$\lambda^R(X_t) := \gamma^R + \Gamma^R X_t,$$

where

$$\begin{aligned}\gamma^R &:= \gamma^N - \sigma_q \\ \Gamma^R &:= \Gamma^N.\end{aligned}$$

A.2 Decomposing the Inflation Risk Premium in the Latent Factor Model

In this section, we decompose the IRP in the latent factor model into two separate terms. To start with, we know that

$$P_{t,T}^N = \mathbb{E}_t\left[\frac{M_T^N}{M_t^N}\right]$$

and that

$$M_t^R = M_t^N Q_t$$

so

$$\begin{aligned}P_{t,T}^N &= \mathbb{E}_t\left[\frac{M_T^R}{M_t^R}\frac{Q_t}{Q_T}\right] \\ &= \mathbb{E}_t\left[\frac{M_T^R}{M_t^R}\right]\mathbb{E}_t\left[\frac{Q_t}{Q_T}\right] + \mathbb{C}\mathrm{ov}_t\left[\frac{M_T^R}{M_t^R}\frac{Q_t}{Q_T}\right] \\ &= \mathbb{E}_t\left[\frac{M_T^R}{M_t^R}\right]\mathbb{E}_t\left[\frac{Q_t}{Q_T}\right]\left[1 + \frac{\mathbb{C}\mathrm{ov}_t\left[\frac{M_T^R}{M_t^R}\frac{Q_t}{Q_T}\right]}{\mathbb{E}_t\left[\frac{M_T^R}{M_t^R}\right]\mathbb{E}_t\left[\frac{Q_t}{Q_T}\right]}\right] \\ &= P_{t,T}^R\,\mathbb{E}_t\left[\frac{Q_t}{Q_T}\right]\exp\left\{\mathbb{E}_t\left[\log\left(\frac{Q_t}{Q_T}\right)\right] - \mathbb{E}_t\left[\log\left(\frac{Q_t}{Q_T}\right)\right]\right\}\left[1 + \frac{\mathbb{C}\mathrm{ov}_t\left[\frac{M_T^R}{M_t^R}\frac{Q_t}{Q_T}\right]}{\mathbb{E}_t\left[\frac{M_T^R}{M_t^R}\right]\mathbb{E}_t\left[\frac{Q_t}{Q_T}\right]}\right].\end{aligned}$$

Now,

$$y_{t,T}^N = -\frac{1}{\tau}\log\left(P_{t,T}^N\right)$$

and

$$y_{t,T}^R = -\frac{1}{\tau}\log\left(P_{t,T}^R\right),$$

so

$$y_{t,T}^N = y_{t,T}^R + \frac{1}{\tau}\mathbb{E}_t\left[\log\left(\frac{Q_T}{Q_t}\right)\right] - \frac{1}{\tau}\left[\log\left(\mathbb{E}_t\left[\frac{Q_t}{Q_T}\right]\right) - \mathbb{E}_t\left[\log\left(\frac{Q_t}{Q_T}\right)\right]\right] - \frac{1}{\tau}\log\left[1 + \frac{\mathbb{C}\text{ov}_t\left[\frac{M_T^R}{M_t^R}\frac{Q_t}{Q_T}\right]}{\mathbb{E}_t\left[\frac{M_T^R}{M_t^R}\right]\mathbb{E}_t\left[\frac{Q_t}{Q_T}\right]}\right].$$

Since we know that the extended Fisher equation is given by

$$y_{t,T}^N = y_{t,T}^R + i_{t,T}^e + \phi_{t,T},$$

and

$$i_{t,T}^e = \frac{1}{\tau}\mathbb{E}_t\left[\log\left(\frac{Q_T}{Q_t}\right)\right]$$

we have that

$$\phi_{t,T} = -\frac{1}{\tau}\left[\log\left(\mathbb{E}_t\left[\frac{Q_t}{Q_T}\right]\right) - \mathbb{E}_t\left[\log\left(\frac{Q_t}{Q_T}\right)\right]\right] - \frac{1}{\tau}\log\left[1 + \frac{\mathbb{C}\text{ov}_t\left[\frac{M_T^R}{M_t^R}\frac{Q_t}{Q_T}\right]}{\mathbb{E}_t\left[\frac{M_T^R}{M_t^R}\right]\mathbb{E}_t\left[\frac{Q_t}{Q_T}\right]}\right].$$

Defining

$$\mathcal{J}_{t,T} := -\frac{1}{\tau}\left[\log\left(\mathbb{E}_t\left[\frac{Q_t}{Q_T}\right]\right) - \mathbb{E}_t\left[\log\left(\frac{Q_t}{Q_T}\right)\right]\right]$$

$$\mathcal{C}_{t,T} := -\frac{1}{\tau}\log\left[1 + \frac{\mathbb{C}\text{ov}_t\left[\frac{M_T^R}{M_t^R}, \frac{Q_t}{Q_T}\right]}{\mathbb{E}_t\left[\frac{M_T^R}{M_t^R}\right]\mathbb{E}_t\left[\frac{Q_t}{Q_T}\right]}\right].$$

we get that

$$\phi_{t,T} = \mathcal{J}_{t,T} + \mathcal{C}_{t,T}.$$

A.3 Deriving the Expected Inflation Dynamics in the Latent Factor Model

Here we outline how to show that

$$\frac{1}{\tau}\mathbb{E}_t\left[\log\left(\frac{Q_T}{Q_t}\right)\right] = a_\tau^e + b_\tau^{e\top} X_t,$$

where

$$a_\tau^e = \eta_0^e + \frac{1}{\tau}\eta_1^{e\top}\int_0^\tau \left(\mathbf{I}_n - e^{-\mathcal{K}s}\right)\theta ds$$

$$b_\tau^e = \frac{1}{\tau}\int_0^\tau e^{-\mathcal{K}^\top s}\eta_1^e ds.$$

Firstly, we have from (2.2) and the short-rate process for inflation that

$$\log\left(\frac{Q_T}{Q_t}\right) = \int_t^T \eta_0^e ds + \int_t^T \eta_1^{e\top} X_s ds + \int_t^T \sigma_q^\top dZ_s + \int_t^T \varsigma_q dW_s. \tag{A.1}$$

Next, it is commonly known (see, for instance, Filipovic (2009) [22]) that the solution of the Vasicek process can be expressed as

$$X_s = e^{-\mathcal{K}(s-t)} X_t + \left(\mathbf{I}_n - e^{-\mathcal{K}(s-t)}\right)\theta + \Sigma \int_t^s e^{-\mathcal{K}(s-t)} dZ_u \tag{A.2}$$

for $t \leq s$. Inserting (A.2) into (A.1) and taking expectations, we get that

$$\begin{aligned}\mathbb{E}_t\left[\log\left(\frac{Q_T}{Q_t}\right)\right] &= \int_t^T \eta_0^e ds + \int_t^T \eta_1^{e\top} e^{-\mathcal{K}(s-t)} X_t ds + \int_t^T \eta_1^{e\top}\left(\mathbf{I}_n - e^{-\mathcal{K}(s-t)}\right)\theta ds \\ &= \eta_0^e \tau + \left(\int_0^\tau e^{-\mathcal{K}^\top s}\eta_1^e ds\right)^\top X_t + \eta_1^{e\top}\int_0^\tau \left(\mathbf{I}_n - e^{-\mathcal{K}s}\right)\theta ds,\end{aligned}$$

where $\tau = T - t$. This is possible, since the integrands of the above stochastic integrals are all bounded and their expectations are all equal to 0. Dividing the above expression by τ and grouping the terms, we get the desired expression.

Appendix B

Optimisation Routines

B.1 The Nelder-Mead Simplex Algorithm

The Nelder-Mead simplex algorithm is used in Matlab's unconstrained optimiser, *fminsearch*. The algorithm is simply explained in Lagarias, Reeds, Wright and Wright (1998) [32] and we draw from this paper for our brief overview of the scheme here.

The Nelder-Mead simplex method is a member of the family of direct search methods, as it does not compute any derivatives of the function it is trying to optimise. It operates through the use of a non-degenerate simplex - a convex, non-zero volumed N-dimensional figure with $N+1$ vertices - at each step in the algorithm. The $N+1$ vertices of the simplex are defined on the parameter space (so that N represents the number of parameters) and the function values at each of these is computed. We define the function that we are trying to optimise as $g(x)$, where x is a real-valued, N-dimensional vector. The algorithm then proceeds as follows.

Initialisation. Specify the four parameters that define the algorithm: $a > 0$, $b > \max(1, a)$, $0 < c < 1$ and $0 < d < 1$ (often[1] $a = 1$, $b = 2$, $c = \frac{1}{2}$, $d = \frac{1}{2}$).

Then, at any iteration k in the algorithm, **do**:

Order. Order the x_i, $i = 1, \ldots, N+1$ such that $g(x_1) \leq g(x_2) \leq \cdots \leq g(x_{N+1})$.

Reflect. Compute the reflection point $x_r = \hat{x} + a(\hat{x} - x_{N+1})$, where $\hat{x} = \frac{1}{N}\sum_{i=1}^{N} x_i$, and calculate $g(x_r)$. If $g(x_1) \leq g(x_r) < g(x_N)$, replace x_{N+1} with x_r and move on to iteration $k+1$. Otherwise continue.

[1] See Lagarias, Reeds, Wright and Wright (1998) [32].

Expand. If $g(x_r) < g(x_1)$, calculate the expansion point $x_e = \hat{x} + b(x_r - \hat{x})$ and calculate $g(x_e)$. If $g(x_e) < g(x_r)$, replace x_{N+1} with x_e and move on to iteration $k+1$. Otherwise, replace x_{N+1} with x_r and move on to iteration $k+1$.

Contract. If $g(x_r) \geq g(x_N)$, perform a contraction:

Contract Outside. If $g(x_N) \leq g(x_r) < g(x_{N+1})$, perform an outside contraction $x_{co} = \hat{x} + c(x_r - \hat{x})$ and calculate $g(x_{co})$. If $g(x_{co}) \leq g(x_r)$, replace x_{N+1} with x_{co} and move on to iteration $k+1$. Otherwise, continue.

Contract Inside. If $g(x_r) \geq g(x_{N+1})$, perform an inside contraction $x_{ci} = \hat{x} - c(\hat{x} - x_{N+1})$ and calculate $g(x_{ci})$. If $g(x_{ci}) < g(x_{N+1})$, replace x_{N+1} with x_{ci} and move on to iteration $k+1$. Otherwise, continue.

Shrink. Calculate $g(y_i)$ for $i = 2, \ldots, N+1$, where $y_i = x_1 + d(x_i - x_1)$ and replace $x_2, \ldots, x_{N+1}$ with (the unordered vertices) $y_2, \ldots, y_{N+1}$ in the next iteration. Move on to iteration $k+1$.

It is also important to adopt tie-breaking rules for re-ordering the vertices when the function value evaluated at the new vertex matches that at (at least) another vertex. In this case, Lagarias, Reeds, Wright and Wright (1998) [32] assign to the new vertex the greatest possible index such that the ordering rule is still observed.

The Nelder-Mead simplex algorithm is useful for high-dimensional optimisation problems, where it is difficult or impossible to calculate the derivatives of the objective function at various points.

B.2 The Genetic Algorithm

Another optimisation routine that we make use of is a form of the genetic algorithm[2] (GA). GAs apply the principles of natural selection and evolution to the optimisation of an objective function. In this way, individual points in the parameter space that best optimise the objective function are selected over those that do not. Such an algorithm begins by choosing a population of individuals (that is a set of initial points in the parameter space) and assigning fitness values to these individuals depending on how well they optimise the objective function. These fitness values are used to decide which individuals are allowed to "reproduce" in order to create subsequent population generations. As such, individuals in

[2]This section gives a brief overview of the form of the genetic algorithm employed in this thesis. The actual code used to run the genetic algorithm for calibration purposes in this thesis was developed by the author. The content here is based on that in Poklewski-Koziell (2012) [37].

the population with low fitness values (that do not provide good solutions to the optimisation problem) start to die out and those with high fitness values (that do provide good solutions to the optimisation problem) survive. Once the algorithm has finished, the fittest individual at the end should provide the user with the point in the parameter space at which the global optimum of the objective function lies. We refer to the book by Coley (2010) [15] regularly in our treatment of GAs. Coley (2010) [15] presents the principles behind GAs in a concise manner and demonstrates how such algorithms could be implemented in practice.

To introduce the concept behind the algorithm that we use, consider the situation where we are trying to optimise an objective function with respect to a number of parameters. We initialise the algorithm by randomly generating a population of N individuals in the form of N strings of binary digits. The bit strings are all of equal length and each one can be thought of (in a biological sense) as the chromosome of the relevant individual. The next step in the algorithm is to compute the fitness of each individual in the population. This is done by first converting the bit strings of all the individuals into points in the parameter space. Each point represents a possible solution to the optimisation problem and individuals are then assigned fitness values according to how well these points satisfy the optimisation task. Next, the fitness values assigned to the individuals are scaled to prevent an individual, or a group of individuals, from dominating the algorithm. This can impact negatively on the convergence of the algorithm to a global optimum. From here, the individuals undergo the processes of selection, crossover, mutation and elitism in order to produce a new, hopefully fitter, population of individuals. The processes of fitness evaluation, selection, crossover and mutation are then repeated over and over to create successive generations of populations, until the algorithm converges. The fittest individual in the last generation of the algorithm should then provide a global optimum for the objective function. We briefly outline the selection, crossover and mutation aspects of the algorithm below.

Selection. In the selection component of the GA, certain individuals in the population are chosen to "reproduce", whilst the rest of population is discarded. Individuals are selected according to their scaled fitness values such that individuals with higher fitness values have a greater chance of being selected than those with lower ones. This operation can be implemented in the following way:

1. A random number between 0 and the total scaled fitness of all individuals in the population is generated.

2. Starting from the first individual in the population, the cumulative sum of the scaled fitness values is calculated.

3. Comparing the random number to the cumulative sum of scaled fitness values, the first individual responsible for making this sum larger than the random number is selected.

Generally, two individuals are selected simultaneously in this manner and are then allowed to "reproduce". Obviously, this method allows a single individual to be selected more than once.

Crossover. Crossover is the component of the algorithm where selected individuals "reproduce". Generally, this step is performed in conjunction with the selection step. To perform crossover, we first draw a random integer between 1 and the bit string length of the individuals in the population, giving us the point in the bit strings of two selected individuals where the crossover is to be performed. The actual crossover occurs by swapping the tails of the two bit strings after this point, thus creating two new individuals. Often, a probability is assigned to the crossover operation so that individuals sometimes "reproduce" exact replicas of themselves. Once selection and crossover have been performed, a new population of individuals arises and replaces the old population.

Mutation. The operation of mutation is performed after the selection and crossover steps of the algorithm. It is a simple operation and is performed by randomly swapping some of the bits in the bit strings of each individual in the new population from a 0 to a 1 or a 1 to a 0. This is performed with a small probability, usually given as 1 over the total bit string length of the individuals. This operation adds a further element of randomness to the algorithm and helps to prevent the algorithm from converging to a local optimum.

Elitism. Elitism is the final operation that we consider in our implementation of the GA. This operation is carried out by ensuring that the fittest individual across all generations remains in the population until the end of the algorithm. To do so, we ensure that if the fittest individual in the previous generation of the algorithm has a greater fitness value than that in the current generation, then that individual is selected to replace a random individual in the current generation.

GAs are effective tools to use when conducting optimisation routines on objective functions which are non-linear, non-convex and multi-modal. In such a situation, a GA is usually more effective than local optimisation schemes, although GAs are generally computationally intensive and often take a long time to converge to a solution. They also do not guarantee that a global optimum will be found, however they should at least find a point very close to the global optimum (see Coley [15]).

Appendix C

Selected Matlab Code

C.1 Instrument Prices in the Vasicek Latent Factor Model

C.1.1 Nominal Zero-Coupon Yields

```
%-------------------------------------------------------------------------
% Warrick Poklewski-Koziell
% MSc UZH/ETH QF Thesis
% Inflation Modelling: Risk Premia and Derivative Pricing
%-------------------------------------------------------------------------
% Title: ODE Solver for Nominal Yields in the Vasicek Latent Factor Model.
% Description: This function solves the ODE equations dAdtau and dBdtau in
% the nominal bond pricing problem for the Vasicek latent factor inflation
% model.
% Date: May 2013
%-------------------------------------------------------------------------

function [aNom,bNom] = VasicekFactorModelNomYieldODE(tau,eta1N,eta0N,...
    Kappa,theta,Sigma,gammaN,GammaN)

[rows,cols] = size(tau);
if rows > 1 && cols > 1
    error('tau must be a vector input of instrument maturities')
end

lenA = length(eta0N);
lenB = length(eta1N);
lentau = length(tau);
aNom = zeros(lentau,lenA);
bNom = zeros(lentau,lenB);
```

```
for t = 1:lentau
    % ODE solver for dBdtau
    dBdtau =@(t,x) -eta1N - (Kappa + Sigma*GammaN)'*x;
    [~,B] = ode23(dBdtau,[0 tau(t)],[0 0 0]');
    B = B(end,:)';
    % ODE solver for dAdtau
    dAdtau =@(t,x) -eta0N + B'*(Kappa*theta-Sigma*gammaN)...
        + 0.5*B'*(Sigma*Sigma')*B;
    [~,A] = ode23(dAdtau,[0,tau(t)],0);
    aNom(t,:) = -A(end)/tau(t);
    bNom(t,:) = -B/tau(t);
end
end
```

C.1.2 Real Zero-Coupon Yields

```
%-------------------------------------------------------------------------
% Warrick Poklewski-Koziell
% MSc UZH/ETH QF Thesis
% Inflation Modelling: Risk Premia and Derivative Pricing
%-------------------------------------------------------------------------
% Title: ODE Solver for Real Yields in the Vasicek Latent Factor Model.
% Description: This function solves the ODE equations dAdtau and dBdtau in
% the real bond pricing problem for the Vasicek latent factor inflation
% model.
% Date: May 2013
%-------------------------------------------------------------------------

function [aReal,bReal] = VasicekFactorModelRealYieldODE(tau,eta1R,eta0R,...
    Kappa,theta,Sigma,gammaR,GammaR)

[rows,cols] = size(tau);
if rows > 1 && cols > 1
    error('tau must be a vector input of instrument maturities')
end

lenA = length(eta0R);
lenB = length(eta1R);
lentau = length(tau);
aReal = zeros(lentau,lenA);
bReal = zeros(lentau,lenB);
for t = 1:lentau
    % ODE solver for dBdtau
    dBdtau =@(t,x) -eta1R - (Kappa + Sigma*GammaR)'*x;
```

```
    [~,B] = ode23(dBdtau,[0 tau(t)],[0 0 0]');
    B = B(end,:)';
    % ODE solver for dAdtau
    dAdtau =@(t,x) -eta0R + B'*(Kappa*theta-Sigma*gammaR)...
       + 0.5*B'*(Sigma*Sigma')*B;
    [~,A] = ode23(dAdtau,[0,tau(t)],0);
    aReal(t,:) = -A(end)/tau(t);
    bReal(t,:) = -B/tau(t);
end
end
```

C.1.3 Zero-Coupon Inflation-Indexed Swap Rates

```
%-------------------------------------------------------------------------
% Warrick Poklewski-Koziell
% MSc UZH/ETH QF Thesis
% Inflation Modelling: Risk Premia and Derivative Pricing
%-------------------------------------------------------------------------
% Title: ODE Solver for ZCIIS Rates in the Vasicek Latent Factor Model.
% Description: This function solves the ODE equations dAdtau and dBdtau in
% both the real and nominal bond pricing problems and combines the
% solutions to solve the ZCIIS pricing problem for the Vasicek latent
% factor inflation model.
% Date: May 2013
%-------------------------------------------------------------------------

function [aZCIIS,bZCIIS] = VasicekFactorModelZCIISRateODE(tau,eta1N,...
    eta0N,eta1R,eta0R,Kappa,theta,Sigma,gammaN,GammaN,gammaR,GammaR)

[rows,cols] = size(tau);
if rows > 1 && cols > 1
    error('tau must be a vector input of instrument maturities')
end

lenA = length(eta0N);
lenB = length(eta1N);
lentau = length(tau);
aZCIIS = zeros(lentau,lenA);
bZCIIS = zeros(lentau,lenB);
for t = 1:lentau
    % Nominal
    % ODE solver for dBdtau
    dBdtau =@(t,x) -eta1N - (Kappa + Sigma*GammaN)'*x;
    [~,B] = ode23(dBdtau,[0 tau(t)],[0 0 0]');
```

```
    B = B(end,:)';
    % ODE solver for dAdtau
    dAdtau =@(t,x) -eta0N + B'*(Kappa*theta-Sigma*gammaN)...
        + 0.5*B'*(Sigma*Sigma')*B;
    [~,A] = ode23(dAdtau,[0,tau(t)],0);
    aNom = -A(end)/tau(t);
    bNom = -B/tau(t);

    % Real
    % ODE solver for dBdtau
    dBdtau =@(t,x) -eta1R - (Kappa + Sigma*GammaR)'*x;
    [~,B] = ode23(dBdtau,[0 tau(t)],[0 0 0]');
    B = B(end,:)';
    % ODE solver for dAdtau
    dAdtau =@(t,x) -eta0R + B'*(Kappa*theta-Sigma*gammaR)...
       + 0.5*B'*(Sigma*Sigma')*B;
    [~,A] = ode23(dAdtau,[0,tau(t)],0);
    aReal = -A(end)/tau(t);
    bReal = -B/tau(t);

    % ZCIIS
    aZCIIS(t,:) = aNom - aReal;
    bZCIIS(t,:) = bNom - bReal;
end
end
```

C.1.4 Expected Inflation

```
%-------------------------------------------------------------------------
% Warrick Poklewski-Koziell
% MSc UZH/ETH QF Thesis
% Inflation Modelling: Risk Premia and Derivative Pricing
%-------------------------------------------------------------------------
% Title: Solver for expected inflation in the Vasicek Latent Factor Model.
% Description: This function finds the factor loadings aEInf and bEInf for
% calculating expected inflation is the Vasicek latent factor inflation
% model.
% Date: June 2013
%-------------------------------------------------------------------------

function [aEInf,bEInf] = VasicekFactorModelEInflat(tau,eta0e,eta1e,...
    Kappa,theta)

    [rows,cols] = size(tau);
```

```
    if rows > 1 && cols > 1
        error('tau must be a vector input of instrument maturities')
    end

    lenA = length(eta0e);
    lenB = length(eta1e);
    lentau = length(tau);
    aEInf = zeros(lentau,lenA);
    bEInf = zeros(lentau,lenB);
    for t = 1:lentau
        % Expected inflation
        Integranda =@(s) (eye(size(Kappa))-exp(Kappa*s));
        Integrandb =@(s) exp(-Kappa'*s);
        aEInf(t,:) = eta0e + 1/tau(t)*eta1e'...
            *integral(Integranda,0,tau(t),'ArrayValued',true)*theta;
        bEInf(t,:) = 1/tau(t)*integral(Integrandb,0,tau(t),...
            'ArrayValued',true)*eta1e;
    end
end
```

C.2 The Kalman-Filter

```
%-------------------------------------------------------------------------
% Warrick Poklewski-Koziell
% MSc UZH/ETH QF Thesis
% Inflation Modelling: Risk Premia and Derivative Pricing
%-------------------------------------------------------------------------
% Title: General implementation of the Kalman-filter with MLE
% Description: General implementation of the Kalman-filter with MLE
% Date: May 2013
%-------------------------------------------------------------------------

function [logl neglogl x yest] = KalmanFilterMLE(y,x_0,Q_0,A,B,e,C,D,...
    eta,ntpts)

    % This function implements the Kalman-filter on the following system:
    % y(t) = A + Bx(t) + v(t)
    % x(t) = C + Dx(t-1) + w(t)
    % where v ~ N(0,e)
    %       w ~ N(0,eta)

    ninsts = size(y,1);
    logl = zeros(ntpts-1,1);
```

```
    x = zeros(length(x_0),ntpts);
    x(:,1) = x_0;
    yest = zeros(ninsts,ntpts-1);
    for iter = 1:ntpts-1

       % Prediction
       x_1 = C + D*x_0;
       Q_1 = D*Q_0*D' + eta;

       % Error decomposition
       yest(:,iter) = A + B*x_1;
       v = -(yest(:,iter) - y(:,iter));
       V = B*Q_1*B' + e;

       % Log-likelihood function
       Vinv = V\eye(length(V));
       detV = det(V);
       if detV <= 0
            detV = 1e-10;
       end
       logl(iter) = -ninsts/2*log(2*pi)-0.5*log(detV)-0.5*v'*Vinv*v;

       % Updating equations
       Kgain = Q_1*B'*Vinv;
       x_1 = x_1 + Kgain*v;
       Q_1 = Q_1 - Kgain*B*Q_1;
       x_0 = x_1;
       Q_0 = Q_1;
       x(:,iter+1) = x_1;
    end
    logl = sum(logl);
    neglogl = -logl;

end
```

C.3 The Unscented Kalman-Filter

The following code is based on that by Cao (2010) [11].

```
%-------------------------------------------------------------------------
% Warrick Poklewski-Koziell
% MSc UZH/ETH QF Thesis
% Inflation Modelling: Risk Premia and Derivative Pricing
%-------------------------------------------------------------------------
```

```
% Title: General implementation of the unscented Kalman-filter with MLE
% Description: General implementation of the unscented Kalman-filter with
% MLE. Based on code by Yi Cao at Cranfield University.
% Date: June 2013
%-------------------------------------------------------------------------

function [logl neglogl x y1] = UnscentedKalmanFilterMLE(y,x_0,Q_0,...
    hfun,e,ffun,eta)

    % This function implements the unscented Kalman-filter for nonlinear
    % systems. Noises are assumed to be additive. Solves the system:
    % y_t   = h(x_t) + v_t
    % x_t   = f(x_t-1) + w_t
    % where v ~ N(0,e)
    %       w ~ N(0,eta)

    % Initialisation
    [ninsts,ntpts] = size(y);
    numfacts = numel(x_0);
    logl = zeros(ntpts-1,1);
    x = zeros(length(x_0),ntpts);
    x(:,1) = x_0;
    Q = Q_0;

    % Calculate constants for sigma points
    M = numfacts;
    nu = 1e-3;
    kappa = 3-M;
    lambda = nu^2*(M+kappa)-M;
    gamma = M+lambda;

    for iter = 1:ntpts-1

        % Calculate sigma points
        X = sigmavect(x(:,iter),Q,sqrt(gamma));

        % Weights
        varpi = 2;
        wMU = [lambda/gamma repmat(0.5/gamma,1,2*M)];
        wQ = wMU;
        wQ(1) = wQ(1)+(1-nu^2+varpi);

        % Time-update equations
        [x1,~,Q1,~] = unscentedtransform(ffun,X,wMU,wQ,M,eta);
        % Calculate augmented sigma points
```

```
        X1 = sigmavect(x1,Q1,sqrt(gamma));
        X2 = X1 - x1(:,ones(1,size(X1,2)));
        [y1,~,Q2,Y2]=unscentedtransform(hfun,X1,wMU,wQ,ninsts,e);

        % Measurement-update equations
        Q12 = X2 * diag(wQ) * Y2';
        invQ2 = eye(size(Q2))/Q2;
        K = Q12 * invQ2;
        v = y(:,iter) - y1;
        x(:,iter+1) = x1 + K * v;
        Q = Q1 - K * Q12';

        % Log-likelihood
        detQ2 = det(Q2);
        if detQ2 <= 0
             detQ2 = 1e-10;
        end
        logl(iter) = -ninsts/2*log(2*pi)-0.5*log(detQ2)-0.5*v'*invQ2*v;
    end
    logl = sum(logl);
    neglogl = -logl;
end

function [y,Y,Q,Y1] = unscentedtransform(f,X,wMU,wQ,n,R)
    m = size(X,2);
    y = zeros(n,1);
    Y = zeros(n,m);
    for k = 1:m
        Y(:,k) = f(X(:,k));
        y = y + wMU(k) * Y(:,k);
    end
    Y1 = Y - y(:,ones(1,m));
    Q = Y1 * diag(wQ) * Y1' + R;
end

function X = sigmavect(x,Q,gamma)
    shift = gamma*chol(Q,'lower');
    Y = x(:,ones(1,numel(x)));
    X = [x Y+shift Y-shift];
end
```

Bibliography

[1] Abrahams, M., Adrian, T., Crump, R., Moench, E., *Pricing TIPS and Treasuries with Linear Regressions*, FRB of New York Staff Report (2012), no. 570.

[2] Ang, A., Bekaert, G., Wei, M., *The Term Structure of Real Rates and Expected Inflation*, The Journal of Finance **63** (2008), no. 2, 797–849.

[3] Barclays, *Barclays Capital Indices*, Available at https://indices.barcap.com/index.dxml.

[4] Bekaert, G., Wang, X., *Inflation Risk and The Inflation Risk Premium*, Economic Policy **25** (2010), no. 64, 755–806.

[5] Belgrade, N., Benhamou, E., *Reconciling Year on Year and Zero Coupon Inflation Swap: A Market Model Approach*, (2004), Available at http://ssrn.com/abstract=583641 or http://dx.doi.org/10.2139/ssrn.583641.

[6] Berndt, E., Hall, B., Hall, R., Hausman, J., *Estimation and Inference in Nonlinear Structural Models*, Annals of Economic and Social Measurement, vol. 3, National Bureau of Economic Research, 1974, pp. 653–665.

[7] Brigo, D., Mercurio, F., *Interest Rate Models - Theory and Practice: With Smile, Inflation and Credit*, Springer Finance, Springer Berlin Heidelberg, 2006.

[8] Buraschi, A., Jiltsov, A., *Inflation Risk Premia and the Expectations Hypothesis*, Journal of Financial Economics **75** (2005), no. 2, 429–490.

[9] Campbell, J., Shiller, R., *A Scorecard for Indexed Government Debt*, NBER Macroeconomics Annual **11** (1996), 155–208.

[10] Campbell, J., Shiller, R., Viceira, L., *Understanding Inflation-Indexed Bond Markets*, Brookings Papers on Economic Activity **2009** (2009), no. 1, 79–120.

[11] Cao, Y., *Learning the Unscented Kalman-Filter*, 2010, Available Online at Matlab Central http://www.mathworks.com/matlabcentral/fileexchange/18217-learning-the-unscented-kalman-filter.

[12] Chen, R., Liu, B., Cheng, X., *Inflation, Fisher Equation, and the Term Structure of Inflation Risk Premia: Theory and Evidence from TIPS*, (2005), Available at http://papers.ssrn.com/sol3/papers.cfm?abstract_id=809346.

[13] Chernov, M., Mueller, P., *The Term Structure of Inflation Expectations*, Journal of Financial Economics (2012).

[14] Christensen, J., Lopez, J., Rudebusch, G., *Inflation Expectations and Risk Premiums in an Arbitrage Free Model of Nominal and Real Bond Yields*, Journal of Money, Credit and Banking **42** (2010), 143–178.

[15] Coley, D., *An Introduction to Genetic Algorithms for Scientists and Engineers*, World Scientific, 2010.

[16] Dai, Q., Singleton, K., *Specification Analysis of Affine Term Structure Models*, The Journal of Finance **55** (2000), no. 5, 1943–1978.

[17] D'Amico, S., Kim, D., Wei, M., *Tips from TIPS: the Informational Content of Treasury Inflation-Protected Security prices*, (2008), Available at http://www.federalreserve.gov/pubs/feds/2010/201019.

[18] Deacon, M., Derry, A., Mirfendereski, D., *Inflation-Indexed Securities: Bonds, Swaps and other Derivatives*, John Wiley & Sons, 2004.

[19] Duffie, D., Kan, R., *A Yield-Factor Model Of Interest Rates*, Mathematical Finance **6** (1996), no. 4, 379–406.

[20] Ejsing, J., Garcia, J., Werner, T., *The Term Structure of Euro Area Break-Even Inflation Rates and the Impact of Seasonality*, ECB Working Paper Series (2007), no. 830.

[21] Evans, D., *Real Rates, Expected Inflation, and Inflation Risk Premia*, The Journal of Finance **53** (1998), no. 1, 187–218.

[22] Filipović, D., *Term-Structure Models: A Graduate Course*, Springer, 2009.

[23] Garcia, J., Werner, T., *Inflation Risks and Inflation Risk Premia*, ECB Working Paper Series (2010), no. 1162.

[24] Grishchenko, O., Huang, J., *The Inflation Risk Premium: Evidence from the TIPS Market*, (2012), Available at http://papers.ssrn.com/sol3/papers.cfm?abstract_id=2147016.

[25] Hamilton, J., *Time Series Analysis*, Princeton University Press, 1994.

[26] Harvey, A., *Forecasting, structural time series models and the Kalman filter*, Cambridge University Press, 1989.

[27] Haubrich, J., Pennacchi, G., Ritchken, P., *Inflation Expectations, Real Rates, and Risk Premia: Evidence from Inflation Swaps*, Review of Financial Studies **25** (2012), no. 5, 1588–1629.

[28] Ho, H., Huang, H., Yildirim, Y., *Affine Model of Inflation-Indexed Derivatives and Inflation Risk Premium*, (2012), Available at http://dx.doi.org/10.2139/ssrn.1945575.

[29] iShares, *iShares by Blackrock Website*, Available at http://www.ishares.com/.

[30] Jarrow, R., Yildirim, Y., *Pricing Treasury Inflation Protected Securities and Related Derivatives using an HJM Model*, Journal of Financial and Quantitative Analysis **38** (2003), no. 2, 409–430.

[31] Kitsul, Y., Wright, J., *The Economics of Options-Implied Inflation Probability Density Functions*, Tech. report, National Bureau of Economic Research, 2012.

[32] Lagarias, J., Reeds, J., Wright, M., Wright, P., *Convergence Properties of the Nelder–Mead Simplex Method in Low Dimensions*, SIAM Journal on Optimization **9** (1998), no. 1, 112–147.

[33] Lemaire, N., Plante, J., *Boost Your Bonds*, Canadian Investment Review (2009).

[34] Litterman, R., Scheinkman, J., *Common factors affecting bond returns*, The Journal of Fixed Income **1** (1991), no. 1, 54–61.

[35] Peat, T., Segreti, R., *Inflation Derivatives: A User's Guide*, January 2005.

[36] Piazzesi, M., *Affine Term Structure Models*, Handbook of Financial Econometrics **1** (2010), 691–766.

[37] Poklewski-Koziell, W., *Stochastic Volatility Models: Calibration, Pricing and Hedging*, Master Thesis, The University of the Witwatersrand, Johannesburg, 2012.

[38] Risa, S., *Nominal and Inflation Indexed Yields: Separating Expected Inflation and Inflation Risk Premia*, Tech. report, Working Paper, Columbia University, 2001.

[39] Salas, S., *Inflation Derivatives in a Nutshell*, Societe Generale Presentation.

[40] Segreti, R., *Global Inflation-Linked Products: A User's Guide*, Barclays Capital Research Booklet, February 2008.

[41] Shen, P., *How Important is the Inflation Risk Premium?*, Economic Review - Federal Reserve Bank OF Kansas City **83** (1998), 35–48.

[42] The European Central Bank, *Website of the ECB*, Available at http://www.ecb.europa.eu/.

[43] Ungari, S., *Inflation Market Handbook*, Societe Generale Cross Asset Research, April 2009.

[44] Vasicek, O., *An equilibrium characterization of the term structure*, Journal of Financial Economics **5** (1977), no. 2, 177–188.

[45] Wan, E., van der Merwe, R., *Kalman Filtering and Neural Networks*, ch. 7, pp. 221–280, John Wiley and Sons, Inc., 2001.